The Graduate University for Advanced Studies
School of High Energy Accelerator Science
Department of Particle and Nuclear Physics

Higgs interactions in physics beyond the standard model

Yohei Kikuta

A dissertation submitted in partial fulfillment
of the requirement for the degree of
Doctor of Science in Physics

Abstract

In this thesis we study the Higgs interactions in physics beyond the Standard Model. After the discovery of the Higgs boson at the LHC, it is the time to study the Higgs interactions from various aspects. The precise measurement of the Higgs boson properties provides tests of the Standard Model, and perhaps the first signal of new physics beyond the Standard Model can be indirectly found in Higgs physics. In this thesis we concentrate on the following two issues: the scattering amplitudes of the longitudinal gauge bosons and the Higgs boson, and the couplings of the Higgs boson to other particles. The first one is related to the perturbative unitarity of a theory with spontaneously broken symmetries and expected to be important information for the scalar sector, especially the origin of the electroweak symmetry breaking. The second one reflects the structure of the Higgs interactions and gives a clue for the mass generation of the particles. Various new physics models show the deviations of these properties from the Standard Model prediction, which may be investigated at the future collider experiments. We examine the unitarity violation caused by the dimension-six derivative interactions of the Higgs doublets, which indicates the new physics scale associated with an extended Higgs sector. We compute the strongest unitarity bound for several models and find it gives rather low cut-off scale compared with that of the naive dimensional analysis. We also examine the possible deviations of the Higgs couplings in agreement with the experimental constraints, focusing on the three models: the minimal composite Higgs models, the Randall-Sundrum model, and the extra singlet Higgs model. It is found that the correlation of Higgs couplings is quite powerful to discriminate models at the future collider experiments.

This thesis is composed of five chapters. In chapter 1 we give an overview of the current status of phenomenological particle physics, especially about Higgs physics. While all the particles of the Standard Model are observed, we know the phenomena the Standard Model seems not to cover; hence there are many proposals for new physics beyond the Standard Model. In chapter 2 we provide a brief overview of Higgs physics in the Standard Model. The Higgs sector is introduced to account for the low energy breaking of the $SU(2)_L \times U(1)_Y$ electroweak gauge symmetry to the $U(1)_{EM}$, and all of the interactions including the Higgs boson is determined by its mass value. In chapter 3 we analyze the perturbative unitarity bound given by the dimension-six derivative interactions consisting of the Higgs doublets. The bound is obtained by diagonalizing the scattering amplitude matrix of two-body to two-body scattering processes which include the longitudinal gauge bosons and the Higgs boson. We formulate it in terms of the parameters of the Lagrangian. In chapter 4 we present the deviations of the Higgs couplings in some models, compared with the Standard Model prediction, mainly focusing on the minimal composite Higgs model. In order to classify the features of the models we consider, we elucidate the correlation of the coupling deviations. The future experiments are able to distinguish the models well by using both the tree level and loop induced Higgs couplings. In the concluding remarks we summarize our results and give an outlook for the future prospects of Higgs physics.

Contents

---

1 Introduction

The Higgs boson which is predicted by the Standard Model (SM) has been discovered by the ATLAS and CMS experiments at the LHC in 2012 [1]. This observation means that the spontaneous symmetry breaking (SSB) by the condensation of the scalar field, Brout-Englert-Higgs mechanism [2], occurs in the real world. The vacuum expectation value (VEV) of the Higgs field gives the masses of W/Z bosons, quarks, charged leptons and the Higgs boson itself; the strength of the interaction with the Higgs field is completely determined by the mass of the interacting particle. Although we have observed only the gauge interactions as a fundamental interaction so far, the discovery of the Higgs boson and the SSB strongly implies the existence of the yukawa interaction (at least the top yukawa interaction) and the Higgs self interaction. Now the experiments shed light on the Higgs sector, and the SM is being confirmed; the establishment of the SM is one of the greatest achievement of human intellect.

While the SM can explain extraordinarily well physical phenomena observed at the microscopic scale, there exists a number of the experimental and the theoretical problems which the SM cannot answer: neutrino masses and oscillations, dark matter, baryon asymmetry of the universe, inflation, fine tuning problems, impossibility of the unification of the gauge couplings, and so forth. We have to introduce a new element into the theory to solve these problems: symmetries, particles, mechanisms. Such extensions of the SM probably leave traces of physics beyond the SM; we try to find them by means of direct and indirect measurements. A direct measurement is the method to search new phenomena which are undoubtedly signals of new physics. An indirect measurement is the method to investigate the deviations from the SM prediction, which can be more powerful than a direct one in some cases. These two ways are complementary, and they allow us to investigate various features and properties of the model we consider.

With regard to the Higgs sector, one of the important problems is the mystery of why the electroweak (EW) symmetry is spontaneously broken. This mystery is deeply connected with the Higgs fine tuning problem which requires unnatural adjustment of the dimension-full Higgs mass parameter to produce the correct EW scale. Since the EW symmetry is

broken by hand via the negative mass-squared term in the case of the SM, the model does not tell us the origin of the SSB and cannot avoid the unacceptable fine tuning of the Higgs mass parameter. It would be undesirable for the fundamental theory of nature, and we expect that some mechanism or dynamics naturally explains the EW symmetry breaking and stabilizes the EW scale. In order to provide the natural description of the Higgs sector at the EW scale, we have to construct a TeV-scale theory that will replace the SM.

Many models describing the physics beyond the SM have been proposed: supersymmeric (SUSY) models, composite Higgs models and models with extra dimensions, etc. The Higgs sector of these models is extended as it is naturally responsible for the EW symmetry breaking with a certain dynamics or mechanism. Such an extension of the Higgs sector causes the modification of Higgs physics from that of the SM. The modification can affect various observables at the collider experiments; maybe its effect could be firstly observed as deviations from the SM prediction at the energy scale which is lower than a typical new physics scale (such as the dynamical scale or the masses of new resonances). From the perspective of the effective theory, we can examine these deviations in terms of higher dimensional operators including the Higgs field. Higgs physics is therefore important not only for the establishment of the SM Higgs sector but also for the indirect search of the new physics. After the discovery of the Higgs boson, it is becoming more important and interesting to investigate the phenomena beyond the SM by focusing on Higgs physics. In this thesis we concentrate on Higgs physics as a window to new physics and especially study the following two subjects.

One of the topics we study is the perturbative unitarity of the scattering amplitudes of the longitudinal gauge bosons and Higgs bosons [3]. Since the massive gauge boson has the longitudinal polarization state whose wave function is proportional to the four momentum in the high energy limit, the massive gauge boson scattering amplitudes grow as the center of mass energy increases. In the case of the SM the contribution from the Higgs boson cancels the positive power dependence of energy on the amplitudes, and the amplitudes are expressed as a function of the Higgs mass; hence the unitarity of the theory is ensured [4]. This is the striking feature of the renormalizable spontaneously broken gauge theory. However, if there is a deviation of the coupling between the gauge bosons and the Higgs boson, such a cancellation would be lost. The amplitudes therefore keep growing until the energy scale where the perturbative unitarity breaks down, which suggests that some new physics has to appear at this energy scale and recover the unitarity of the theory. Typically, the dimension-six derivative interactions of the Higgs field give rise to the unitarity violation in the high energy region [5]. It is meaningful to estimate the energy scale of the unitarity violation within the effective theory in which heavy particles are integrated out and only the SM particles including the Higgs bosons are treated as a dynamical degrees of freedom (DOF). According to the Ref [6], the general form of the dimension-six derivative interactions including any number of the Higgs doublets is constructed. With this consequence we examine the condition of the tree level unitarity violation in terms of the coefficients of the dimension-six Higgs derivative operators for the one Higgs doublet and two Higgs doublets cases. By way of example, we show the typical unitarity violation scales in various composite Higgs models; however our result can be

applied to any theory where the dimension-six Higgs derivative interactions are generated.

The other topic is the couplings of the Higgs boson to other particles. For the SM the strength of the couplings is expressed in terms of the particle mass and the VEV of the Higgs field, and we already know all of the mass parameters in the theory. Hence the deviation of the couplings from those of the SM is undoubtedly evidence of new physics. In most cases new physics models predict the modified Higgs couplings at tree or loop level. These modified couplings are good observables for the search of new physics. At this stage, the Higgs couplings begin to be observed at the LHC [7]. At the future collider experiments we can measure the various couplings with high accuracy, $\leq \mathcal{O}(1)\%$, which is a powerful tool for probing new physics; the more precise the experiment, the higher scale physics we can probe. In addition, the correlations of the modified Higgs couplings are useful to discriminate new physics models because they tend to show different features for each model. In this work we especially study the partial decay widths and the couplings of the Higgs boson in the minimal composite Higgs model (MCHM) [8] in detail. It is notable that we compute all of the loop induced effective couplings, $hgg, h\gamma\gamma$ and $hZ\gamma$, including exact mass dependences of the heavy resonances and show their correlations. Then the result is compared with those of other models, the Randall-Sundrum (RS) model [9] and the extra singlet Higgs model. Using the correlations of the deviations of the Higgs couplings, we clarify how we can discriminate each model in the future experiments.

2 Higgs physics in the Standard Model

In this chapter we briefly review the Higgs physics in the SM. The Higgs field is introduced as $(\mathbf{1}, \mathbf{2}, +1/2)$[1] under $SU(3)_C \times SU(2)_L \times U(1)_Y$, and its VEV breaks $SU(2)_L \times U(1)_Y$ down to $U(1)_{EM}$ [10]. The Higgs interactions are completely determined by the masses of the interacting particles.

2.1 Lagrangian including the Higgs field

The Lagrangian including the Higgs field is divided into three parts:

$$\mathcal{L} \supset \mathcal{L}_V + \mathcal{L}_{Hkin} + \mathcal{L}_{yukawa}, \tag{2.1}$$

where $\mathcal{L}_V, \mathcal{L}_{Hkin}$ and $\mathcal{L}_{yukawa}$ are Higgs potential part, Higgs kinetic part and yukawa interaction part. The Higgs field can be parametrized using four real DOFs as

$$H(x) = \frac{1}{\sqrt{2}} \begin{pmatrix} h_1(x) + ih_2(x) \\ h_3(x) + ih_4(x) \end{pmatrix}. \tag{2.2}$$

[1] We define the hypercharge as $Y = Q - T_L^3$.

2.1.1 Higgs potential part

Higgs potential is described by two parameters:

$$\mathcal{L}_V = \mu^2|H|^2 - \lambda|H|^4 = -\lambda\left(|H|^2 - \frac{\mu^2}{2\lambda}\right)^2 + \frac{\mu^4}{4\lambda}. \tag{2.3}$$

The VEV reads $\langle|H|\rangle \equiv v/\sqrt{2} = \sqrt{\mu^2/2\lambda}$. This non-trivial VEV is essential for the EW symmetry breaking; the trigger is the sign of the mass parameter μ^2 which is chosen by hand and the reason cannot be explained in the SM. After expanding around the VEV and using an $SU(2)_W$ rotation, the Higgs doublet can be expressed as

$$H(x) = U(x)\frac{1}{\sqrt{2}}\begin{pmatrix} 0 \\ v + h(x) \end{pmatrix}, \tag{2.4}$$

where $U(x)$ is a gauge transformation of $SU(2)_W$. We can always rotate away this $U(x)$ by transforming $H(x) \to U^{-1}(x)H(x)$, which means that only one DOF remains physical after the SSB. The other three DOFs are called Nambu Goldstone (NG) bosons and "eaten" by gauge bosons as we will see.

In the basis where $U(x)$ is rotated away, so-called unitary gauge, we are able to rewrite $\mathcal{L}_V$:

$$\begin{aligned}\mathcal{L}_V &= -\lambda v^2 h^2 - \lambda v h^3 - \frac{\lambda}{4}h^4 \\ &= -\frac{1}{2}m_h^2 h^2 - \frac{m_h^2}{2v}h^3 - \frac{m_h^2}{8v^2}h^4,\end{aligned} \tag{2.5}$$

where m_h is the Higgs mass. Now we have measured the value of the mass of the Higgs boson:

$$m_h = 125.9 \pm 0.4 \text{ [GeV]}. \tag{2.6}$$

Note that we drop the vacuum energy term in the Eq. (2.5); we need not care about it as long as neglecting the gravity.

2.1.2 Higgs kinetic part

The Higgs kinetic term reads

$$\mathcal{L}_{Hkin} = (D_\mu H)^\dagger D^\mu H, \qquad D_\mu = \partial_\mu - igW_\mu^a\frac{\sigma^a}{2} - i\frac{g'}{2}B_\mu \mathbb{I}_{2\times 2}, \tag{2.7}$$

where σ^a (a=1,2,3) is the Pauli matrices. We then move to the electromagnetic eigenbasis since $U(1)_{EM}$ gauge symmetry still remains after the EW symmetry breaking:

$$W_\mu^\pm = \frac{1}{\sqrt{2}}(W_\mu^1 \mp iW_\mu^2), \tag{2.8}$$

$$Z_\mu = \frac{1}{\sqrt{g^2 + g'^2}}(gW_\mu^3 - g'B_\mu) = \cos\theta_W W_\mu^3 - \sin\theta_W B_\mu, \tag{2.9}$$

$$A_\mu = \frac{1}{\sqrt{g^2 + g'^2}}(g'W_\mu^3 + gB_\mu) = \sin\theta_W W_\mu^3 + \cos\theta_W B_\mu, \tag{2.10}$$

where θ_W is the Weinberg angle. In this basis we get

$$\begin{aligned}\mathcal{L}_{Hkin} &= \frac{1}{2}\partial_\mu h \partial^\mu h + \left(\frac{gv}{2}\right)^2 W_\mu^+ W^{-\mu}\left(1+\frac{h}{v}\right)^2 + \left(\frac{\sqrt{g^2+g'^2}v}{2}\right)^2 \frac{Z_\mu Z^\mu}{2}\left(1+\frac{h}{v}\right)^2 \\ &= \frac{1}{2}\partial_\mu h \partial^\mu h + m_W^2 W_\mu^+ W^{-\mu}\left(1+\frac{h}{v}\right)^2 + m_Z^2 \frac{Z_\mu Z^\mu}{2}\left(1+\frac{h}{v}\right)^2. \end{aligned} \tag{2.11}$$

2.1.3 Yukawa interaction part

The yukawa interaction Lagrangian is the following:

$$\mathcal{L}_{yukawa} = -\sum_{I,J}^{3} \bar{L}_I^g y_{IJ}^{l,g} e_J^g H - \sum_{I,J}^{3} \bar{Q}_I^g y_{IJ}^{d,g} d_J^g H - \sum_{I,J}^{3} \bar{Q}_I^g y_{IJ}^{u,g} u_J^g \tilde{H} + (h.c.), \tag{2.12}$$

where superscript g means the gauge eigenbasis, and l, d and u stand for lepton, down quark and up quark respectively. We also define

$$\tilde{H} = i\sigma^2 H^*, \tag{2.13}$$

$$L_I = \begin{pmatrix}\nu_e \\ e\end{pmatrix}_L, \quad \begin{pmatrix}\nu_\mu \\ \mu\end{pmatrix}_L, \quad \begin{pmatrix}\nu_\tau \\ \tau\end{pmatrix}_L, \tag{2.14}$$

$$Q_I = \begin{pmatrix}u \\ d\end{pmatrix}_L, \quad \begin{pmatrix}c \\ s\end{pmatrix}_L, \quad \begin{pmatrix}t \\ b\end{pmatrix}_L, \tag{2.15}$$

$$e_I = e_R, \mu_R, \tau_R, \tag{2.16}$$

$$d_I = d_R, s_R, b_R, \tag{2.17}$$

$$u_I = u_R, c_R, t_R. \tag{2.18}$$

Here $L(R)$ denotes the left (right) handedness. It is notable that in the Eq. (2.12) only the left handed neutrino is introduced; hence the neutrinos are massless in the SM. Let us count the DOFs of the yukawa couplings. If $y = 0$, the Lagrangian is invariant under the chiral transformations:

$$L_I^g \to F_{LIJ} L_J^g, \quad e_I^g \to F_{eIJ} e_J^g, \tag{2.19}$$

$$Q_I^g \to F_{QIJ} Q_J^g, \quad d_I^g \to F_{dIJ} d_J^g, \quad u_I^g \to F_{uIJ} u_J^g, \tag{2.20}$$

where F is 3×3 unitary matrix acting on flavor space. The yukawa couplings break these symmetries explicitly. Let us treat the yukawa couplings as spur ions transforming as follows:

$$y_{IJ}^{lg} \to F_{LII'} y_{I'J'}^{lg} F_{eJ'J}^\dagger, \tag{2.21}$$

$$y_{IJ}^{dg} \to F_{QII'} y_{I'J'}^{dg} F_{dJ'J}^\dagger, \tag{2.22}$$

$$y_{IJ}^{ug} \to F_{QII'} y_{I'J'}^{ug} F_{uJ'J}^\dagger. \tag{2.23}$$

The Lagrangian is still invariant under these transformations. Note that if we choose $F_Q = F_u = F_d = e^{iB}$ and $F_L = W\mathrm{diag}(e^{i\alpha}, e^{i\beta}, e^{i\gamma}), F_e = W\mathrm{diag}(e^{i\alpha}, e^{i\beta}, e^{i\gamma})$ where $W^\dagger y^{lg} W = \mathrm{diag}(y_1, y_2, y_3)$, the yukawa Lagrangian remains invariant. These are corresponding to the baryon number conservation and the lepton number conservation for each generation. Similarly to the NG boson case, we could write the physical DOF of the yukawa couplings as

$$N_{y\,phys} = N_y - N_G + N_{G'}, \tag{2.24}$$

where a chiral symmetry G is broken explicitly by the yukawa sector to a group G'. For the lepton sector, $G = U(3)_L \otimes U(3)_e$ and $G' = U(1)^3$. Then we get

$$\text{moduli} : N_{y\,phys} = 3^2 - 2\frac{3(3-1)}{2} = 6, \tag{2.25}$$

$$\text{phases} : N_{y\,phys} = 3^2 - 2\frac{3(3+1)}{2} + 3 = 0. \tag{2.26}$$

The half of moduli is related to masses, and the others are corresponding to physical yukawa couplings. For the quark sector, $G = U(3)_Q \otimes U(3)_u \otimes U(3)_d$ and $G' = U(1)_B$, leading to

$$\text{moduli} : N_{y\,phys} = 2 \times 3^2 - 3\frac{3(3-1)}{2} = 9, \tag{2.27}$$

$$\text{phases} : N_{y\,phys} = 2 \times 3^2 - 3\frac{3(3+1)}{2} + 1 = 1. \tag{2.28}$$

The moduli are divided into three masses, three mixing angles and three yukawa couplings. We have one phase DOF in the quark sector which is the unique source of the CP-violation in the SM.

In order to get the mass eigenstates we perform the singular value decomposition (SVD) by defining the following unitary matrices:

$$\sum_{I,J=1}^{3} (U^l_{iI})^\dagger y^{l,g}_{IJ} V^l_{Jj} = \delta_{ij} y^l_i, \tag{2.29}$$

$$\sum_{I,J=1}^{3} (U^d_{iI})^\dagger y^{d,g}_{IJ} V^d_{Jj} = \delta_{ij} y^d_i, \tag{2.30}$$

$$\sum_{I,J=1}^{3} (U^u_{iI})^\dagger y^{u,g}_{IJ} V^u_{Jj} = \delta_{ij} y^u_i. \tag{2.31}$$

The relations between the gauge eigenstates and the mass eigenstates are

$$e^g_I = V^l_{Ii} e_i, \tag{2.32}$$

$$d^g_I = V^d_{Ii} d_i, \tag{2.33}$$

$$u^g_I = V^u_{Ii} u_i, \tag{2.34}$$

$$\bar{L}^g_I = \bar{L}_i (U^l_{iI})^\dagger, \tag{2.35}$$

$$\begin{aligned}\bar{Q}^g_I &= (\bar{u}_i (U^u_{iI})^\dagger,\ \bar{d}_i (U^d_{iI})^\dagger)_L = (\bar{u}_i,\ \bar{d}_j (V^{CKM}_{ji})^\dagger)_L\ (U^u_{iI})^\dagger \\ &= (\bar{u}_i,\ \bar{d'}_i)_L\ (U^u_{iI})^\dagger = \bar{Q}_I (U^u_{iI})^\dagger,\end{aligned} \tag{2.36}$$

where we define the Cabibo-Kobayashi-Maskawa (CKM) matrix as $V_{ij}^{CKM} = (U_{iJ}^{u})^{\dagger} U_{Jj}^{d}$. The fit results for the magnitudes of all nine CKM elements are

$$V_{CKM} = \begin{pmatrix} 0.97427 \pm 0.00015 & 0.22534 \pm 0.00065 & 0.00351^{+0.00015}_{-0.00014} \\ 0.22520 \pm 0.00065 & 0.97344 \pm 0.00016 & 0.0412^{+0.0011}_{-0.0005} \\ 0.00867^{+0.00029}_{-0.00031} & 0.0404^{+0.0011}_{-0.0005} & 0.999146^{+0.000021}_{-0.000046} \end{pmatrix}. \tag{2.37}$$

The CP phase is often represented by the Jarlskog invariant J defined by

$$\mathrm{Im}[V_{ij} V_{kl} V_{il}^{*} V_{kj}^{*}] = J \sum_{m,n} \epsilon_{ikm} \epsilon_{jln}. \tag{2.38}$$

This is a base-independent, and its fitted value is

$$J = 2.91^{+0.19}_{-0.11} \times 10^{-5}. \tag{2.39}$$

In the mass eigenbasis $\mathcal{L}_{yukawa}$ is rewritten as

$$\mathcal{L}_{yukawa} = -\sum_{i=1}^{3} y_i^{l} \bar{L}_i H e_i - \sum_{i,j=1}^{3} y_i^{d} \bar{Q}_j V_{ji}^{CKM} H d_i - \sum_{i=1}^{3} y_i^{u} \bar{Q}_i \tilde{H} u_i + (h.c.). \tag{2.40}$$

The CKM matrix appears in the second term. The reason is that the up quarks and the down quarks cannot be simultaneously diagonalized since the left handed up and down quarks form the $SU(2)_L$ doublets. Interactions between the down quarks and the neutral components of the Higgs field, however, are diagonal due to the cancellation of the CKM matrix. This means the CKM matrix, especially the CP violation, appears in the charged current interaction of the quarks.

In the unitary gauge we get

$$\begin{aligned} \mathcal{L}_{yukawa} &= -\sum_{l=e,\mu,\tau} \frac{y_l v}{\sqrt{2}} \left(1 + \frac{h}{v}\right) \bar{l}l - \sum_{d=d,s,b} \frac{y_d v}{\sqrt{2}} \left(1 + \frac{h}{v}\right) \bar{d}d - \sum_{u=u,c,t} \frac{y_u v}{\sqrt{2}} \left(1 + \frac{h}{v}\right) \bar{u}u \\ &= -\sum_{l=e,\mu,\tau} m_l \left(1 + \frac{h}{v}\right) \bar{l}l - \sum_{d=d,s,b} m_d \left(1 + \frac{h}{v}\right) \bar{d}d - \sum_{u=u,c,t} m_u \left(1 + \frac{h}{v}\right) \bar{u}u. \end{aligned} \tag{2.41}$$

2.2 Higgs interactions with other particles

As we saw in the previous section, the interactions of the physical Higgs field with other particles (as well as itself) are determined by the masses of the particles. We summarize the Higgs interactions at the tree and one-loop levels. We also show the accuracies on Higgs coupling measurements that experiments are capable of reaching in the future collider experiments.

2.2.1 Tree level interactions

The Higgs boson interacts with all massive particles at tree level via mass dependent couplings. We parametrize the couplings as follows:

$$\mathcal{L} \supset -\sum_f g_{h\bar{f}f} h\bar{f}f + \sum_V g_{hVV} h \frac{VV}{1+\delta_{VZ}} + \sum_V g_{hhVV} \frac{h^2}{2!}\frac{VV}{1+\delta_{VZ}} - g_{hhh}\frac{h^3}{3!} - g_{hhhh}\frac{h^4}{4!}, \tag{2.42}$$

where f runs all species of the massive fermions, $V = W^{\pm}/Z$ and δ_{VZ} is introduced to denote the symmetric factor for the Z boson. In the case of the SM we get the following couplings from the result of previous section.

$$g_{h\bar{f}f} = \frac{m_f}{v}, \tag{2.43}$$

$$g_{hVV} = \frac{2m_V^2}{v}, \tag{2.44}$$

$$g_{hhVV} = \frac{2m_V^2}{v^2}, \tag{2.45}$$

$$g_{hhh} = \frac{3m_h^2}{v}, \tag{2.46}$$

$$g_{hhhh} = \frac{3m_h^2}{v^2}, \tag{2.47}$$

The important feature is that the Higgs couplings are controlled by the masses of the interacting particles. In particular, the couplings $g_{h\bar{f}f}$, $\sqrt{g_{hhVV}/2}$ and $\sqrt{g_{hhhh}/3}$ are aligned on the linear line as we can see in the Fig. 1.

We can compute the decay widths of the Higgs boson to two vector bosons and two fermions; for the vector boson modes one vector boson is on-shell and the other is off-shell because $m_h < 2m_V$. The results are the following:

$$\Gamma(h \to \bar{f}f)_{SM} = \frac{\sqrt{2}G_F N_c}{8\pi} m_f^2 m_h \sqrt{1 - \frac{4m_f^2}{m_h^2}}, \tag{2.48}$$

$$\Gamma(h \to WW^*)_{SM} = \frac{3\alpha^2 m_h}{32\sin^4\theta_W} G\left(\frac{m_W}{m_h}\right), \tag{2.49}$$

$$\Gamma(h \to ZZ^*)_{SM} = \frac{\alpha^2 m_h}{128\pi\sin^4\theta_W(1-\sin\theta_W)^2}\left(7 - \frac{40}{3}\sin\theta_W + \frac{160}{9}\sin^2\theta_W\right) G\left(\frac{m_Z}{m_h}\right), \tag{2.50}$$

where N_c is the color factor, and we define the function $G(x)$ as

$$\begin{aligned} G(x) = &-|1-x^2|\left(\frac{47}{2}x^2 - \frac{13}{2} + \frac{1}{x^2}\right) - 3(1-6x^2+4x^4)|\ln x| \\ &+ 3\frac{1-8x+20x^4}{\sqrt{4x^2-1}}\arccos\left(\frac{3x^2-1}{2x^3}\right). \end{aligned} \tag{2.51}$$

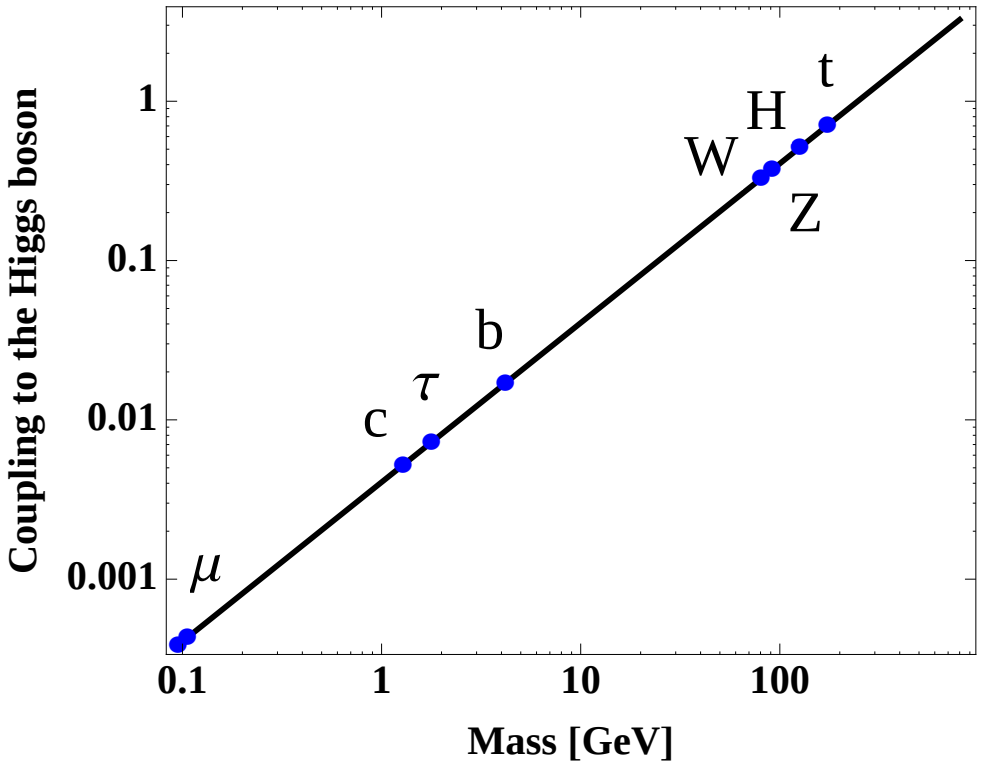

Figure 1. The strength of the Higgs coupling to other particles as a function of the masses of the interacting particles. The Higgs couplings are linearly dependent on the particle mass. A similar figure is seen in the Refs. [11, 12].

2.2.2 One-loop level interactions

The quantum number of the Higgs field forbids the Higgs couplings with $gg, \gamma\gamma$ and $Z\gamma$ at tree level. At loop level, however, the Higgs boson can decay into these particles. The loop induced decay modes are also important to clarify the Higgs properties; in some cases, the loop induced decays are fairly sensitive to new physics because the smallness of the SM effect leads to identifying easily a contribution from new physics.

First we consider the decay of the Higgs boson into two gluons. Since the gluon is $SU(3)_c$ gauge boson, in the SM only the quarks appear in the loop; top and bottom quarks give large contribution to this process, and the other quarks are negligible due to their small masses, namely, small couplings to the Higgs boson. We here represent the formula including spin-0, 1/2 and 1 contributions for the sake of generality. The decay width is given by

$$\Gamma(h \to gg) = \frac{\alpha_s^2 m_h^3}{128\pi^3} \left| \delta_R T(V) \frac{g_{hVV}}{m_V^2} A_1(\tau_V) + \delta_R T(f) \frac{2 g_{h\bar{f}f}}{m_f} A_{1/2}(\tau_f) + \delta_R T(S) \frac{g_{hSS}}{m_S^2} A_0(\tau_S) \right|^2 . \tag{2.52}$$

In the above the notation V,f and S refer to spin-1, spin-1/2 and spin-0 particles, respectively. The loop functions are defined in the App. A, and the argument of the loop function is defined as $\tau_i = \left(\frac{2m_i}{m_h}\right)^2$. $T(i)$ is the Dynkin index of the matter representation defined by the following relation on the group generators:

$$\mathrm{Tr}[T^a T^b] = T(i)\delta^{ab}. \tag{2.53}$$

For $SU(N)$ fundamental representations and adjoint representations $T(i) = \frac{1}{2}$ and N, respectively. In addition, $\delta_R = \frac{1}{2}$ for real matter fields and 1 otherwise. In the case of the SM, we can rewrite the coupling as

$$\frac{2g_{hf\bar{f}}}{m_f} = \frac{2}{v}, \tag{2.54}$$

and the width becomes

$$\begin{aligned}\Gamma(h \to gg)_{SM} &= \frac{\sqrt{2}G_F\alpha_s^2 m_h^3}{128\pi^3}\left|A_{1/2}(\tau_t) + A_{1/2}(\tau_b)\right|^2 \\ &\sim 2.0 \times 10^{-4}\ [\mathrm{GeV}],\end{aligned} \tag{2.55}$$

where we use $\alpha_s = 0.119, m_t = 173$ [GeV] and $m_b = 4.8$ [GeV].[2]

Next we provide the decay width of the Higgs boson into two photons. In this process the particles which get mass from the Higgs field and are electrically charged can enter the loop; $W^\pm$, quarks and charged leptons for the SM case. The decay width is expressed as

$$\Gamma(h \to \gamma\gamma) = \frac{\alpha^2 m_h^3}{1024\pi^3}\left|\frac{g_{hVV}}{m_V^2}Q_V^2 A_1(\tau_V) + \frac{2g_{h\bar{f}f}}{m_f}N_{c,f}Q_f^2 A_{1/2}(\tau_f) + \frac{g_{hSS}}{m_S^2}N_{c,S}Q_S^2 A_0(\tau_S)\right|^2, \tag{2.56}$$

where Q_i is the electric charge in $|e|$ unit, $N_{c,i}$ is the number colors for each particle. For the SM case

$$\frac{g_{hWW}}{m_W^2} = \frac{2g_{hf\bar{f}}}{m_f} = \frac{2}{v}, \tag{2.57}$$

and the width is

$$\begin{aligned}\Gamma(h \to \gamma\gamma)_{SM} &= \frac{\sqrt{2}G_F\alpha^2 m_h^3}{256\pi^3}\left|1^2 A_1(\tau_W) + 3\left(\frac{2}{3}\right)^2 A_{1/2}(\tau_t) + 3\left(\frac{-1}{3}\right)^2 A_{1/2}(\tau_b)\right|^2 \\ &\sim 1.1 \times 10^{-5}\ [\mathrm{GeV}],\end{aligned} \tag{2.58}$$

where we use $\alpha^{-1} = 129$ and $m_W = 80.4$ [GeV].

Finally we also consider the Higgs to Z photon decay mode. The particles appearing in the loop are the same as those of $h \to \gamma\gamma$. In this mode, however, there could be two particles with different masses inside the loop. Let us consider the case that the theory

[2] Of course the QCD correction is significant in such a calculation, and we have to care about the renormalization scheme, see e.g. [13]. In this section we just put the pole mass into the equation.

includes the SM $W^{\pm}$ boson and the fermions which are interacting with the Higgs boson and the Z boson with off-diagonal couplings in the mass eigenbasis. The Lagrangian is described as

$$\begin{aligned}\mathcal{L} \supset\ & m_W^2 W_\mu^+ W^{-\mu} + g_{hWW} h W_\mu^+ W^{-\mu} - m_i \bar{\psi}_i \psi_i + Q_i |e| \bar{\psi}_i \gamma^\mu \psi_i A_\mu \\ & - \bar{\psi}_i (c_{ij}^L P_L + c_{ij}^R P_R) \psi_j h + \bar{\psi}_i \gamma^\mu (\lambda_{ij}^L P_L + \lambda_{ij}^R P_R) \psi_j Z_\mu, \end{aligned} \tag{2.59}$$

where P_L and P_R are the projection operators defined by $P_{L,R} = \frac{1 \mp \gamma^5}{2}$. The decay width of this mode is expressed by the following:

$$\begin{aligned}\Gamma(h \to Z\gamma) =& \frac{\alpha^2 m_h^3}{512\pi^3} \left(1 - \frac{m_Z^2}{m_h^2}\right)^3 \left| \frac{g_{hWW}}{\sin\theta_W \cos\theta_W} A_V(m_W) \right. \\ & \left. + \frac{2N_c}{g \sin\theta_W} \sum_{i,j} Q_i m_i (c_{ij}^L + c_{ij}^R)(\lambda_{ji}^L + \lambda_{ji}^R) A_F(m_i, m_j) \right|^2 . \end{aligned} \tag{2.60}$$

For the SM case we get

$$\begin{aligned}\Gamma(h \to Z\gamma)_{SM} =& \frac{\sqrt{2} G_F \alpha^2 m_h^3}{128\pi^3} \left(1 - \frac{m_Z^2}{m_h^2}\right)^3 \left| \frac{m_W^2}{\sin\theta_W \cos\theta_W} A_V(m_W) \right. \\ & + \frac{2 \times 3}{\sin\theta_W \cos\theta_W} \left\{ \left(\frac{2}{3}\right) m_t^2 \left(\frac{1}{2} - 2\sin^2\theta_W \left(\frac{2}{3}\right)\right) A_F(m_t, m_t) \right. \\ & \left. \left. + \left(\frac{-1}{3}\right) m_b^2 \left(-\frac{1}{2} - 2\sin^2\theta_W \left(\frac{-1}{3}\right)\right) A_F(m_b, m_b) \right\} \right|^2 \\ \sim & 7.0 \times 10^{-6}\ [\text{GeV}]. \end{aligned} \tag{2.61}$$

There doesn't appear to be the off-diagonal contributions in the SM.

2.2.3 Experimental sensitivity to the Higgs couplings

It is important to precisely measure the Higgs couplings in order not only to confirm the SM, but also to investigate the physics beyond the SM. For the SM case, as we looked, the decay widths of the Higgs boson are determined by the mass of the particles and the EW parameters. The total decay width, $\Gamma_H = \sum_{\text{all modes}} \Gamma$, is dependent on the Higgs mass and the result is shown in the Fig. 2. The total width sharply changes around the two vector boson threshold, and in the high mass region the width becomes too broad to be identified as a particle. For $m_h = 126$ [GeV], total width is $\Gamma_H = 4.2 \times 10^{-3}$ [GeV] which is too small to be experimentally measurable from the shape of the resonance.

The branching ratio (BR) for a particular decay mode is defined by Γ/Γ_H. The result of various modes is shown in the Fig. 3. We can see the BR is sensitive to the Higgs mass. For $m_h = 125.9$ [GeV], the branching ratios are $\text{BR}(bb) = 0.563, \text{BR}(WW^*) = 0.229, \text{BR}(gg) = 0.0849, \text{BR}(\tau\tau) = 0.0617, \text{BR}(ZZ^*) = 0.0287, \text{BR}(cc) = 0.0284, \text{BR}(\gamma\gamma) = 0.00228$ and $\text{BR}(Z\gamma) = 0.00162$ [12]. Fortunately it is possible to measure various modes at the collider

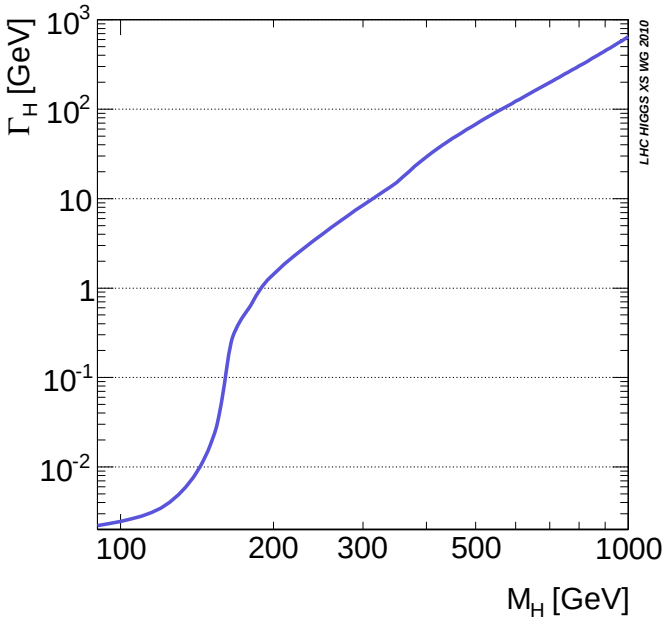

Figure 2. The total decay width as the function of the Higgs mass. The width is monotonic increasing with the Higgs mass. This figure is taken from the Refs. [14].

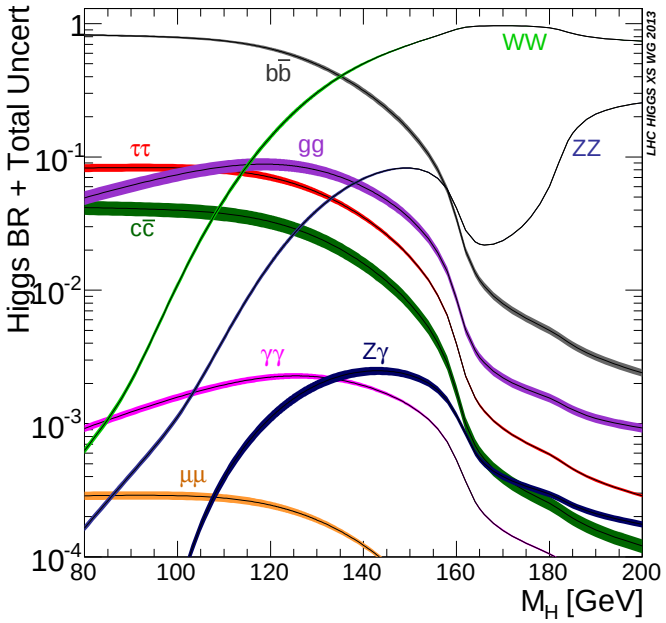

Figure 3. The branching ratio of the Higgs decay modes. In the light mass region (below the WW threshold) the main decay mode is bb. If the Higgs boson is sufficiently heavy the decay mode is dominated by WW and ZZ modes. This figure is taken from the Ref. [14].

experiments; the Higgs coupling is interesting target for the future physics.

Many studies of the Higgs coupling measurements are done. For example, the accuracies that can be achieved by experiments at the LHC and at the ILC are estimated by the Refs. [15, 16]. The Fig. 4 show the 1σ experimental sensitivities to the Higgs couplings. At the LHC, due to the QCD back ground, the hbb and $h\tau\tau$ couplings are difficult to be determined well. The loop induced couplings can be relatively well measured. Using ILC sensitivities, we can determine the couplings within 5% accuracy. Especially, tree level couplings, hVV and hbb, can be measured less than about 1%. Note that $h \to Z\gamma$ mode has not studied yet although this process is as important as the other loop induced processes, $h \to gg$ and $h \to \gamma\gamma$; we need to study this mode and clarify its validity for the search of new physics.

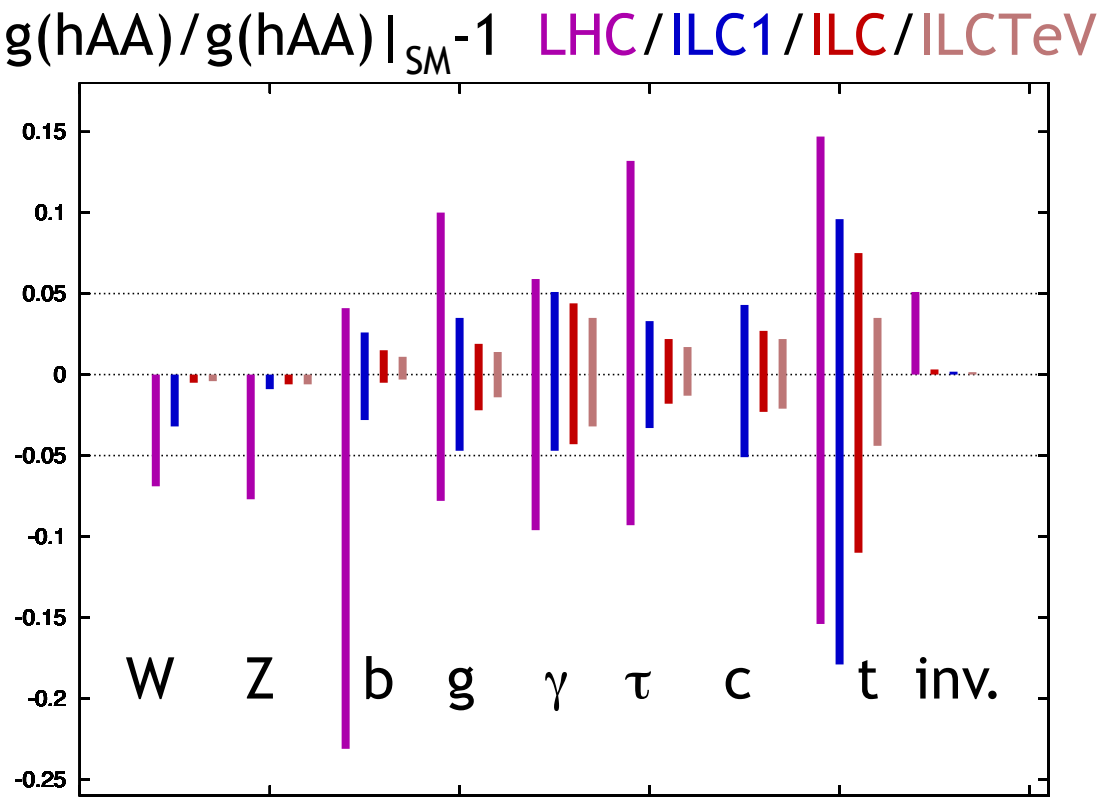

Figure 4. Comparison of the capabilities of the LHC and the ILC model independent measurements of the Higgs couplings. The plot shows (from left to right in each set of error bars) 1 σ confidence intervals for LHC at 14 [TeV] with 300 [fb^{-1}], for ILC at 250 [GeV] and 250 [fb^{-1}] ('ILC1'), for the full ILC program up to 500 [GeV] with 500 [fb^{-1}] ('ILC'), and for a program with 1000 [fb^{-1}] for an upgraded ILC at 1 [TeV] ('ILCTeV'). The marked horizontal band represents a 5% deviation from the Standard Model prediction for the coupling. This figure is taken from the Ref. [15].

2.3 Theoretical aspects of Higgs physics

In this section we provide several theoretical aspects of Higgs physics. The Higgs field is introduced as the only scalar field in the SM to cause the EW symmetry breaking. Therefore, its theoretical properties are various and important to understand what the Higgs field is. They are also useful to investigate new physics because models with extended Higgs sector likely modify the properties.

2.3.1 Perturbative unitarity

In this subsection we discuss the perturbative unitarity of the scattering amplitudes. The amplitudes of elastic scattering satisfy the following relation for each partial wave:

$$M_n^I = \lambda(a,b)\left|M_n^R + iM_n^I\right|^2, \tag{2.62}$$

$$\lambda(a,b) = \sqrt{(1-(a+b)^2)(1-(a-b)^2)}, \tag{2.63}$$

where $M_n^R(M_n^I)$ is the real (imaginary) part of the partial wave amplitude, a and b are the ratios between the mass of each particle and the center of mass energy, $m_{a,b}/\sqrt{s}$, and partial waves are defined as below with the Legendre polynomials $P_m(x)$:

$$\mathcal{M}(\cos\theta) = 16\pi\sum_{n=0}^{\infty}(2n+1)M_nP_n(\cos\theta), \tag{2.64}$$

$$\int_{-1}^{1} dx\, P_m(x)P_n(x) = \frac{2}{2n+1}\delta_{mn}. \tag{2.65}$$

Eq. (2.62) is the equation of the circle with radius $\frac{1}{2\lambda}$ and center $\left(0,\frac{1}{2\lambda}\right)$. In the high-energy limit where the masses of produced particles can be neglected, the radius of the circle becomes the maximum. Therefore, the actual amplitudes are in the maximal circle. Finally, partial wave amplitudes at least satisfy $M_n^R \in \left[-\frac{1}{2},\frac{1}{2}\right]$ and $M_n^I \in [0,1]$. If we consider processes involving identical particles in the final state, the bound becomes weaker as $M_n^R \in [-1,1]$ and $M_n^I \in [0,2]$.

As an example, let us consider the two-body to two-body scattering amplitudes of the longitudinal gauge bosons. The polarization vector of the massive gauge boson is expressed as

$$\epsilon_L^\mu = \frac{E}{m_V}\begin{pmatrix}\frac{|\mathbf{p}|}{E}\\ \frac{\mathbf{p}}{|\mathbf{p}|}\end{pmatrix}, \tag{2.66}$$

where E and $\mathbf{p}$ are energy and three momentum, respectively. Naive estimation of a two body to two body scattering amplitude is then

$$\begin{aligned}\mathcal{M}(V_L^aV_L^b \to V_L^cV_L^d) &\propto |\epsilon_L^\mu|^4\\ &\sim \frac{E^4}{m_V^4}.\end{aligned} \tag{2.67}$$

This amplitude seems to be divergent in the ultraviolet region. First we consider the process of longitudinal gauge boson two-body to two-body scatterings with $g' = 0$ case. Diagrams including only the gauge bosons are comprised of one with four point interaction and ones with three point interaction.

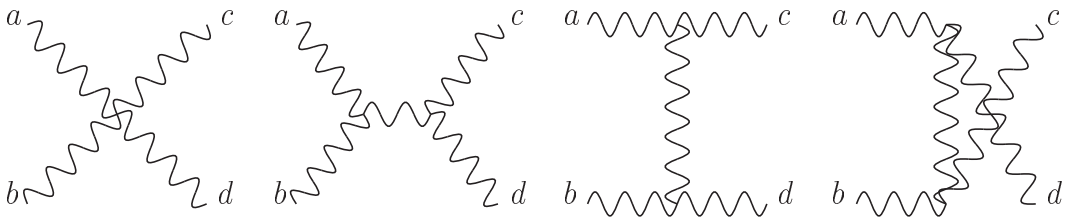

Figure 5. Two-body to two-body scattering process of longitudinal gauge bosons, including only the gauge bosons. Indices, a, b, c and d, denote the component of the gauge boson.

Focusing on the contributions which diverse as energy increases, we can write the amplitude of the four point interaction diagram as

$$\mathcal{M}_4(ab \to cd) = g_{WWWW} \frac{E^4}{m_W^4} \left(-6 + 2\cos^2\theta + 4\frac{m_W^2}{E^2} \right) \delta^{ab}\delta^{cd} + \cdots . \tag{2.68}$$

The t-channel and u-channel contributions are

$$\mathcal{M}_t(ab \to cd) = g_{WWW}^2 \frac{E^4}{m_W^4} \left(3 - 2\cos\theta - \cos^2\theta + \left(-\frac{3}{2} + \frac{15}{2}\cos\theta \right) \frac{m_W^2}{E^2} \right) \delta^{ab}\delta^{cd} + \cdots , \tag{2.69}$$

$$\mathcal{M}_t(ab \to cd) = g_{WWW}^2 \frac{E^4}{m_W^4} \left(3 + 2\cos\theta - \cos^2\theta + \left(-\frac{3}{2} - \frac{15}{2}\cos\theta \right) \frac{m_W^2}{E^2} \right) \delta^{ab}\delta^{cd} + \cdots . \tag{2.70}$$

Note that s-channel contribution to this term vanishes due to the nature of the structure constant. The gauge symmetry guarantees the following relation:

$$g_{WWWW} = g_{WWW}^2 = g^2. \tag{2.71}$$

Thanks to this relation the sum of these contribution becomes

$$\mathcal{M}_4 + \mathcal{M}_t + \mathcal{M}_u = g^2 \frac{E^2}{m_W^2} \delta^{ab}\delta^{cd}, \tag{2.72}$$

We can see E^4 dependence vanishes. The E^2 dependence, however, still remains and violates the tree level unitarity in the high energy region. The Higgs boson mediated diagram, see the Fig.6, plays an crucial role to save this difficulty.

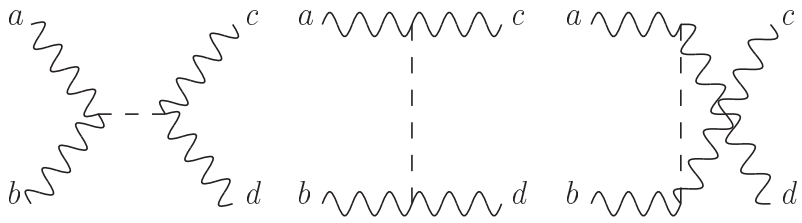

Figure 6. Two-body to two-body scattering process of longitudinal gauge bosons, including the Higgs propagator. Indices, a, b, c and d, denote the component of the gauge boson.

The amplitude of the sum of the Higgs mediated diagrams can be calculated as

$$\begin{aligned}\mathcal{M}_h(ab \to cd) &= g_{hWW}^2 \frac{4E^4}{m_W^4} \frac{1}{m_h^2 - 4E^2} \delta^{ab}\delta^{cd} \\ &= g^2 \frac{4E^4}{m_W^2} \frac{1}{m_h^2 - 4E^2} \delta^{ab}\delta^{cd}. \end{aligned} \tag{2.73}$$

Combining Eq. (2.72) and Eq. (2.73), we get

$$\mathcal{M}_4 + \mathcal{M}_t + \mathcal{M}_u + \mathcal{M}_h = \frac{g^2}{m_W^2} \frac{m_h^2 E^2}{m_h^2 - 4E^2} \delta^{ab}\delta^{cd}. \tag{2.74}$$

This amplitude converges into -2λ in $E^2 \gg m_h^2$ limit, and the terms with other combinations of indices behave the same way. Therefore, the Higgs field performs an important role for constructing the renormalizable theory with massive gauge bosons. If the Higgs boson is too much heavy the Higgs boson decouples from the theory and the perturbative unitarity again violates in the high energy region. Conversely, one can constraint the Higgs mass from the perspective of the unitarity. From this process the Higgs mass is bounded by about 1300 [GeV].

In order to get the most strongest bound, we need to consider all of the same charge initial (final) states [4]. Let us analyze the charge neutral and s-wave states for the SM case. The matrix of the scattering amplitudes for the $J = 0$ modes, $M_0(X \to Y)$ where $X, Y = W_L^+ W_L^-, \frac{1}{\sqrt{2}} Z_L Z_L, \frac{1}{\sqrt{2}} HH, HZ_L$, takes the form

$$(\text{amplitude matrix}) \simeq \frac{m_h^2}{8\pi v^2} \begin{pmatrix} 1 & \frac{1}{\sqrt{8}} & \frac{1}{\sqrt{8}} & 0 \\ \frac{1}{\sqrt{8}} & \frac{3}{4} & \frac{1}{4} & 0 \\ \frac{1}{\sqrt{8}} & \frac{1}{4} & \frac{3}{4} & 0 \\ 0 & 0 & 0 & \frac{1}{2} \end{pmatrix} \tag{2.75}$$

where we use the the $s \gg m_h^2$. The largest eigenvalue gives the strongest bound; we get

$$m_h \leq \sqrt{\frac{16\pi v^2}{3}} \tag{2.76}$$

$$\simeq 1.01 \times 10^3 \text{ [GeV]}. \tag{2.77}$$

2.3.2 Custodial symmetry

At lowest order the W and Z boson masses are related by

$$\rho = \frac{m_W^2}{m_Z^2 \cos^2\theta_W} = 1. \tag{2.78}$$

This relation is the consequence of the custodial symmetry which is an approximate global symmetry of the Lagrangian including the Higgs field. In order to make the discussion clear, we introduce the bi-doublet notation:

$$\Phi = (\tilde{H}\ H) = (i\sigma^2 H^*\ H). \tag{2.79}$$

This bi-doublet field is two by two matrix and its VEV is proportional to the identity matrix, $\langle\Phi\rangle \propto v\mathbb{I}_{2\times 2}$.

First we consider the Higgs potential in terms of doublet field:

$$\mathcal{L}_V = \frac{\mu^2}{2}\,\mathrm{Tr}[\Phi^\dagger\Phi] - \frac{\lambda}{4}(\mathrm{Tr}[\Phi^\dagger\Phi])^2. \tag{2.80}$$

This Lagrangian is invariant under the transformation

$$\Phi \to L\Phi R^\dagger, \tag{2.81}$$

where $L(R)$ is $SU(2)_{L(R)}$ transformation. After the EW symmetry breaking the $SU(2)_V$ symmetry is still preserved; this is called the custodial symmetry. Because of $SO(4) \simeq SU(2)_L \times SU(2)_R$, we can replace the bi-doublet representation with the fundamental representation of $SO(4)$. In this case the Higgs VEV breaks $SO(4)$ into $SO(3)$, and this $SO(3)$ is the custodial symmetry.

We next discuss the Higgs kinetic term. The EW $SU(2)_W \times U(1)_Y$ symmetry is gauged as

$$D_\mu\Phi = \partial_\mu\Phi - igW_\mu^a\frac{\sigma^a}{2}\Phi - ig'B_\mu\Phi\frac{\sigma^3}{2}. \tag{2.82}$$

If $g' = 0$, the custodial symmetry is exact and the covariant derivative in the vacuum reads

$$D_\mu\langle\Phi\rangle = \frac{gv}{2\sqrt{2}}\begin{pmatrix} W_\mu^3 & W_\mu^1 - iW_\mu^2 \\ W_\mu^1 + iW_\mu^2 & -W_\mu^3 \end{pmatrix}. \tag{2.83}$$

The gauge field mass term is obtained as follows:

$$\frac{1}{2}\,\mathrm{Tr}[(D_\mu\langle\Phi\rangle)^\dagger D^\mu\langle\Phi\rangle] = \frac{g^2v^2}{4}\frac{W_\mu^a W^{a\mu}}{2}. \tag{2.84}$$

The ρ parameter is obviously equal to one since $\cos\theta_W = 1$ and $Z_\mu = W_\mu^3$ in this case. Then, we put $g' \neq 0$; the custodial symmetry is explicitly broken since the $SU(2)_R$ generators are not commutable with $U(1)_Y$ generator. The covariant derivative in the vacuum is replaced as

$$D_\mu\langle\Phi\rangle = \frac{gv}{2\sqrt{2}}\begin{pmatrix} W_\mu^3 - \frac{g'}{g}B_\mu & W_\mu^1 - iW_\mu^2 \\ W_\mu^1 + iW_\mu^2 & -W_\mu^3 + \frac{g'}{g}B_\mu \end{pmatrix}. \tag{2.85}$$

From this expression we can see the combination, $W^3_\mu - \frac{g'}{g}B_\mu = \frac{Z_\mu}{\cos\theta_W}$, acts like W^3_μ for $g' = 0$ case. The ρ parameter, therefore, is again equal to one at tree level. Although the symmetry is violated at loop level, the effect is not significant because the strength of the hypercharge gauge coupling is small.

Finally we comment on the yukawa interaction part. If the up type yukawa coupling is identical to the down type one in the same generation, the yukawa interactions can be rewritten as

$$\mathcal{L}_{yukawa} \supset \sum_i y_i \bar{Q}_i \Phi \begin{pmatrix} u_{iR} \\ d_{iR} \end{pmatrix}. \tag{2.86}$$

Provided the right handed doublet linearly transforms under $SU(2)_R$, the custodial symmetry is preserved. In reality, $y^u_i \neq y^d_i$ and the custodial symmetry is broken; however, the contribution to the ρ parameter from the loop diagram is not large.

As stated above the custodial symmetry is approximately good symmetry within the renormalizable EW theory. However, higher dimensional operators could violate the custodial symmetry at tree level. For example, consider the following dimension-six operator:

$$\frac{1}{\Lambda^2}\,\mathrm{Tr}\left[(\Phi^\dagger \overleftrightarrow{D}_\mu \Phi)^\dagger \sigma^3\right]\mathrm{Tr}\left[(\Phi^\dagger \overleftrightarrow{D}_\mu \Phi)\sigma^3\right], \tag{2.87}$$

where Λ is a cutoff scale, and $\Phi^\dagger \overleftrightarrow{D}_\mu \Phi = \Phi^\dagger D_\mu \Phi - (D_\mu \Phi)^\dagger \Phi$. This operator affects the ρ parameter because it gives the contribution to the Z boson mass. The experimental value of the ρ parameter, $\rho^{exp} = 1.0008^{+0.0017}_{-0.0007}$, severely constraints a cutoff scale.

If we consider another representation of the Higgs field, the tree level ρ parameter is not always equal to one. For an arbitrary number of Higgs multiplets, the ρ parameter becomes

$$\rho = \frac{\sum_i \left(I_{H_i}(I_{H_i}+1) - Y^2_{H_i}\right)\langle H_i\rangle^2}{2\sum_i Y^2_{H_i}\langle H_i\rangle^2}, \tag{2.88}$$

where I_{H_i} and Y_{H_i} are the isospin and hypercharge for H_i; in the SM $I_{H_i} = Y_{H_i} = \frac{1}{2}$, and then $\rho = 1$. Even if $\rho = 1$ at tree level, higher representations give interesting phenomenologies, see e.g. the Ref. [17].

Hence the custodial symmetry is important for considering the Higgs physics beyond the SM.

2.3.3 Equivalence theorem

The equivalence theorem [18] is a striking feature of gauge theories with spontaneous symmetry breaking; it relates the amplitude for a process with longitudinally polarized vector bosons to the amplitude in which the longitudinal vector bosons are replaced by the corresponding NG bosons. The proof of the theorem is based on the Ward-Takahashi identity. We now consider, as the most simplest case, a single massive $U(1)$ vector boson

is emitted or absorbed in a scattering process. We can schematically write the amplitude of the process:

$$\mathcal{M}(V_L, \dots) = \mathcal{M}(\phi, \dots) + \mathcal{O}\left(\frac{m_V}{E}\right), \tag{2.89}$$

where V_L and ϕ are the longitudinal gauge boson and the corresponding NG boson.

Let us define the longitudinal polarization vector:

$$\epsilon_L^\mu(k) = \left(\frac{|\mathbf{k}|}{m_V}, 0, 0, \frac{E}{m_V}\right) \tag{2.90}$$

$$= \frac{k^\mu}{m_V} + \mathcal{O}\left(\frac{m_V}{E}\right), \tag{2.91}$$

where this polarization vector satisfies $\epsilon_L^\mu k_\mu = 0$ and $\epsilon_L^\mu \epsilon_{L\mu} = 1$. The Ward-Takahashi identity for a process of the process with a single external gauge boson is

$$k_\mu \mathcal{M}^\mu(k) = 0, \tag{2.92}$$

where we denote the amplitude as $\mathcal{M}(k) = \epsilon_\mu \mathcal{M}^\mu(k)$. In the Landau gauge, this amplitude can be decomposed into two peaces. One is the diagram where the current can couple directly into an one particle irreducible vertex function $\Gamma^\mu(k)$. The other is the diagram where the current creates a NG boson that couples to an one particle vertex $\Gamma(k)$. The interaction term is given by

$$\mathcal{L} \supset -gV_\mu J^\mu, \tag{2.93}$$

where $J^\mu = (\partial^\mu \phi)\phi$. In the vacuum, $J^\mu = (\partial^\mu \phi)\langle\phi\rangle$, the relation linking the gauge current and the NG boson state is

$$\langle 0|J^\mu|\phi(k)\rangle = -i\langle\phi\rangle k^\mu. \tag{2.94}$$

The Ward-Takahashi identity, Eq. (2.92), can be written in terms of two one particle irreducible diagrams:

$$k_\mu \left(\Gamma^\mu(k) + ig\langle\phi\rangle k^\mu \frac{i}{k^2}\Gamma(k)\right) = 0. \tag{2.95}$$

By using the gauge boson mass relation, $m_V = g\langle\phi\rangle$, we find

$$\frac{k_\mu}{m_V}\Gamma^\mu(k) = \Gamma(k). \tag{2.96}$$

In the high energy region $\epsilon_L^\mu = \frac{k^\mu}{m_V}$; this means that the longitudinal mode of the massive gauge boson can be identified to by the NG boson.

We can reconfirm this fact at the field variable level. In the Ferynman-'t Hooft gauge the gauge constraint is

$$\partial_\mu V^\mu + im_V \phi = 0. \tag{2.97}$$

If we denote the longitudinal gauge boson as

$$V_L(k) = \epsilon_L^\mu(k) V_\mu(k), \tag{2.98}$$

we get

$$\begin{aligned} V_L(k) &= \frac{k^\mu}{m_V} V_\mu(k) + \mathcal{O}\left(\frac{m_V}{E}\right) \\ &= \phi(k) + \mathcal{O}\left(\frac{m_V}{E}\right), \end{aligned} \tag{2.99}$$

where we use the relation of the Eq. (2.97).

As an example we see the process where the Higgs boson decays into two longitudinal W bosons. The amplitude is

$$\begin{aligned} \mathcal{M}(h \to W_L^+ W_L^-) &= g m_W \epsilon_{+L\mu}^* \epsilon_{-L}^{*\mu} \\ &= \frac{g m_W}{2} \left(\frac{m_h^2}{m_W^2} - 2\right). \end{aligned} \tag{2.100}$$

Meanwhile, the Higgs self interaction, $\mathcal{L} \supset -\frac{m_h^2}{v} h \phi^+ \phi^-$, leads to the amplitude:

$$\mathcal{M}(h \to \phi^+ \phi^-) = \frac{m_h^2}{v} = \frac{g m_h^2}{2 m_W}. \tag{2.101}$$

This amplitude is identical to the Eq. (2.100) in the limit of $E(= m_h) \gg m_W$.

We consider an another example, $V_L V_L \to V_L V_L$, discussed before. In the case $a = b = 1$ and $c = d = 2$, the Eq. (2.74) becomes $\mathcal{M} \sim -2\lambda$ in the high energy region ($E \gg m_h$). On the other hand, NG four-point interaction, $\mathcal{L} \supset -\frac{\lambda}{2} \phi_1^2 \phi_2^2$, gives

$$\mathcal{M}(\phi_1 \phi_1 \to \phi_2 \phi_2) = -2\lambda. \tag{2.102}$$

This amplitude also agrees with the result computed using the longitudinal gauge boson in the high energy limit.

2.3.4 Higgs low energy theorem

We give a brief review of the Higgs low energy theorem [19] and its application.

First we consider the tree level coupling case. The Higgs interactions in the EW theory are

$$\mathcal{L} \supset -\left(1 + \frac{h}{v}\right) \sum_f m_f \bar{f} f - \left(1 + \frac{h}{v}\right)^2 \left(m_w^2 W^{+\mu} W_\mu^- + \frac{m_Z^2}{2} Z^\mu Z_\mu\right). \tag{2.103}$$

If we consider the constant Higgs field ($p_h = 0$), these interactions can be derived by redefining the mass parameters as

$$m_i \to m_i \left(1 + \frac{h}{v}\right). \tag{2.104}$$

This leads to the following expression of the Higgs low energy theorem:

$$\lim_{p_h=0} \mathcal{M}(Xh) = \sum_{i=f,V} \frac{1}{v} m_i \frac{\partial}{\partial m_i} \mathcal{M}(X), \tag{2.105}$$

where X is any particle configuration.

The interesting and useful point of this theorem is that we can apply to this theorem to the loop process. Now we give a sketch of the proof, taking the loop induced Higgs-gauge-gauge interaction as an example. Let us consider the renormalization group flow of the gauge coupling. If the beta function changes from b to δb at the threshold M, the gauge coupling can be expressed as

$$\frac{1}{g^2(\mu)} = \frac{1}{g^2(\Lambda)} + \frac{b}{8\pi^2} \log \frac{\Lambda}{\mu} + \frac{\delta b}{8\pi^2} \log \frac{\Lambda}{M}, \tag{2.106}$$

where M is a renormalization scale and Λ is a cut off scale. In this expression we denote δb as a coefficient of the beta function. We assume that threshold M has the Higgs field dependence:

$$\frac{1}{g^2(\mu, h(x))} = \frac{1}{g^2(\Lambda)} + \frac{b}{8\pi^2} \log \frac{\Lambda}{\mu} + \frac{\delta b}{8\pi^2} \log \frac{\Lambda}{M(h(x))}. \tag{2.107}$$

The gauge coupling depends on the space-time through the Higgs field. Subtracting the Eq. (2.106) from the Eq. (2.107), we get

$$\frac{1}{g^2(\mu, h(x))} - \frac{1}{g^2(\mu)} = -\frac{\delta b}{8\pi^2} \log \frac{M(h(x))}{M}. \tag{2.108}$$

Using this expression we can rewrite the gauge kinetic term $-\frac{1}{4g^2} V^a_{\mu\nu} V^{a\mu\nu}$ as

$$-\frac{1}{4g(\mu)^2} V^a_{\mu\nu} V^{a\mu\nu} + \frac{\delta b}{32\pi^2} \log M(h(x)) V^a_{\mu\nu} V^{a\mu\nu} + (M \text{ term}). \tag{2.109}$$

After the expansion of $h(x) \to v + h(x)$, the second term reads

$$\begin{aligned} \frac{\delta b}{32\pi^2} \log M(h(x)) V^a_{\mu\nu} V^{a\mu\nu} &\supset \frac{\delta b}{32\pi^2} \frac{h}{v} \frac{v}{M(v)} \frac{\partial M(v)}{\partial v} V^a_{\mu\nu} V^{a\mu\nu} \\ &= \frac{\delta b}{32\pi^2} \frac{h}{v} \frac{\partial \log M(v)}{\partial \log v} V^a_{\mu\nu} V^{a\mu\nu}. \end{aligned} \tag{2.110}$$

Then we can derive the loop induced Higgs coupling by reading the coefficient of the beta function. Although we provide the one-loop result, the Higgs low energy theorem is studied at two-loop level [20].

As an explicit application of the theorem, we show the hgg coupling induced by the top loop. After the wave function renormalization of the gauge field we get

$$-\frac{1}{4} V^a_{\mu\nu} V^{a\mu\nu} + \frac{g_s^2 \delta b}{32\pi^2} \frac{h}{v} \frac{\partial \log M(v)}{\partial \log v} G^a_{\mu\nu} G^{a\mu\nu}. \tag{2.111}$$

The coefficient of the beta function is

$$\delta b = \frac{4}{3} C(r), \tag{2.112}$$

where $C(r)$ is defined as $\mathrm{Tr}[t^a t^b] = C(r)\delta^{ab}$. In the case of the SM, $C(r) = \frac{1}{2}$ and $\frac{\partial \log M(v)}{\partial \log v} = 1$; then we obtain

$$\mathcal{L}_{hgg} = \frac{\alpha_s}{12\pi} \frac{h}{v} G^a_{\mu\nu} G^{a\mu\nu}. \tag{2.113}$$

This result becomes identical to the exact result in the limit of $\frac{m_t}{m_h} \to \infty$.

2.3.5 Fine tuning problem

Although the SM is the most successful theory ever, the theory is less than satisfactory in both experimental and theoretical points of view. One of the most important problem is the fine tuning of the Higgs boson mass parameter; the question is why the Higgs boson is so much lighter than the plank scale.

Unlike fermions and gauge bosons, the Higgs boson mass is not protected a symmetry, such as the chiral symmetry and the gauge symmetry. The Higgs boson mass is naively expected to be the planck scale, $m_{pl} \sim 10^{18}$ [GeV]. In fact, the quantum correction to the Higgs boson mass from the top quark is

$$\delta m_h^2 = -\frac{3y_t^2}{8\pi^2} \left(\Lambda^2 - 3m_t^2 \ln \left(\frac{\Lambda^2 + m_t^2}{m_t^2} \right) + \cdots \right), \tag{2.114}$$

where Λ is a cutoff scale (we naively expect $\Lambda \sim m_{pl}$). One can express the bare mass parameter as

$$m_{h,bare}^2 = m_{h,phys}^2 + \delta m_h^2. \tag{2.115}$$

In order to get $m_{h,pays}^2 = (126\,[\mathrm{GeV}])^2$, the nature has to finely adjust the Lagrangian parameter $m_{h,bare}^2$. This is an indication that within the SM m_h^2 is an unnatural parameter. The smallness of the Higgs boson mass cannot be explained in the SM; setting $m_h^2 = 0$ doesn't enhance the symmetry of the theory.

The measure of the fine tuning may be defined as

$$\Delta = \frac{2\delta m_h^2}{m_{h,phys}^2}. \tag{2.116}$$

The degree of the fine tuning is expressed by $\frac{100}{\Delta}[\%]$, and we naively expect $\Delta \leq 1$. In the SM case this requirements reads $\Lambda \leq 5 \times 10^2$ [GeV]. Note that definition of the measure is not unique, and the standard of naturalness is totally depending on the human sense.

Several models beyond the SM which solve the fine tuning problem are proposed. A supersymmetric model is one of the promising candidates. The quadratic divergence of the Higgs boson mass from a certain particle is cancelled by the contribution from a superpartner particle. In other words, the supersymmetry links fermions and bosons, which

means that the chiral symmetry is extended to the scalar sector. A composite Higgs model is another possibility. In this case the Higgs boson is realized as a NG boson arising from the spontaneous global symmetry breaking. An approximate global symmetry ensures the light Higgs boson. Some models, e.g. Little Higgs models, introduce the same spin particles for the cancellation of the one-loop quadratic divergence of the Higgs boson mass. In addition, models which extend the dimension of the space-time are also advocated. Note that even is the quadratic divergence is killed, the logarithmic term still remains and leads the little hierarchy problem [21]. It is becoming interesting to reconsider the degree of the fine tuning which is permissible in the nature and the question whether the fine tuning is a serious problem or not.

Perhaps our understanding of the fine tuning is wrong [22]. The uncomputable power divergences are removed by an unknown UV gravitational dynamics. If it is true we can discuss only the finite Higgs mass (presumably up to a logarithmic divergence). Such an idea is a good match for the model in which the EW symmetry breaking is due to the dimensional transmutation with an extended Higgs sector.

In any case the fine tuning problem is the important stepping stone to the physics beyond the SM.

3 Perturbative unitarity of Higgs derivative interactions

This chapter is based on the Ref. [23]. When we consider physics beyond the SM with extended Higgs sector, its low energy effective theory probably includes dimension six derivative interactions as a part of higher dimensional operators. These operators have two origins: expansion of kinetic terms if the Higgs doublet is realized as a part of pseudo NG field; integrating out heavy new scalar/vector bosons that interact with the Higgs field. The latter case appears even in models including elementary Higgs field.

If the Higgs boson were removed from the SM, the Higgs sector would be described by $SU(2)_L \times SU(2)_R/SU(2)_V$ nonlinear sigma model. Derivative interactions of NG fields emerge from the kinetic term. These interactions contribute to scattering among longitudinal massive gauge bosons through the equivalence theorem and cross sections of these processes become larger and larger as energy increases. They finally become so large as to violate the perturbative unitarity around 1[TeV] [4]. Of course, the recent observation of the Higgs boson told us the absence of the unitarity violation and validity of the SM description even much above the TeV scale. We confront the similar problem in studying derivative interactions of Higgs doublets. In this chapter, we examine the scales where the given perturbative description is available in several models that include derivative interactions of the Higgs doublets.

Before going to the detail, let us discuss the general form of the unitarity constraint. Considering the scattering amplitude which is linearly dependent on the Mandelstam vari-

ables. We can express the amplitude as

$$\mathcal{M} = \frac{C_s \hat{s} + C_t \hat{t}}{M^2} \tag{3.1}$$

$$= \frac{\hat{s}}{M^2} \left(\left(C_s - \frac{C_t}{2} \right) P_0 + \frac{C_t}{2} P_1 \right), \tag{3.2}$$

where $\hat{s}(\hat{t})$ is the Mandelstam variable and M is a typical new physics scale. The zeroth and the first modes of partial wave amplitudes appear:

$$M_0 = \frac{\hat{s}}{16\pi M^2} \left(C_s - \frac{C_t}{2} \right), \tag{3.3}$$

$$M_1 = \frac{\hat{s}}{16\pi M^2} \frac{C_t}{6}. \tag{3.4}$$

Eventually, the following conditions are respectively obtained,

$$\frac{\hat{s}}{M^2} \lesssim \frac{16\pi}{|2C_s - C_t|}, \tag{3.5}$$

$$\frac{\hat{s}}{M^2} \lesssim \frac{48\pi}{|C_t|}. \tag{3.6}$$

If the condition, $|C_t| \leq 3|C_s| \leq 2|C_t|$, is satisfied, the unitarity bound given by the first mode of the partial wave amplitude is stronger than that given by the zeroth mode.

3.1 Unitarity of derivative interactions on one Higgs doublet models

The perturbative unitarity bounds given by the derivative interaction are discussed on 1HDMs.

Firstly, we derive the formula of the unitarity bound and investigate its general properties. The formulae of the perturbative unitarity are shown before.

Then results are applied to explicit models. We study the unitarity bounds on two models: the minimal composite Higgs model [8] and the littlest Higgs model with T-parity [24]. The latter model has previously been studied in the Refs. [25, 26]. In the Ref. [26], several Little Higgs models are also investigated.[3] Since the normalization of decay constants can be changed, the combination $\frac{f^2}{c^H}$ is meaningful. Here, we follow the normalization given in the original papers. Decay constants have physical meanings through masses of additional massive vector bosons and fermions in each model. The Higgs doublet is embedded in such a way as to preserve the custodial symmetry in both models.

[3] They obtained the unitarity bounds with all NG bosons. However, we focus on the Higgs doublets because other NG bosons are too heavy to treat as massless particles. Our results are conservative compared to theirs.

3.1.1 Formulae and general properties of the unitarity bound

The effective Lagrangian of derivative interactions in 1HDM is[4]

$$\mathcal{L} \supset \frac{c^H}{2f^2}\partial(H^\dagger H)\partial(H^\dagger H) + \frac{c^T}{2f^2}(H^\dagger \overleftrightarrow{\partial} H)(H^\dagger \overleftrightarrow{\partial} H), \tag{3.7}$$

where f is a scale related to new physics and $H^\dagger \overleftrightarrow{\partial} H := H^\dagger(\partial H) - (\partial H)^\dagger H$. For the second operator, we replace the covariant derivatives with partial ones because in this paper we consider only longitudinal modes of the gauge bosons. Since the latter term violates the custodial symmetry, our analysis is based on the Lagrangian with $c^T = 0$.[5]

Since our focus is entirely on the four point scattering processes given by Eq. (3.7), the VEV of the Higgs boson plays no role in the following calculation. Therefore, we use

$$H = \begin{pmatrix} C^+ \\ N \end{pmatrix}, \qquad H^\dagger = \begin{pmatrix} C^- & N^\dagger \end{pmatrix}, \tag{3.8}$$

where $C^+(N)$ is a charged (complex-neutral) scalar field. The charged scalar and imaginary part of the neutral scalar are respectively eaten by $W^\pm$ and Z bosons. Using the above notation, the following amplitudes are obtained[6]:

$$\begin{aligned} \mathcal{M}(C^+C^- \to C^+C^-) =& \mathcal{M}(NN^\dagger \to NN^\dagger) \\ =& \frac{\hat{s}+\hat{t}}{f^2}c^H, \end{aligned} \tag{3.9}$$

$$\mathcal{M}(C^+C^- \to NN^\dagger) = \frac{\hat{s}}{f^2}c^H, \tag{3.10}$$

where $\hat{s}$ and $\hat{t}$ are the Mandelstam variables and we consider the energy scale where particles can be treated as massless, i.e. $\hat{s}+\hat{t}+\hat{u} = 0$.

Following the Ref. [4], we construct matrices with partial wave amplitudes. The largest eigenvalue of these matrices gives us the strongest bound to the perturbative unitarity. We

[4] Using the field redefinition $H \to H + \left(\frac{a}{f^2}\right)(H^\dagger H)H$, where a is chosen as an appropriate value, any other dimension-six derivative interaction of the Higgs doublet can be expressed with the kinds of operators given here [5].

[5] Since the remaining term, $\partial(H^\dagger H)\partial(H^\dagger H)$, changes the normalization of the Higgs field, in addition to the SM contributions, the oblique parameters receive $O\left(\frac{v^2}{f^2}\right)$ corrections. After eliminating tree-level corrections, models including additional heavy particles probably obtain the oblique corrections at the same order. They can be canceled with tuning parameters. The derivative interactions receive no sizable corrections from the tuning. Therefore, we consider only tree-level contributions to the oblique corrections.

[6] We neglect the effects of EW symmetry breaking because they are below the leading order around the unitarity violation scale. For example, the ratio of contributions generated by the SM and the demension-six derivative interactions in the 1HDMs is

$$\frac{(\text{SM})}{(\text{dim6})} = \frac{2m_h^2 f^2}{v^2 c^H \hat{s}} \sim \frac{1}{2c^H}\frac{f^2}{\hat{s}},$$

where we have assumed $\hat{s} \gg m_h^2$ and have used the result given by Eq. (3.11). As we will see later, the typical unitarity violation scale is a few times larger than the decay constant. Therefore, the above effects are small enough to be neglected.

have found that the zeroth mode gives the strongest bound in 1HDMs, so we focus on this case. With the formulae in the Subsec. 2.3.1, the strongest bound is given by the largest eigenvalue of the following matrix:

$$\begin{pmatrix} M_0(C^+C^- \to C^+C^-) & M_0(C^+C^- \to NN^\dagger) \\ M_0(NN^\dagger \to C^+C^-) & M_0(NN^\dagger \to NN^\dagger) \end{pmatrix} = \frac{\hat{s}}{16\pi f^2} \begin{pmatrix} \frac{c^H}{2} & c^H \\ c^H & \frac{c^H}{2} \end{pmatrix}. \tag{3.11}$$

The perturbative unitarity condition is therefore

$$\frac{\hat{s}}{f^2} \lesssim \frac{16\pi}{3c^H}. \tag{3.12}$$

Assuming that derivative interactions are purely given by the kinetic term of the nonlinear sigma model, the conservative cut-off scale is expressed in terms of the decay constant, i.e. $\Lambda \sim 4\pi f$.[7] Using the relation, the unitarity bound is related to the cut-off scale as

$$\frac{\hat{s}}{\Lambda^2} \sim \frac{1}{3\pi c^H}. \tag{3.13}$$

Therefore, if the relation

$$c^H \lesssim \frac{1}{3\pi} \tag{3.14}$$

is satisfied, models reach the cut-off scale before accessing the unitarity violation scale. Then, the effective Lagrangian, Eq. (3.7), is available up to the cut-off scale. On the other hand, if the coefficient c^H is much larger than unity, the unitarity violation scale is comparable to the scale of the new physics, f, so that the description of the effective Lagrangian is invalid even in the energy region around f. In the case c^H is $\mathcal{O}(1)$, the unitarity violation scale lies between the new physics scale and the cut-off. Most of examples shown later are involved in this case. Around the unitarity bound, we have to include resonance effects; see, for example, the Ref. [28]. It is therefore necessary to clarify the valid energy scale in the description for each model.

We apply the result to cross sections of the scattering of the Higgs boson and longitudinal modes of massive gauge bosons, so called vector boson scattering (VBS) processes, with the equivalence theorem. Since these energy scatterings are dominated by the coefficient, c^H, with the custodial symmetry, all of the cross sections are proportional to each other. Here we focus only on the process $W_L^+W_L^- \to hh$, and relations with the others are shown in the Tab. 1. Considering this sort of process, we must remember the importance of the central region[8] which is pointed out in the Ref. [29], so that we also show the ratios between the cross section of the Higgs pair production and those of the other processes with the central region cut. The cross section of $W_L^+W_L^- \to hh$ is

$$\sigma(W_L^+W_L^- \to hh) = \frac{\hat{s}}{32\pi}\left(\frac{c^H}{f^2}\right)^2 \lesssim \frac{8\pi}{9\hat{s}} \simeq \frac{1.1\times 10^6}{\hat{s}\,[\mathrm{TeV}]^2}[\mathrm{fb}]. \tag{3.15}$$

For this process, Fig. 7 shows the region where perturbative unitarity is violated.

[7] If UV completions are specified, the generalized dimensional analysis may introduce lower cut-off scales [27].

[8] This region is defined as $\cos\theta \in \left[-\frac{1}{2}, \frac{1}{2}\right]$ in detectors, where θ is an angle from the beam axis.

Process			Full	Central
$W_L^+W_L^-$	$\to$	hh	1	1/2
$W_L^+W_L^-$	$\to$	$W_L^+W_L^-$	2/3	13/48
$W_L^+W_L^-$	$\to$	Z_LZ_L	1	1/2
Z_LZ_L	$\to$	hh	1	1/2
Z_LZ_L	$\to$	$W_L^+W_L^-$	2	1
$W_L^+Z_L$	$\to$	$W_L^+Z_L$	2/3	13/48
$W_L^+W_L^+$	$\to$	$W_L^+W_L^+$	1	1/2

Table 1. Cross-sections of VBS processes in the units of $\sigma(W_L^+W_L^- \to hh)$. In the Full/Central column, the cross sections of VBS subprocesses with/without the central region cut are shown.

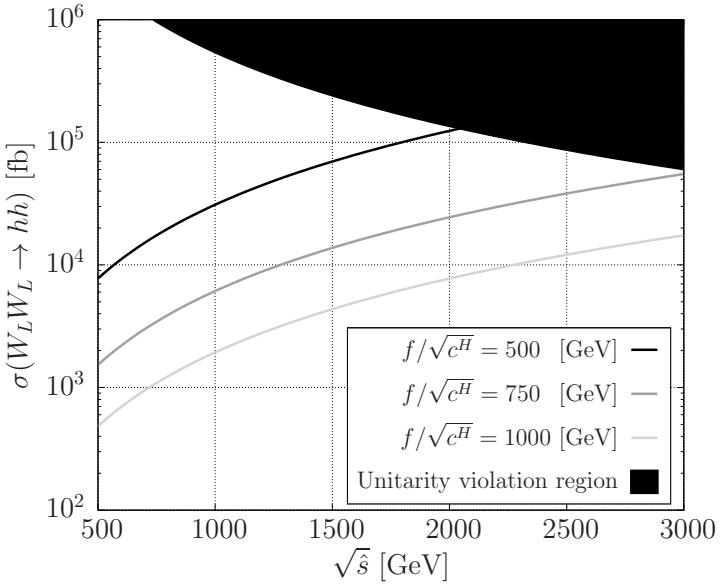

Figure 7. The upper bound of the cross section for $W_L^+W_L^- \to hh$ with the perturbative unitarity condition. The horizontal axis is the collision energy of this VBS subprocess. In the upper shaded region, the unitarity is broken down. The black, dark gray and light gray lines are the cross sections where $\frac{f}{\sqrt{c^H}} = 500, 750$, and 1000 [GeV], respectively. For the other processes, the bounds can be obtained with a shift of the vertical axis by the factors given in the Tab. 1.

Assuming that cross sections reach the above bound at $\sqrt{\hat{s}} = 3$ [TeV], we can obtain the relation:

$$\frac{f}{\sqrt{c^H}} \sim \sqrt{\frac{3\hat{s}}{16\pi}} \sim 733 \text{ [GeV]}. \tag{3.16}$$

If $c^H \sim 1$, the effect of the derivative interaction in the process is comparable to the SM background of about $\sqrt{\hat{s}} = 2$ [TeV], where the cross section is 3×10^4 [fb] without the central region cut; see the Ref. [29]. Note that the value of f is typically related to new particle masses. For example, in the little Higgs scenario [30], the top partner mass is given by $O(f)$. From the viewpoint of the fine tuning, f is required to be below about 1 [TeV].

3.1.2 The minimal composite Higgs model

This model is described by the $SO(5)/SO(4)$ nonlinear sigma model including four NG fields [8]. They are identified as the Higgs doublet.

The Lagrangian is

$$\mathcal{L} = \frac{f^2}{2} (\partial\Sigma)^\dagger (\partial\Sigma), \tag{3.17}$$

with

$$\Sigma = \begin{pmatrix} \sin[h/f]\ \vec{h}/h \\ \cos[h/f] \end{pmatrix}, \tag{3.18}$$

where $\vec{h}$ is the real scalar multiplet of four NG bosons and h is its norm. Expanding these trigonometric functions, we obtain

$$c^H = 1. \tag{3.19}$$

Using the Eq. (3.12), the relation between the decay constant and the energy scale of the unitarity violation is

$$\frac{\hat{s}}{f^2} \sim \frac{16\pi}{3}. \tag{3.20}$$

Assuming that perturbative unitarity is violated at 3 [TeV], the decay constant is about 750 [GeV]. On the other hand, if the decay constant is chosen as 500 [GeV], the perturbativity is preserved up to about 2 [TeV], where the cross section of $W_L^+ W_L^- \to hh$ is 7×10^5 [fb]. In this case, the cross section of the Higgs boson pair production is one order of magnitude larger than that given by the SM. However, it is challenging to observe this process because the main decay mode is $hh \to 4b$, which is overwhelmed by the QCD background.

3.1.3 The littlest Higgs model with T-parity

Derivative interactions on the littlest Higgs model with T-parity [24] are shown below. Scalar fields are described by the $SU(5)/SO(5)$ nonlinear sigma model which includes 14 NG bosons.

The kinetic term of this model is

$$\mathcal{L} = \frac{f^2}{8} \mathrm{tr} \left[\left(\partial e^{-2i\Pi/f} \right) \left(\partial e^{2i\Pi/f} \right) \right], \tag{3.21}$$

where Π is the NG field. The Higgs doublet is assigned in the NG field as

$$\Pi = \frac{1}{\sqrt{2}} \begin{pmatrix} & H & \\ H^\dagger & & H^T \\ & H^* & \end{pmatrix}. \tag{3.22}$$

We omitted the other NG bosons since they don't contribute to the current analysis. Extracting the derivative interaction from the kinetic term, we obtain

$$c^H = \frac{1}{2}. \tag{3.23}$$

This result is consistent with previous works [25, 26].

If we suppose that $f = 750$ [GeV], the perturbative unitarity is preserved up to about 4 [TeV]. Hence this model description is valid in higher energy scales while the signals of the derivative interaction are smaller than the previous model. For $f = 750$ [GeV], the cross section of $W_L^+ W_L^- \to hh$ in this model almost corresponds to the line where $\frac{f}{\sqrt{c^H}}$ is 1000 [GeV] in the Fig. 7.

3.2 Unitarity of derivative interactions on two Higgs doublet models

In this section we extend the previous discussion to dimension-six derivative interactions including two Higgs doublets.

The modification is straightforward, and the prescription is also simple. However, the formulae become too complex because of the many DOF. Then we cannot obtain the formula of the strongest bound like the Eq. (3.12) with the largest eigenvalue of a matrix that consists of partial wave amplitudes. Since the matrix can be diagonalized in individual models, three models are investigated as examples.

We study the consequences of the above result with several models including two Higgs doublets. The following three models are studied: the bestest little Higgs model [31]; the UV friendly T-parity little Higgs model [32]; and an inert doublet model. The first and second ones are composite Higgs models and the last one is a toy model including elementary Higgs doublets.

In this section, we consider processes whose initial states are electromagnetically neutral. Matrices giving the unitarity bounds for singly or doubly charged initial states are also shown in the App. B.

3.2.1 Formulae and general properties of the unitarity bound

The analyses in this section are based on the following effective Lagrangian:

$$\begin{aligned}
\mathcal{L} \supset & \frac{c^H_{1111}}{f^2} O^H_{1111} + \frac{c^H_{1112}}{f^2}(O^H_{1112} + O^H_{1121}) \\
& + \frac{c^H_{1122}}{f^2} O^H_{1122} + \frac{c^H_{1221}}{f^2} O^H_{1221} + \frac{c^H_{1212}}{f^2}(O^H_{1212} + O^H_{2121}) \\
& + \frac{c^H_{2221}}{f^2}(O^H_{2221} + O^H_{2212}) + \frac{c^H_{2222}}{f^2} O^H_{2222} \\
& + \frac{c^T_{1122}}{f^2} O^T_{1122} + \frac{c^T_{1221}}{f^2} O^T_{1221} + \frac{c^T_{1212}}{f^2}(O^T_{1212} + O^T_{2121}),
\end{aligned} \tag{3.24}$$

where

$$O^H_{ijkl} = \frac{1}{1+\delta_{ik}\delta_{jl}} \partial(H_i^\dagger H_j)\partial(H_k^\dagger H_l), \tag{3.25}$$

$$O^T_{ijkl} = \frac{1}{1+\delta_{ik}\delta_{jl}} (H_i^\dagger \overleftrightarrow{\partial} H_j)(H_k^\dagger \overleftrightarrow{\partial} H_l), \tag{3.26}$$

and

$$H_i = \begin{pmatrix} C_i^+ \\ N_i \end{pmatrix}, \qquad H_i^\dagger = \begin{pmatrix} C_i^- & N_i^\dagger \end{pmatrix}. \tag{3.27}$$

In the case where we study the custodial symmetric models, the above coefficients are real and follow the relation derived in the App. C:

$$3c^T_{1122} + c^H_{1221} - c^H_{1212} = 0, \tag{3.28}$$

$$c^T_{1122} + c^T_{1221} + c^T_{1212} = 0. \tag{3.29}$$

The 2HDMs require mixing angles to get mass eigenstates of scalar fields. In this paper, we use the equivalence theorem and focus on only derivative interactions, that is, masses of scalar fields are neglected. In this case, the perturbative unitarity bound is independent of mixing angles. This is also true for models including N Higgs doublets.

The unitarity bound is expressed as

$$\frac{\hat{s}}{f^2} \lesssim \frac{8\pi}{|C_{\max}|}, \tag{3.30}$$

where $C_{\max}$ is the largest eigenvalue of the matrices given in App. B.[9]

As we will see later, the largest eigenvalue $|C_{\max}|$ can be as large as about 10. In this case, the unitarity bound becomes quite strong and leads us to an interesting remark. Consider, for instance, the pair production of a heavy particle whose mass is $O(f)$ in VBS processes; the energy scale where the pair is produced could be as large as the unitarity violation scale. This means that we couldn't discuss this kind of process by means of these low-energy descriptions.

3.2.2 The bestest little Higgs model

The bestest little Higgs model [31] is a little Higgs model which includes two Higgs doublets. We obtain 15 NG fields that parametrize the $SO(6) \times SO(6)/SO(6)$ coset. The normalization of the kinetic term is the same as the Eq. (3.21), and the NG field is

$$\Pi = \frac{i}{\sqrt{2}} \begin{pmatrix} & h_1 & h_2 \\ -h_1^T & & \\ -h_2^T & & \end{pmatrix}, \tag{3.31}$$

[9] The Eq. (3.30) and the viewpoint explained below are also stated in the Ref. [26].

where $h_{1,2}$ are real scalar multiplets considered two Higgs doublets and the other NG bosons are eliminated. In this model, Higgs doublets interact with heavy gauge bosons and a singlet scalar. The masses of the heavy gauge bosons depend on the other decay constant that is larger than f in order to avoid the constraints from the EW precision measurement. Thus the effects coming from the heavy gauge bosons are tiny, and we neglect them. The interaction with a singlet is required to obtain a collective quartic coupling. For simplicity, we introduce the following terms to see the effect:

$$\mathcal{L}_\sigma \supset -\frac{m_\sigma^2}{2}\sigma^2 + \lambda f \sigma (H_1^\dagger H_2 + \text{H.c.}), \tag{3.32}$$

where σ is a neutral singlet scalar.[10] Including this contribution, the coefficients of the derivative interactions are

$$c^H_{1111} = \frac{1}{2}, \qquad c^H_{1112} = 0, \tag{3.33}$$

$$c^H_{1122} = 0, \qquad c^H_{1221} = \frac{1}{4} + c^\sigma, \qquad c^H_{1212} = \frac{1}{4} + c^\sigma, \tag{3.34}$$

$$c^H_{2221} = 0, \qquad c^H_{2222} = \frac{1}{2}, \tag{3.35}$$

$$c^T_{1122} = 0, \qquad c^T_{1221} = \frac{1}{4}, \qquad c^T_{1212} = -\frac{1}{4}, \tag{3.36}$$

where

$$c^\sigma = \frac{\lambda^2 f^4}{m_\sigma^4}. \tag{3.37}$$

The unitarity bound depends on the value of c^σ because the largest eigenvalue is a function of it. For $0 \leq c^\sigma < \frac{1}{8}$, the bound is

$$\frac{\hat{s}}{f^2} \lesssim \frac{16\pi}{2 - c^\sigma}. \tag{3.38}$$

For $c^\sigma = 0$, it is bounded as

$$\frac{\hat{s}}{f^2} \lesssim 8\pi, \tag{3.39}$$

and it becomes weak as c^σ increases. For $c^\sigma = \frac{1}{8}$, the bound is the weakest:

$$\frac{\hat{s}}{f^2} \lesssim 8\frac{16\pi}{15}. \tag{3.40}$$

In the region, $\frac{1}{8} < c^\sigma$, the bound is

$$\frac{\hat{s}}{f^2} \lesssim \frac{16\pi}{1 + 7c^\sigma}, \tag{3.41}$$

where the right-hand side decreases as c^σ increases and the bound becomes the same as the case of $c^\sigma = 0$ at $c^\sigma = \frac{1}{7}$.

[10] In the original paper [31], $m_\sigma = \sqrt{\lambda_{65} + \lambda_{56}}\, f$ and $\lambda = \frac{\lambda_{65} - \lambda_{56}}{\sqrt{2}}$.

The unitarity bounds for the cross sections of $W_L^+W_L^- \to hh$ and $W_L^+W_L^+ \to W_L^+W_L^+$ are displayed below. We define the mass eigenstates, h and $W_L^\pm$, as follows:

$$\frac{h}{\sqrt{2}} = N_1^R \cos\alpha + N_2^R \sin\alpha, \tag{3.42}$$

$$W_L^\pm = C_1^\pm \cos\beta + C_2^\pm \sin\beta, \tag{3.43}$$

where N_i^R is the real part of N_i and α and β are mixing angles. Unitarity bounds for these processes are

$$\sigma(W_L^+W_L^- \to hh) = \frac{\hat{s}}{32\pi f^4} B_h(\alpha,\beta)^2 \lesssim \frac{2\pi}{\hat{s}} \frac{B_h(\alpha,\beta)^2}{{C_{\max}}^2}, \tag{3.44}$$

$$\sigma(W_L^+W_L^+ \to W_L^+W_L^+) = \frac{\hat{s}}{32\pi f^4} B_w(\beta)^2 \lesssim \frac{2\pi}{\hat{s}} \frac{B_w(\beta)^2}{{C_{\max}}^2}, \tag{3.45}$$

where

$$B_h(\alpha,\beta) = \frac{1}{4}\left(1 + (1 + 2c^\sigma(1 - c_{4\beta}))c_{2(\alpha-\beta)} + 2c^\sigma s_{4\beta} s_{2(\alpha-\beta)}\right), \tag{3.46}$$

$$B_w(\beta) = \frac{1}{2}\left(1 + c^\sigma(1 - c_{4\beta})\right). \tag{3.47}$$

Here the parameters c_x and s_x are $\cos x$ and $\sin x$, and $C_{\max} = \frac{2-c^\sigma}{2}$ for $0 \le c^\sigma < \frac{1}{8}$ and $C_{\max} = \frac{1+7c^\sigma}{2}$ for $\frac{1}{8} \le c^\sigma$. If $\alpha = \beta$ is satisfied, the so-called decoupling limit, we get the relation: $B_h(\beta,\beta) = B_w(\beta)$.

The perturbative unitarity bounds of $W_L^+W_L^- \to hh$ are shown in the Fig. 8. In order to see the effects of the new parameters, we fix the decay constant to be 750 [GeV]. The shaded regions in these figures are changed in response to the mixing angles because the cross section depends on the angles. However, the unitarity bound itself depends only on the coefficient, c^σ. Hence we can see that the energy scales where each cross section line intersects the unitarity violation regions are independent of the angles, e.g. $\sqrt{\hat{s}} \sim 1.9$ [TeV] for $c^\sigma = 1$. For $\beta = 0$ and $\alpha - \beta = \frac{\pi}{6}$, the cross sections are independent of the value of c^σ; thus, we have only one line but still the intersecting points are the same.

3.2.3 The UV friendly little Higgs model

The UV friendly T-parity little Higgs model [32] also includes two Higgs doublets as a part of the 14 NG bosons given by the $SU(6)/Sp(6)$ nonlinear sigma model. The normalization of the kinetic term is also the same as the Eq. (3.21). This model possesses Z_2 symmetry, so-called T-parity, and one of the Higgs doublets is T-odd. This doublet has no VEV. Since we study only Higgs doublets, the NG field Π can be considered as follows:[11]

$$\Pi = \frac{1}{2}\begin{pmatrix} & -\epsilon(H_1 - H_2) & H_1 + H_2 & \\ \epsilon(H_1^\dagger - H_2^\dagger) & & & -H_1^T - H_2^T \\ H_1^\dagger + H_2^\dagger & & & \epsilon(H_1^T - H_2^T) \\ & -H_1^* - H_2^* & -\epsilon(H_1^* - H_2^*) & \end{pmatrix}, \tag{3.48}$$

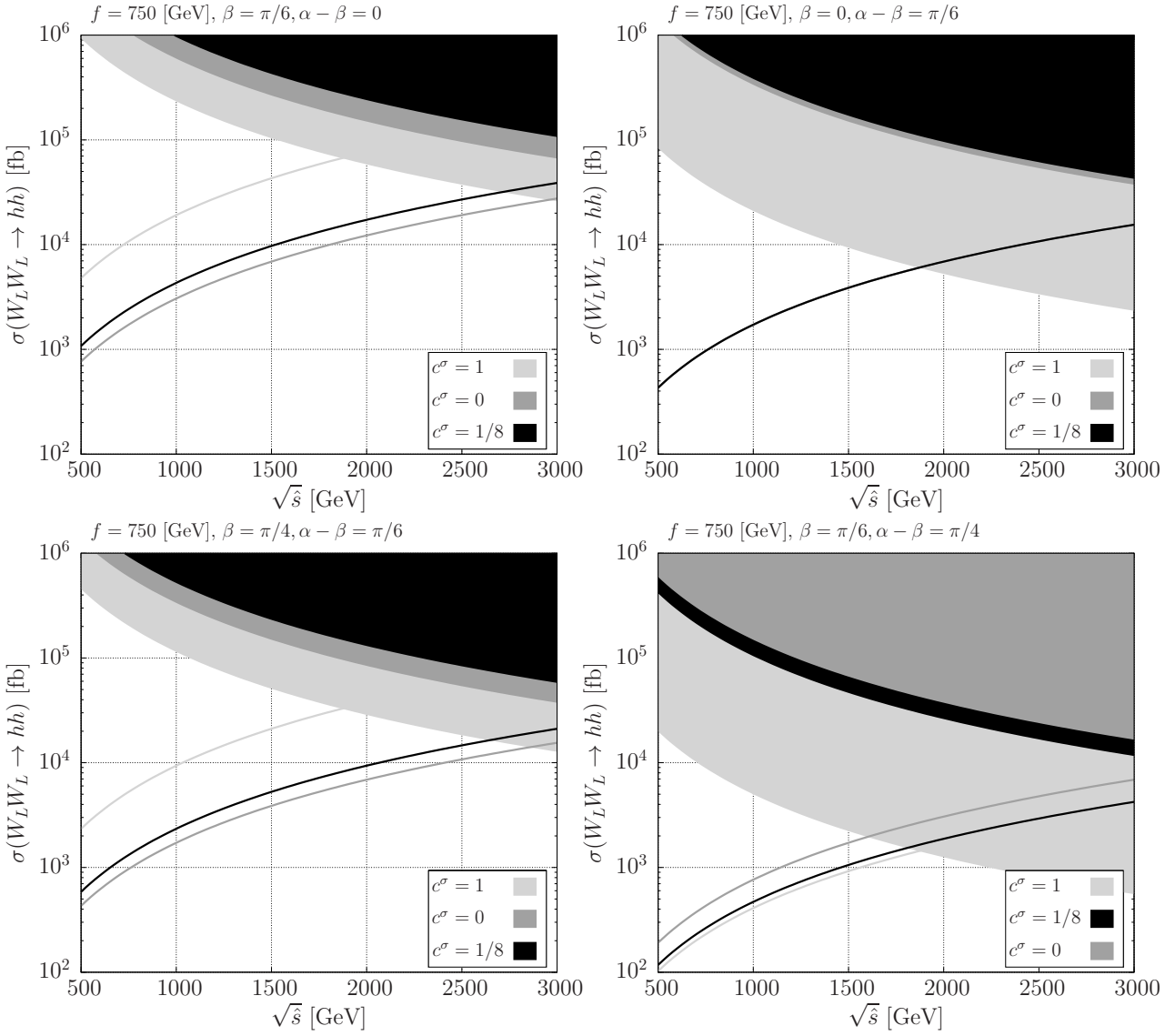

Figure 8. The perturbative unitarity bounds of $W_L^+ W_L^- \to hh$ for various c^σ and mixing angles. The decay constant is fixed to be 750 [GeV]. The mixing angles are set to be $(\beta, \alpha - \beta) = \left(\frac{\pi}{6}, 0\right)$ (upper left), $\left(0, \frac{\pi}{6}\right)$ (upper right), $\left(\frac{\pi}{4}, \frac{\pi}{6}\right)$ (lower left) and $\left(\frac{\pi}{6}, \frac{\pi}{4}\right)$ (lower right). The light gray, dark gray and black lines are cross sections for $c^\sigma = 1, 0$, and $\frac{1}{8}$, respectively. The unitarity violation regions depend on the value of c^σ, and their brightness corresponds to each line.

where ϵ is the totally antisymmetric tensor, $\epsilon^{12} = 1$. Since contributions of heavy new particles can be ignored in this model, derivative interactions are generated only by the

[11] Assignment and normalization of NG bosons given by the original paper are different from the ordinary prescription of the nonlinear sigma model. Since we study only the part of two Higgs doublets, normalization of these fields are changed in order to get the canonical kinetic term.

kinetic term. The coefficients of the derivative interactions are as follows:

$$c^H_{1111}=4, \qquad c^H_{1112}=0, \tag{3.49}$$

$$c^H_{1122}=1, \qquad c^H_{1221}=0, \qquad c^H_{1212}=-3, \tag{3.50}$$

$$c^H_{2221}=0, \qquad c^H_{2222}=4, \tag{3.51}$$

$$c^T_{1122}=1, \qquad c^T_{1221}=0, \qquad c^T_{1212}=1. \tag{3.52}$$

These coefficients apparently violate the custodial invariant conditions, the Eqs. (3.28) and (3.29). In this model only one of the Higgs doublets has the VEV, so that tree-level contributions to ρ parameter do not appear. With these coefficients, the strongest bound is

$$\frac{\hat{s}}{f^2} \lesssim \pi. \tag{3.53}$$

Assuming that perturbative unitarity is violated at 3 [TeV], the decay constant, f, is determined as 1.7 [TeV]. This value looks large from the viewpoint of fine tuning as we have already seen. On the other hand, if the decay constant is about 1 [TeV], the unitarity is broken below about 1.7 [TeV].

The unitarity bounds of $W^+_L W^-_L \to hh$ and $W^+_L W^+_L \to W^+_L W^+_L$ are

$$\sigma(W^+_L W^-_L \to hh) = \frac{\hat{s}}{2\pi f^4} \lesssim \frac{\pi}{2\hat{s}}, \tag{3.54}$$

$$\sigma(W^+_L W^+_L \to W^+_L W^+_L) = \frac{\hat{s}}{2\pi f^4} \lesssim \frac{\pi}{2\hat{s}}. \tag{3.55}$$

Note that the cross sections have no mixing angle dependence because only one of the Higgs doublet gets a VEV. These bounds to the cross sections are shown in the Fig. 9. They correspond to the case $c^\sigma = \frac{15}{7}$ for the bestest little Higgs model. The unitarity bound of this model is severe because the largest eigenvalue is much larger than the previous models.

3.2.4 Inert doublet models with odd scalars

We investigate the following Lagrangian consisting of elementary scalar and vector fields:

$$\begin{aligned}
\mathcal{L} \supset & -\frac{m^2_{s0}}{2}\phi_0^2 + \lambda_0 f \phi_0 \left(H_1^\dagger H_2 + \text{H.c.}\right) \\
& - \frac{m^2_{sL}}{2}\phi_L^a \phi_L^a + \lambda_L f \phi_L^a \left(H_1^\dagger \sigma^a H_2 + \text{H.c.}\right) \\
& - m^2_{sL}\phi_T^{a\dagger}\phi_T^a + \sqrt{2}\lambda_L f \left(\phi_T^{a\dagger}(H_1^T \sigma^2 \sigma^a H_2) + \text{H.c.}\right) \\
& + \frac{m^2_{v0}}{2} V_0 \cdot V_0 + g_0 V_0 \cdot \left(i H_1^\dagger \overleftrightarrow{\partial} H_2 + \text{H.c.}\right) \\
& + m^2_{v0} V_S^\dagger \cdot V_S + \sqrt{2} g_0 \left(i V_S^\dagger \cdot H_1^T \sigma^2 \overleftrightarrow{\partial} H_2 + \text{H.c.}\right) \\
& + \frac{m^2_{vL}}{2} V_L^a \cdot V_L^a + g_L V_L^a \cdot \left(i H_1^\dagger \sigma^a \overleftrightarrow{\partial} H_2 + \text{H.c.}\right).
\end{aligned} \tag{3.56}$$

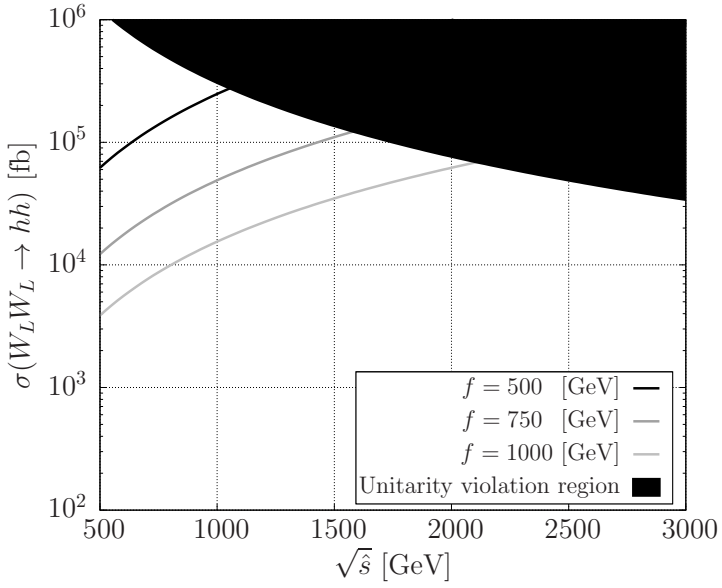

Figure 9. The perturbative unitarity bounds of $W_L^+ W_L^- \to hh$ in the UV friendly T-parity little Higgs model. The horizontal axis is the collision energy of this VBS subprocess. In the upper shaded region, unitarity is broken down. The black, dark gray and light gray lines are the cross sections corresponding to $f = 500, 750$, and 1000 [GeV], respectively.

Scalar fields ϕ_0, ϕ_L^a, and ϕ_T^a, are respectively $\mathbf{1}_0$, $\mathbf{3}_0$, and $\mathbf{3}_1$ representations of $SU(2)_L \times U(1)_Y$, and vector fields V_0, V_S, and V_L^a, are, respectively, $\mathbf{1}_0$, $\mathbf{1}_1$, and $\mathbf{3}_0$ representations. We suppose that these new particles and H_2 are odd under an additional Z_2 symmetry, and H_1 and the other SM particles are even under the discrete symmetry. We consider the case that only one of the Higgs doublets has a VEV, such as in the model in the Subsec. 3.2.3. These choices of couplings and masses for ϕ_L^a and ϕ_T^a, and V_0 and V_S are required to respect $SO(4)$ symmetry.[12] This set up suppresses contributions to the oblique corrections.

After integrating out heavy particles, we obtain the following coefficients of the derivative interactions:

$$c_{1111}^H = 0, \qquad c_{1112}^H = 0, \tag{3.57}$$

$$c_{1122}^H = -2s_L + 3v_0 + 3v_L, \quad c_{1221}^H = s_0 - 2s_L + 3v_0, \quad c_{1212}^H = s_0 - 2s_L + 3v_L, \tag{3.58}$$

$$c_{2221}^H = 0, \qquad c_{2222}^H = 0, \tag{3.59}$$

$$c_{1122}^T = -v_0 + v_L, \quad c_{1221}^T = -s_L - v_L, \quad c_{1212}^T = s_L + v_0, \tag{3.60}$$

[12] This structure should be broken by the renormalization group running of the couplings even if the UV completion possesses the structure. We assume that this $SO(4)$ symmetry is still good symmetry so as to suppress large corrections to the ρ parameter in the scale where the Lagrangian (3.56) is available.

where

$$s_0 = \left(\frac{\lambda_0 f^2}{m_{s0}^2}\right)^2, \qquad s_L = \left(\frac{\lambda_L f^2}{m_{sL}^2}\right)^2, \tag{3.61}$$

$$v_0 = \left(\frac{g_0 f}{m_{v0}}\right)^2, \qquad v_L = \left(\frac{g_L f}{m_{vL}}\right)^2. \tag{3.62}$$

Even if additional particles exist, their contributions are included in these four coefficients. We cannot discriminate these multiple contributions from a large contribution of a particle with a large coupling. Using these coefficients, the eigenvalues of the Eq. (B.1) are fortunately obtained as the following simple forms:

$$c_1^I = -\frac{s_0 - 7s_L + 3v_0 + 3v_L}{2}, \tag{3.63}$$

$$c_2^I = \frac{7s_0 - 9s_L + 9v_0 + 9v_L}{2}, \tag{3.64}$$

$$c_3^I = \frac{s_0 - 3s_L + 3v_0 - 9v_L}{2}, \tag{3.65}$$

$$c_4^I = \frac{s_0 - 3s_L - 9v_0 + 3v_L}{2}, \tag{3.66}$$

$$c_{5\pm}^I = \pm\frac{s_0 + s_L + 3v_0 + 3v_L}{2}, \tag{3.67}$$

$$c_{6\pm}^I = \pm\frac{s_0 + 9s_L - 9v_0 - 9v_L}{2}. \tag{3.68}$$

The strongest unitarity condition is given by the Eq. (3.30) with the largest eigenvalue in the above.

Derivative interactions generated by integrating out T-odd heavy particles must include two H_1 and two H_2, as in the Eqs. (3.58) and (3.60). Furthermore there are no mixing angles in the Higgs doublets because only one of the Higgs doublets has a VEV. They are the reason why cross sections of $W_L^+W_L^- \to hh$ and $W_L^+W_L^- \to W_L^+W_L^-$ vanish.

In this model we have four coefficients the Eqs. (3.61) and (3.62) to parametrize the dimension-six differential operators. If we suppose that $s_0 = s_L = v_0 = v_L = 1$, the eigenvalue c_2^I becomes the largest: $c_2^I = 8$. This value gives us a perturbative unitarity condition which is the same as the Eq. (3.53).

The unitarity bound, the Eq. (3.30), can be interpreted as the perturbativity condition of couplings. For example, if $s_0 = s_L = v_0 = 0$ and $v_L \neq 0$, we get $|C_{\max}| = \frac{9v_L}{2}$. Then the unitarity bound is

$$\sqrt{\hat{s}} \sim \frac{4\sqrt{\pi}}{3}\frac{m_{vL}}{g_L}. \tag{3.69}$$

In order to preserve unitarity, the unitarity violation scale should be larger than the mass, m_{vL}. As a result, we get the following condition:

$$g_L \lesssim \frac{4\sqrt{\pi}}{3}. \tag{3.70}$$

If the model includes only one $\mathbf{3_0}$ vector, this requirement is stronger than the naive perturbativity condition $g_L < 4\pi$. On the other hand, if it includes several $\mathbf{3_0}$ vectors, the

unitarity bound also limits how many there are.

3.3 Conclusions

We have studied perturbative unitarity for dimension-six derivative interactions of the Higgs doublets. They are generated by kinetic terms in composite Higgs models, or by integrating out heavy particles that interact with the Higgs doublets. The latter case means that derivative interactions appear even in models consisting of elementary Higgs doublets.

We first studied the unitarity bounds in models including only one Higgs doublet. The strongest bounds are expressed by the largest eigenvalue of the matrix given by partial wave amplitudes of VBS processes. We focused on the high-energy region such that derivative interactions could dominate the contributions to the scattering among longitudinal vector bosons. Assuming that the given derivative interactions respect the EW constraints, only a combination of parameters $\frac{c^H}{f^2}$ appears in the analysis. Therefore, the unitarity condition is expressed by the parameter as Eq. (3.12). We have applied it to the cross section of $W_L W_L \to hh$.

We have calculated the bounds on explicit models: the minimal composite Higgs model, the littlest Higgs model. Their structures of global symmetry are significantly different from each other; $SO(5)/SO(4)$ and $SU(5)/SO(5)$. However, the given bounds are similar; $c^H = 1$ and $\frac{1}{2}$. The decay constants f are related to the masses of the top like fermions in composite Higgs models. It is therefore supposed that $\frac{f}{\sqrt{c^H}}$ is larger than about 500 GeV; see e.g. the Ref. [33], where the perturbative unitarity is violated above the region $\sqrt{\hat{s}} \gtrsim 2$ TeV. Even in this case, it is difficult to obtain cross sections large enough to distinguish new physics contributions from the SM ones.

Secondly, similar analyses have been performed in 2HDMs. A simple formula for the unitarity bound could not be obtained in terms of parameters included in the effective Lagrangian (3.24) since the matrix of partial wave amplitudes is too complex to be diagonalized. Hence we have investigated the unitarity bound with explicit models: the bestest little Higgs model; the UV friendly T-parity little Higgs model; and the inert doublet model with heavy Z_2 odd particles. The first and the second ones are literally a kind of little Higgs model and the third one is a toy model including elementary Higgs doublets.

In the first one, derivative interactions are generated not only by the kinetic term but also by the integrating out of a heavy scalar field. The constraints of the former to the unitarity are similar to those given by the 1HDMs discussed in the Sec. 3.1. Including the latter one, the largest eigenvalue depends on the scalar contribution. The unitarity bound can be stronger than the case not including it.

In the second model, the unitarity condition is much more severe compared to the other models mentioned in this paper. This is because the coefficients of the derivative interactions are large in this model. Therefore the unitarity is violated at a low scale compared with the other models. In this kind of model, large coefficients can produce large cross sections which are large enough to exceed the SM background. On the other hand, assuming that the masses of additional particles are near the decay constant, they are

also near the scale of the unitarity violation. Therefore, contributions of vector resonances probably need to be considered when people investigate, for instance, pair productions of these additional particles with vector boson collisions.

In the last model that includes an elementary Higgs doublet, VBS processes of the SM particles are suppressed as we have shown. In this kind of model, the masses of heavy particles should be smaller than the unitarity violation scale. This condition means that couplings between Higgs doublets and heavy particles are much smaller than the strong coupling, 4π, or the number of these particles is limited.

We have clarified the importance of studying the unitarity bound when Higgs derivative interactions are investigated because the bound can be significantly lower than the naive cut-off scale. We could observe the energy-growing behavior of VBS processes at the future collider experiments [29, 34].

4 Higgs couplings beyond the Standard Model

In this chapter we study the Higgs couplings for some models. After the discovery of the Higgs boson, the precise measurement of the Higgs couplings is growing in importance and necessity. If we observe the deviation from the SM, it is a solid evidence of the physics beyond the SM. Such an indirect search of new physics is complementary to the direct search, and this kind of search is quite powerful due to the high sensitivity of the Higgs coupling measurements at the future collider experiments.

Many models beyond the SM predict non-SM Higgs couplings in various ways. In order to discriminate these models, the measurement of a specific coupling is not enough because a new physics theory can possibly explain the coupling by choosing model parameters; hence we need to study correlations among the Higgs couplings and compare them with those of other models. In this thesis we study the three models: the minimal composite Higgs model (MCHM); the Randall-Sundrum (RS) model; the extra singlet Higgs model. The MCHM is the model with the minimal realization of the composite Higgs which is based on a strongly interacting field theory. The RS model is the model with an extra dimension which is considered to be related to a strongly coupled conformal theory through the duality. The extra singlet Higgs model is the minimal extension of the Higgs sector in the SM.

In particular, we focus on the MCHM because the Higgs couplings of this model has not studied comprehensively. From the experimental perspective we examine the following (effective) couplings: hVV, hbb, hgg, $h\gamma\gamma$ and $hZ\gamma$. We first calculate the decay widths of the Higgs boson. Then we define the deviation of the Higgs couplings using them and show the differences among the models. We clarify how we can discriminate the models at the future collider experiments using the correlations of the coupling deviations.

4.1 The minimal composite Higgs model

The MCHM is the model based on the $SO(5)/SO(4)$ symmetry breaking which was originally introduced in the context of 5D theories [8]. This symmetry breaking gives four NG

fields which form a fundamental representation of $SO(4)$ or equivalently a bi-doublet of $SU(2)_L \times SU(2)_R$; these fields are identified as the Higgs fields. This symmetry breaking pattern is the minimal realization including the custodial symmetry. In order to reproduce the fermion quantum numbers an additional local symmetry $U(1)_X$ is introduced, leading to the symmetry breaking pattern $SO(5) \times U(1)_X / SO(4) \times U(1)_X$. The SM EW gauge symmetry $SU(2)_L \times U(1)_Y$ is embedded into $SO(4) \times U(1)_X$ and the hypercharge is defined by $Y = T_R^3 + X$ [8, 35].

The SM fermion is realized by mixing the elementary fermion whose quantum number is the same as the SM one with the composite fermions, so-called the partial compositeness, and there are various possibilities to introduce the composite fermions. The most simplest choice is to introduce a spinorial representation of $SO(5)$. However, this choice leads to the large correction to the $Zb_L\bar{b}_L$ coupling at tree level; the experimental constraint leaves no allowed parameter space [36]. The $Zb_L\bar{b}_L$ constraint can be relaxed if the composite fermions are fundamental or antisymmetric representations of $SO(5)$; in this case a subgroup of the custodial symmetry $O(3) \subset O(4)$ protects the $Zb_L\bar{b}_L$ coupling [37]. In this thesis we focus on the case where a single vector-like fermion whose representation is **5** of $SO(5)$, which is called MCHM5.

4.1.1 The Lagrangian

We decompose the Lagrangian of the MCHM5 into three parts:

$$\mathcal{L} \supset \mathcal{L}_{Hkin} + \mathcal{L}_{Fkin} + \mathcal{L}_{Yukawa+Mass}. \tag{4.1}$$

Here we don't care about the Higgs potential and gauge kinetic terms which are assumed to be unchanged from those of the SM.

First we construct the Higgs kinetic term. Before proceeding, we define the basis for the algebra of $SO(5)$ that is used throughout in this thesis. We use the following explicit expressions of the $SO(4) \simeq SU(2)_L \times SU(2)_R$ and $SO(5)/SO(4)$ generators:

$$T^a_{L,ij} = -\frac{i}{2}\left(\frac{1}{2}\epsilon^{abc}(\delta^b_i\delta^c_j - \delta^b_j\delta^c_i) + (\delta^a_i\delta^4_j - \delta^a_j\delta^4_i)\right), \tag{4.2}$$

$$T^a_{R,ij} = -\frac{i}{2}\left(\frac{1}{2}\epsilon^{abc}(\delta^b_i\delta^c_j - \delta^b_j\delta^c_i) - (\delta^a_i\delta^4_j - \delta^a_j\delta^4_i)\right), \tag{4.3}$$

$$T^{\hat{a}}_{L,ij} = -\frac{i}{\sqrt{2}}(\delta^{\hat{a}}_i\delta^5_j - \delta^{\hat{a}}_j\delta^5_i), \tag{4.4}$$

where $a = 1, 2, 3$, $\hat{a} = 1, \ldots, 4$ and $i, j = 1, \ldots, 5$. Now we introduce the following notations and parametrization of the NG fields:

$$\Sigma = \Sigma_0 e^{\Pi/f}, \quad \Pi = -i\sqrt{2}T^{\hat{a}}h^{\hat{a}}, \quad \Sigma_0 = (0, 0, 0, 0, 1), \tag{4.5}$$

where f is the decay constant and $h^{\hat{a}}$ are the four real NG fields that are identified as the Higgs fields. Using the explicit expressions we obtain

$$\Sigma = \frac{\sin(\tilde{h}/f)}{\tilde{h}}(h_1, \quad h_2, \quad h_3, \quad h_4, \quad \tilde{h}\cot(\tilde{h}/f)), \tag{4.6}$$

where we define $\tilde{h} = \sqrt{\sum_{\hat{a}} h_{\hat{a}}^2}$. The kinetic term is then given by

$$\mathcal{L}_{Hkin} = \frac{f^2}{2}(D_\mu \Sigma)(D^\mu \Sigma)^T, \qquad D_\mu \Sigma = \partial_\mu \Sigma + igW_\mu^a \Sigma T_L^a + ig' B_\mu \Sigma T_R^3. \tag{4.7}$$

It is possible to perform an $SO(4)$ rotation to align the Higgs VEV to the h_3 direction. We denote $h_3 = H = \langle H \rangle + h$, and in the unitary gauge we get

$$\Sigma = \Sigma_0 \begin{pmatrix} 1 & & & & \\ & 1 & & & \\ & & \cos(H/f) & & -\sin(H/f) \\ & & & 1 & \\ & & \sin(H/f) & & \cos(H/f) \end{pmatrix} \tag{4.8}$$

$$= \Sigma_0 \Omega \tag{4.9}$$

$$= (0, \quad 0, \quad \sin(H/f), \quad 0, \quad \cos(H/f)). \tag{4.10}$$

The Higgs kinetic term in terms of H is therefore

$$\mathcal{L}_{Hkin} = \frac{1}{2}\partial_\mu H \partial^\mu H + \frac{g^2 f^2}{4} \sin\left(\frac{H}{f}\right)\left(W_\mu^+ W^{-\mu} + \frac{1}{2\cos^2\theta_W} Z_\mu Z^\mu\right), \tag{4.11}$$

where the VEV is given by $f^2 \sin^2(\langle H \rangle / f) = v^2 = (246\,[\mathrm{GeV}])^2$.

Next we build the fermion kinetic term. In order to describe the SM fermion using the partial compositeness, we introduce vector-like fermions which have quantum numbers such that they can mix with the fundamental fermions $q_L = (t_L, b_L)^T$ and t_R. The composite fermion transforming as $\mathbf{5_{2/3}}$ under $SO(5) \times U(1)_X$ is written as

$$\Psi = \frac{1}{\sqrt{2}} \begin{pmatrix} B - X \\ i(B + X) \\ T + U \\ i(T - U) \\ \sqrt{2}\tilde{T} \end{pmatrix}. \tag{4.12}$$

Under $SU(2)_L \times SU(2)_R$, a $\mathbf{5}$ of $SO(5)$ decomposes into $\mathbf{5} \sim (\mathbf{2},\mathbf{2}) \oplus (\mathbf{1},\mathbf{1})$. The quantum numbers of the composite fields are summarized in the Tab. 2.

The $SU(2)_L$ doublet $Q = (T, B)^T$ have the same quantum number as q_L, whereas $\tilde{T}$ has the same one as t_R. The Lagrangian of the fermion kinetic term is

$$\mathcal{L}_{Fkin} = i\bar{q}_L \not{D} q_L + i\bar{t}_R \not{D} t_R + i\bar{b}_R \not{D} b_R + i\bar{\Psi}_L \not{D} \Psi_L + i\bar{\Psi}_R \not{D} \Psi_R, \tag{4.13}$$

where the covariant derivative acting on each fermion is given by

$$D_\mu q_L = \left[\partial_\mu - ig\frac{\sigma^a}{2} W_\mu^a - ig'\frac{1}{6} B_\mu\right] q_L, \tag{4.14}$$

$$D_\mu t_R = \left[\partial_\mu - ig'\frac{2}{3} B_\mu\right] t_R, \tag{4.15}$$

$$D_\mu b_R = \left[\partial_\mu - ig'\left(\frac{-1}{3}\right) B_\mu\right] b_R, \tag{4.16}$$

$$D_\mu \Psi_{L(R)} = \left[\partial_\mu - igW_\mu^a T_L^a - ig' B_\mu (T_R^3 + X)\right] \Psi_{L(R)}, \tag{4.17}$$

field	T_L^3	T_R^3	X	$Y = T_R^3 + X$	$Q_{EM} = T_L^3 + Y$
X	$1/2$	$1/2$	$2/3$	$7/6$	$5/3$
U	$-1/2$	$1/2$	$2/3$	$7/6$	$2/3$
T	$1/2$	$-1/2$	$2/3$	$1/6$	$2/3$
$\tilde{T}$	0	0	$2/3$	$2/3$	$2/3$
B	$-1/2$	$-1/2$	$2/3$	$1/6$	$-1/3$

Table 2. The quantum numbers of the composite fermions in Ψ. Note that $((X,U)^T,(T,B)^T)$ forms a bi-doublet $(\mathbf{2},\mathbf{2})$ under $SU(2)_L \times SU(2)_R$.

where σ^a are the Pauli matrices, and $U(1)_X$ generator is introduced as $X = \frac{2}{3}\mathbb{I}_{5\times 5}$.

Finally we construct the yukawa and mass terms:

$$\mathcal{L}_{Yukawa+Mass} = -Yf(\bar{\Psi}_L\Sigma^T)(\Sigma\Psi_R) - M\bar{\Psi}_L\Psi_R - \Delta_L\bar{q}_L Q_R - \Delta_R\bar{\tilde{T}}_L t_R + (\text{h.c.}). \quad (4.18)$$

The first term is (proto) yukawa interaction which produces the interaction between the Higgs boson and the composite fermions. The second term is the vector mass of the composite fermions. The third and fourth term is the mixing of the composite sector and the fundamental sector, which is the key factor of the partial compositeness. In this set up, the lightest bottom quark is still massless; hence we add the small breaking term of the partial compositeness:

$$-\mathcal{L}_b = y_b\bar{q}_L H b_R + (\text{h.c.}). \quad (4.19)$$

This term gives the mass term to the fundamental b quark. We expect the coefficient y_b is much smaller than unity. Including this breaking term into the theory we get the mass terms in the vacuum of the Higgs field as

$$-\mathcal{L}_m = \bar{\psi}_{tL}\mathcal{M}_t\psi_{tR} + \bar{\psi}_{bL}\mathcal{M}_b\psi_{bR} + (\text{h.c.}), \quad (4.20)$$

where we introduce the following notations:

$$\psi_t = (t,\ T,\ U,\ \tilde{T})^T, \quad (4.21)$$

$$\psi_b = (b,\ B)^T, \quad (4.22)$$

$$\mathcal{M}_t = \begin{pmatrix} 0 & \Delta_L & 0 & 0 \\ 0 & M + \frac{Yfs^2}{2} & \frac{Yfs^2}{2} & \frac{Yfsc}{\sqrt{2}} \\ 0 & \frac{Yfs^2}{2} & M + \frac{Yfs^2}{2} & \frac{Yfsc}{\sqrt{2}} \\ \Delta_R & \frac{Yfsc}{\sqrt{2}} & \frac{Yfsc}{\sqrt{2}} & M + Yfc^2 \end{pmatrix}, \quad (4.23)$$

$$\mathcal{M}_b = \begin{pmatrix} \frac{y_b\langle H\rangle}{\sqrt{2}} & \Delta_L \\ 0 & M \end{pmatrix}, \quad (4.24)$$

with the definition $s = \sin(\langle H\rangle/f) = v/f$ and $c = \cos(\langle H\rangle/f)$. Note that in the $v \to 0$ limit (no EW symmetry breaking) the lightest top and bottom quarks become massless. For

$v = 0$, we can analytically diagonalize these mass matrices using the following orthogonal transformations:

$$\begin{pmatrix} q_L \\ Q_L \end{pmatrix} = \begin{pmatrix} \cos\phi_L & -\sin\phi_L \\ \sin\phi_L & \cos\phi_L \end{pmatrix} \begin{pmatrix} q_{L,m} \\ Q_{L,m} \end{pmatrix}, \quad \tan\phi_L = \frac{\Delta_L}{M}, \tag{4.25}$$

$$\begin{pmatrix} t_R \\ \tilde{T}_R \end{pmatrix} = \begin{pmatrix} \cos\phi_R & -\sin\phi_R \\ \sin\phi_R & \cos\phi_R \end{pmatrix} \begin{pmatrix} t_{R,m} \\ \tilde{T}_{R,m} \end{pmatrix}, \quad \tan\phi_R = \frac{\Delta_R}{M + Yf}, \tag{4.26}$$

where the subscript m denotes the mass eigenstate. The mass eigenvalues of the composite states are

$$M_Q = \frac{M}{\cos\phi_L}, \tag{4.27}$$

$$M_X = M, \tag{4.28}$$

$$M_{\tilde{T}} = \frac{M + Yf}{\cos\phi_R}. \tag{4.29}$$

When turning on the Higgs VEV, we need to diagonalize the mass matrices by performing the SVD numerically. Before going to the mass eigenbasis we introduce the interaction matrix as follows:

$$\begin{aligned} \mathcal{L} \supset\ & \bar{\psi}_t \gamma^\mu \left(\frac{2|e|}{3}\right) \mathbb{I}_{4\times4} \psi_t A_\mu + \bar{\psi}_b \gamma^\mu \left(\frac{-|e|}{3}\right) \mathbb{I}_{2\times2} \psi_b A_\mu + \bar{\psi}_X \gamma^\mu \left(\frac{5|e|}{3}\right) \psi_X A_\mu \\ & + \bar{\psi}_t \gamma^\mu (\mathcal{C}_L^t P_L + \mathcal{C}_R^t P_R) \psi_b W_\mu^+ + \bar{\psi}_X \gamma^\mu (\mathcal{C}_L^X P_L + \mathcal{C}_R^X P_R) \psi_t W_\mu^+ + (\text{h.c.}) \\ & + \bar{\psi}_a \gamma^\mu (\mathcal{N}_L^a P_L + \mathcal{N}_R^a P_R) \psi_a Z_\mu - \bar{\psi}_a (\mathcal{Y}_L^a P_L + \mathcal{Y}_R^a P_R) \psi_a h \\ & + g_{hWW} h W_\mu^+ W^{-\mu} + g_{hZZ} h \frac{Z_\mu Z^\mu}{2}, \end{aligned} \tag{4.30}$$

where $a = t, b, X$. For the latter convenience we rewrite the Lagrangian of the fermion-massive gauge bosons interaction terms as follows:

$$\mathcal{L}_W = \frac{g}{\sqrt{2}} \bar{\psi}_t \gamma^\mu (\tilde{\mathcal{C}}_L^t P_L + \tilde{\mathcal{C}}_R^t P_R) \psi_b W_\mu^+ + \frac{g}{\sqrt{2}} \bar{\psi}_X \gamma^\mu (\tilde{\mathcal{C}}_L^X P_L + \tilde{\mathcal{C}}_R^X P_R) \psi_t W_\mu^+ + (\text{h.c.}), \tag{4.31}$$

$$\mathcal{L}_Z = \frac{g}{2\cos\theta_W} \bar{\psi}_a \gamma^\mu (\tilde{\mathcal{N}}_L^a P_L + \tilde{\mathcal{N}}_R^a P_R - 2\sin^2\theta_W Q_a) \psi_a Z_\mu. \tag{4.32}$$

In this expression the Q_a reads the product of the corresponding electric charge and the

unit matrix. The interaction matrices are defined as follows:

$$\mathcal{C}_L^t = \begin{pmatrix} \frac{g}{\sqrt{2}} & 0 \\ 0 & \frac{g}{\sqrt{2}} \\ 0 & 0 \\ 0 & 0 \end{pmatrix}, \quad \mathcal{C}_R^t = \begin{pmatrix} 0 & 0 \\ 0 & \frac{g}{\sqrt{2}} \\ 0 & 0 \\ 0 & 0 \end{pmatrix}, \tag{4.33}$$

$$\mathcal{C}_{L,R}^X = \begin{pmatrix} 0 & 0 & \frac{g}{\sqrt{2}} & 0 \end{pmatrix}, \tag{4.34}$$

$$\mathcal{N}_L^t = \begin{pmatrix} \frac{g}{2c_W} - \frac{2gs_W^2}{3c_W} & 0 & 0 & 0 \\ 0 & \frac{g}{2c_W} - \frac{2gs_W^2}{3c_W} & 0 & 0 \\ 0 & 0 & -\frac{g}{2c_W} - \frac{2gs_W^2}{3c_W} & 0 \\ 0 & 0 & 0 & -\frac{2gs_W^2}{3c_W} \end{pmatrix}, \tag{4.35}$$

$$\mathcal{N}_R^t = \begin{pmatrix} -\frac{2gs_W^2}{3c_W} & 0 & 0 & 0 \\ 0 & \frac{g}{2c_W} - \frac{2gs_W^2}{3c_W} & 0 & 0 \\ 0 & 0 & -\frac{g}{2c_W} - \frac{2gs_W^2}{3c_W} & 0 \\ 0 & 0 & 0 & -\frac{2gs_W^2}{3c_W} \end{pmatrix}, \tag{4.36}$$

$$\mathcal{N}_L^b = \begin{pmatrix} -\frac{g}{2c_W} + \frac{gs_W^2}{3c_W} & 0 \\ 0 & -\frac{g}{2c_W} + \frac{gs_W^2}{3c_W} \end{pmatrix}, \tag{4.37}$$

$$\mathcal{N}_R^b = \begin{pmatrix} \frac{gs_W^2}{3c_W} & 0 \\ 0 & -\frac{g}{2c_W} + \frac{gs_W^2}{3c_W} \end{pmatrix}, \tag{4.38}$$

$$\mathcal{N}_{L,R}^X = \frac{g}{2c_W} - \frac{5gs_W^2}{3c_W} \tag{4.39}$$

$$\mathcal{Y}_{L,R}^t = \begin{pmatrix} 0 & 0 & 0 & 0 \\ 0 & sc & sc & \frac{1-2s^2}{\sqrt{2}} \\ 0 & sc & sc & \frac{1-2s^2}{\sqrt{2}} \\ 0 & \frac{1-2s^2}{\sqrt{2}} & \frac{1-2s^2}{\sqrt{2}} & -2sc \end{pmatrix}, \tag{4.40}$$

$$\mathcal{Y}_{L,R}^b = \begin{pmatrix} \frac{y_b}{2} & 0 \\ 0 & 0 \end{pmatrix}, \tag{4.41}$$

$$\mathcal{Y}_{L,R}^X = 0, \tag{4.42}$$

$$g_{hWW} = \frac{2m_W^2}{v}\sqrt{1 - \frac{v^2}{f^2}}, \tag{4.43}$$

$$g_{hZZ} = \frac{2m_Z^2}{v}\sqrt{1 - \frac{v^2}{f^2}}, \tag{4.44}$$

where we introduce the notation $s_W(c_W)$ as the shorthand for $\sin\theta_W(\cos\theta_W)$. In order to

go to the mass eigenbasis, we perform the SVD:

$$\psi_{tL(R)} = V^t_{L(R)}\psi_{tL(R),m}, \tag{4.45}$$

$$\psi_{bL(R)} = V^b_{L(R)}\psi_{bL(R),m}, \tag{4.46}$$

where $V^t_{L(R)}$ and $V^b_{L(R)}$ are the 4×4 and 2×2 unitary matrices respectively, and the diagonalized mass matrices are

$$V_L^{t\dagger}\mathcal{M}_t V_R^t = \mathcal{M}_{t,\text{diag}} = \text{Diag}(m_{t1},\ m_{t2},\ m_{t3},\ m_{t4}), \tag{4.47}$$

$$V_L^{b\dagger}\mathcal{M}_b V_R^b = \mathcal{M}_{b,\text{diag}} = \text{Diag}(m_{b1},\ m_{b2}), \tag{4.48}$$

where the mass eigenvalues are defined as $m_i \geq m_j$ for $i > j$; hence we identify m_{t4} and m_{b2} with m_t and m_b of the SM. The interaction matrices become

$$\mathcal{C}^t_{L(R),m} = V^{t\dagger}_{L(R)}\mathcal{C}^t_{L(R)}V^b_{L(R)}, \tag{4.49}$$

$$\mathcal{C}^X_{L(R),m} = \mathcal{C}^X_{L(R)}V^t_{L(R)}, \tag{4.50}$$

$$\mathcal{N}^t_{L(R),m} = V^{t\dagger}_{L(R)}\mathcal{N}^t_{L(R)}V^t_{L(R)}, \tag{4.51}$$

$$\mathcal{N}^b_{L(R),m} = V^{b\dagger}_{L(R)}\mathcal{N}^b_{L(R)}V^b_{L(R)}, \tag{4.52}$$

$$\mathcal{Y}^t_{L(R),m} = V^{t\dagger}_{R(L)}\mathcal{Y}^t_{L(R)}V^t_{L(R)}, \tag{4.53}$$

$$\mathcal{Y}^b_{L(R),m} = V^{b\dagger}_{R(L)}\mathcal{Y}^b_{L(R)}V^b_{L(R)}. \tag{4.54}$$

From the next section, we work in the mass eigenbasis but omit the subscript m for simplicity.

Here we comment on the Higgs low energy theorem limit. As an explicit example we consider the effective hgg coupling. Following the Higgs low energy theorem, we can express the effective Lagrangian generated by the charge 2/3 loops as

$$\mathcal{L}_{hgg} = \frac{\alpha_s}{12\pi}\frac{h}{v}\frac{\partial \log(\text{Det}\,\mathcal{M}_t^\dagger(v)\mathcal{M}_t(v))}{\partial \log v}G^a_{\mu\nu}G^{a\mu\nu}. \tag{4.55}$$

Using the Eq. (4.23), we get

$$\mathcal{L}_{hgg} = \frac{\alpha_s}{12\pi}\frac{1-2\frac{v^2}{f^2}}{\sqrt{1-\frac{v^2}{f^2}}}\frac{h}{v}G^a_{\mu\nu}G^{a\mu\nu}. \tag{4.56}$$

The important feature is that this coupling is only depending on the v^2/f^2. In order to understand this feature we perform the field redefinition [38] as

$$\Psi \to \Omega^T\Psi. \tag{4.57}$$

In this basis we can rewrite the yukawa and mass terms as follows:

$$\mathcal{L}_{Yukawa+Mass} = -Yf(\bar{\Psi}_L\Sigma_0^T)(\Sigma_0\Psi_R) - M\bar{\Psi}_L\Psi_R - \Delta_L\bar{\lambda}_L\Omega^T\Psi_R - \Delta_R\bar{\Psi}_L\Omega\eta_R + (\text{h.c.}), \tag{4.58}$$

where we introduce the incomplete $SO(5)$ multiplet:

$$\lambda_L = \frac{1}{\sqrt{2}}(b_L \;\; -ib_L \;\; t_L \;\; it_L \;\; 0)^T, \tag{4.59}$$

$$\eta_R = \frac{1}{\sqrt{2}}(0 \;\; 0 \;\; 0 \;\; 0 \;\; \sqrt{2}t_R)^T. \tag{4.60}$$

The mass matrix reads

$$\mathcal{M}_t = \begin{pmatrix} 0 & \frac{\Delta_L}{2}(1+c) & \frac{\Delta_L}{2}(-1+c) & \frac{\Delta_L}{\sqrt{2}}s \\ -\frac{\Delta_R}{\sqrt{2}}s & M & 0 & 0 \\ -\frac{\Delta_R}{\sqrt{2}}s & 0 & M & 0 \\ \Delta_R c & 0 & 0 & M + Yf \end{pmatrix}. \tag{4.61}$$

In this basis it is clear that there is no Higgs dependence in the composite sub-block of the matrix. The determinant becomes

$$\mathrm{Det}\,\mathcal{M}_t^\dagger(v)\mathcal{M}_t(v) = \left(\frac{MYf\Delta_L\Delta_R}{2\sqrt{2}}\sin\left(\frac{2v}{f}\right)\right)^2. \tag{4.62}$$

This determinant can be decomposed into two parts:

$$\mathrm{Det}\,\mathcal{M}_t^\dagger\mathcal{M}_t = P(M, Y, \Delta_L, \Delta_R, f) \times F(v/f), \tag{4.63}$$

where $F(v/f)$ satisfies $F(0) = 0$. Therefore the quantity $\partial \log(\mathrm{Det}\,\mathcal{M}_t^\dagger\mathcal{M}_t)/\partial \log v$ does not depend on the function P whose arguments are the parameter of the composite sector and the linear mixing term. This separation can be realized if there is a single $SO(5)$ invariant constructed by the linear mixing parameters which can be treated as spurions [38, 39]. This fact is quite characteristic and useful for the analysis of the loop induced Higgs couplings.

4.1.2 Experimental constraints

The strongest experimental constraints on composite Higgs models still come from the electroweak precision measurements at the Z pole at the LEP collider. A convenient description of the LEP precision data is given in terms of the parameters $\epsilon_1, \epsilon_2, \epsilon_3$ and ϵ_b [40]. In addition to the SM contribution, there are three contributions in the MCHM5. The first contribution comes from the modified coupling of the Higgs to the massive gauge bosons, which induces a logarithmic contribution to the epsilon parameters ϵ_1 and ϵ_2, or equivalently to $\hat{T}$ and $\hat{S}$. The contribution is cut-off by the mass m_ρ of the first composite Higgs resonance [36],

$$\delta\epsilon_1^{IR} = -\frac{3\alpha(m_Z)}{16\pi c_W^2}\frac{v^2}{f^2}\log\left(\frac{m_\rho^2}{m_h^2}\right), \tag{4.64}$$

$$\delta\epsilon_3^{IR} = \frac{\alpha(m_Z)}{48\pi s_W^2}\frac{v^2}{f^2}\log\left(\frac{m_\rho^2}{m_h^2}\right). \tag{4.65}$$

The contribution to the ϵ_1 parameter is negative and the contribution to the ϵ_3 parameter is positive. The second effect is the direct contribution of the vector and axial vector resonances to the ϵ_3 parameter. This contribution is found to be

$$\delta\epsilon_3^{UV} = \frac{m_W^2}{m_\rho^2}\left(1+\frac{m_\rho^2}{m_a^2}\right) \simeq 1.36\frac{m_W^2}{m_\rho^2}, \tag{4.66}$$

where we use the relation $\frac{m_a}{m_\rho} \simeq \frac{5}{3}$, obtained in the five dimensional realization of the model [8]. The last contribution comes from the quantum correction of the heavy fermions. This contribution affects the both the ϵ_1 and ϵ_b parameters which are corresponding to the $\hat{T}$ parameter and the $Zb\bar{b}$ coupling, respectively. We can compute them at full one-loop level. The contribution to the ϵ_1 parameter is obtained as follows:

$$\begin{aligned}
\epsilon_1^{\text{fermion}} =& \frac{3\alpha(m_Z)}{16\pi\sin^2\theta_W\cos^2\theta_W}\Bigg\{ \\
& \sum_{i,\alpha}(|\tilde{\mathcal{C}}^t_{Li\alpha}|^2+|\tilde{\mathcal{C}}^t_{Ri\alpha}|^2)\theta_+(y_{ti},y_{b\alpha}) + 2\,\mathrm{Re}[\tilde{\mathcal{C}}^t_{Li\alpha}\tilde{\mathcal{C}}^{t*}_{Ri\alpha}]\theta_-(y_{ti},y_{b\alpha}) \\
& \sum_{i}(|\tilde{\mathcal{C}}^X_{L1i}|^2+|\tilde{\mathcal{C}}^X_{R1i}|^2)\theta_+(y_X,y_{ti}) + 2\,\mathrm{Re}[\tilde{\mathcal{C}}^X_{L1i}\tilde{\mathcal{C}}^{X*}_{R1i}]\theta_-(y_X,y_{ti}) \\
& -\frac{1}{2}\sum_{i,j}(|\tilde{\mathcal{N}}^t_{Lij}|^2+|\tilde{\mathcal{N}}^t_{Rij}|^2)\theta_+(y_{ti},y_{tj}) + 2\,\mathrm{Re}[\tilde{\mathcal{N}}^t_{Lij}\tilde{\mathcal{N}}^{t*}_{Rij}]\theta_-(y_{ti},y_{tj}) \\
& -\frac{1}{2}\sum_{\alpha,\beta}(|\tilde{\mathcal{N}}^b_{L\alpha\beta}|^2+|\tilde{\mathcal{N}}^b_{R\alpha\beta}|^2)\theta_+(y_{b\alpha},y_{b\beta}) + 2\,\mathrm{Re}[\tilde{\mathcal{N}}^b_{L\alpha\beta}\tilde{\mathcal{N}}^{b*}_{R\alpha\beta}]\theta_-(y_{b\alpha},y_{b\beta}) \\
& -\frac{1}{2}\left((|\tilde{\mathcal{N}}^X_L|^2+|\tilde{\mathcal{N}}^X_R|^2)\theta_+(y_X,y_X) + 2\,\mathrm{Re}[\tilde{\mathcal{N}}^X_L\tilde{\mathcal{N}}^{X*}_R]\theta_-(y_X,y_X)\right)\Bigg\},
\end{aligned} \tag{4.67}$$

where i,j and α,β run $1\sim4$ and $1\sim2$, and $y_\psi = \frac{m_\psi^2}{m_Z^2}$. The loop functions θ_+ and θ_- are defined in the App. A. This result includes the effect of the SM top and bottom quarks with the modified couplings; then it is corresponding to the $\hat{T}$ parameter as $\delta\epsilon_1^{\text{th}} - \epsilon_1^{\text{SM,fermion}} = \hat{T}$. The SM contribution with the limit $|V_{tb}^{CKM}| = 1$ is obtained as

$$\begin{aligned}
\epsilon_1^{\text{SM,fermion}} &= \frac{3\alpha(m_Z)}{16\pi\sin^2\theta_W\cos^2\theta_W m_Z^2}\left(m_t^2+m_b^2-2\frac{m_t^2m_b^2}{m_t^2-m_b^2}\ln\left(\frac{m_t^2}{m_b^2}\right)\right) \\
&\sim 9.23\times10^{-3}.
\end{aligned} \tag{4.68}$$

The contribution to the ϵ_b parameter is a little bit complicated. We don't care about the right handed bottom quark effect because the fundamental sector doesn't mix with the composite sector with respect to the right handed bottom quark; the effect is negligibly small. The amplitude for the decay of a Z boson to massless left handed bottom quarks can be written

$$\mathcal{M}(Z\to b_L\bar{b}_L) = -g_L\bar{b}\gamma^\mu\left(\frac{1-\gamma^5}{2}\right)b\epsilon_\mu, \tag{4.69}$$

where the g_L coupling is modified from its value in the SM:

$$g_L = g_L^{SM} + \delta g_L. \tag{4.70}$$

The correction δg_L is coming from the heavy fermions via the loop process. At one-loop level we have

$$\delta g_L = \frac{\alpha}{2\pi}\frac{g}{\cos\theta_W}(F - F_{SM}), \tag{4.71}$$

where the function F is the contribution from the heavy fermions, including the SM top quark with the modified coupling. The contribution can be computed as

$$\begin{aligned} F = &\sum_i |\tilde{\mathcal{C}}^t_{Li2}|^2 \left\{ F_{SM}(m_{ti}) + F_1\left(\frac{\tilde{\mathcal{N}}^t_{Lii}-1}{2}, \frac{\tilde{\mathcal{N}}^t_{Rii}}{2}, m_{ti}\right)\right\} \\ &+ \frac{1}{2}\sum_{i,j} \tilde{\mathcal{C}}^{t*}_{Li2}\tilde{\mathcal{C}}^t_{Lj2} F_2\left(\frac{\tilde{\mathcal{N}}^t_{Lij}}{2}, \frac{\tilde{\mathcal{N}}^t_{Rij}}{2}, m_{ti}, m_{tj}\right), \end{aligned} \tag{4.72}$$

where the functions F_{SM}, F_1 and F_2 are defined in the App. A. Using these results we get the contribution to the ϵ_b parameter:

$$\epsilon_b^{\text{fermion}} - \epsilon_b^{\text{SM,fermion}} = -2\frac{\alpha}{2\pi}\frac{g}{\cos\theta_W}\left(F - F_{SM}\right), \tag{4.73}$$

where we extract the effect beyond the SM. Now we can express the ϵ parameters as the following:

$$\epsilon_1^{\text{th}} = 5.38\times10^{-3} + \delta\epsilon_1^{IR} + (\epsilon_1^{\text{fermion}} - \epsilon_1^{\text{SM,fermion}}), \tag{4.74}$$
$$\epsilon_2^{\text{th}} = -7.06\times10^{-3}, \tag{4.75}$$
$$\epsilon_3^{\text{th}} = 5.42\times10^{-3} + \delta\epsilon_3^{IR} + \delta\epsilon_3^{UV}, \tag{4.76}$$
$$\epsilon_b^{\text{th}} = -6.48\times10^{-3} + (\epsilon_b^{\text{fermion}} - \epsilon_b^{\text{SM,fermion}}), \tag{4.77}$$
$$\varepsilon^{\text{th}} = \text{Diag}\left(\epsilon_1^{\text{th}},\ \epsilon_2^{\text{th}},\ \epsilon_3^{\text{th}},\ \epsilon_b^{\text{th}}\right). \tag{4.78}$$

The first terms of each ϵ are the SM contributions with $m_h = 126$ [GeV] and $m_t = 173$ [GeV]. On the other hand, experimental values of the ϵ parameters are well measured [41]:

$$\epsilon_1^{\text{exp}} = (5.4 \pm 1.0)\times10^{-3}, \tag{4.79}$$
$$\epsilon_2^{\text{exp}} = (-7.9 \pm 0.9)\times10^{-3}, \tag{4.80}$$
$$\epsilon_3^{\text{exp}} = (5.34 \pm 0.94)\times10^{-3}, \tag{4.81}$$
$$\epsilon_b^{\text{exp}} = (-5.0 \pm 1.6)\times10^{-3}, \tag{4.82}$$
$$\varepsilon^{\text{exp}} = \text{Diag}\,(5.4,\ -7.9,\ 5.34,\ -5.0)\times10^{-3}, \tag{4.83}$$
$$\Delta\varepsilon^{\text{exp}} = \text{Diag}\,(1.0,\ 0.9,\ 0.94,\ 1.6)\times10^{-3}. \tag{4.84}$$

Note that we include the W mass update [42]. These constraints are not independent but correlated each other; the correlation matrix is obtained as

$$\rho = \begin{pmatrix} 1 & 0.80 & 0.86 & 0.00 \\ 0.80 & 1 & 0.53 & -0.01 \\ 0.86 & 0.53 & 1 & 0.02 \\ 0.00 & -0.01 & 0.02 & 1 \end{pmatrix}. \tag{4.85}$$

Now the χ^2 fit can be peformed. The quantity χ^2 is defined by

$$\chi^2 = \left(\varepsilon^{\rm th} - \varepsilon^{\rm exp}\right) C^{-1} \left(\varepsilon^{\rm th} - \varepsilon^{\rm exp}\right), \tag{4.86}$$

where C^{-1} is the inverse of the variance-covariance matrix:

$$C = \Delta\varepsilon^{\rm exp}\, \rho\, \Delta\varepsilon^{\rm exp}. \tag{4.87}$$

The number of the parameters of the MCHM5 is seven, $\{f, m_\rho, Y, y_b, M, \Delta L, \Delta R\}$. The ratio $\frac{v^2}{f^2}$ is directly connected to the fine tuning; therefore we compute the minimum of the χ^2 for a fixed value of ξ. The parameter y_b is determined by the requirement of the correct bottom mass and its effect to other observables is enough tiny to ignore; which means that we can treat y_b as a fixed parameter. We also have to reproduce the SM top mass, $m_t = 173$ [GeV], which leads one relation between the parameters of the theory. Finally we should perform the χ^2 fit using the following four DOF; one dimension-full parameter m_ρ and three dimension-less parameters

$$\phi_L = \arctan\left(\frac{\Delta L}{M}\right), \tag{4.88}$$

$$\phi_R = \arctan\left(\frac{\Delta R}{M + Yf}\right), \tag{4.89}$$

$$R = \frac{M + Yf}{M}. \tag{4.90}$$

$\phi_{L(R)}$ is the mixing parameter of the left (right) handed elementary and composite sectors, and R is the ratio of the dimension-full parameters M and yf. In this analysis we require the 99% C.L. with four DOFs:

$$\chi^2 \leq 13.277, \tag{4.91}$$

where the value of right handed side is the corresponding χ^2 value at $p = 0.01$. The minimum value of $\chi^2_{\rm min}$ is smaller than the SM value, $\chi^2_{\rm SM} = 5.03$, because of the larger number of fitting parameters.

Other constraints come from the CKM matrix element $|V_{tb}|$ and the direct top partner search at the LHC. The lower limit on $|V_{tb}|$ is obtained from the single top production in $p\bar{p}$ collisions [44]:

$$|V_{tb}| > 0.92, \quad \text{at } 99\% \text{ C.L.}, \tag{4.92}$$

where the top mass is assumed as 172.5 [GeV]. This constraint is significantly upgraded compared with the previous study, $|V_{tb}| > 0.77$ [45]. However, this upgrade does not give a big change to our analysis. In the Fig.10, we plot a sample of parameters passing the χ^2 test for each $|V_{tb}|$ constraint in the case of $f = 750$ [GeV]. We find the small region, especially the light top partner mass region, is excluded by the change of the constraint. From the figure we find that there are two typical regions in the range of relatively small top partner mass: the small compositeness region and the large compositeness region. In

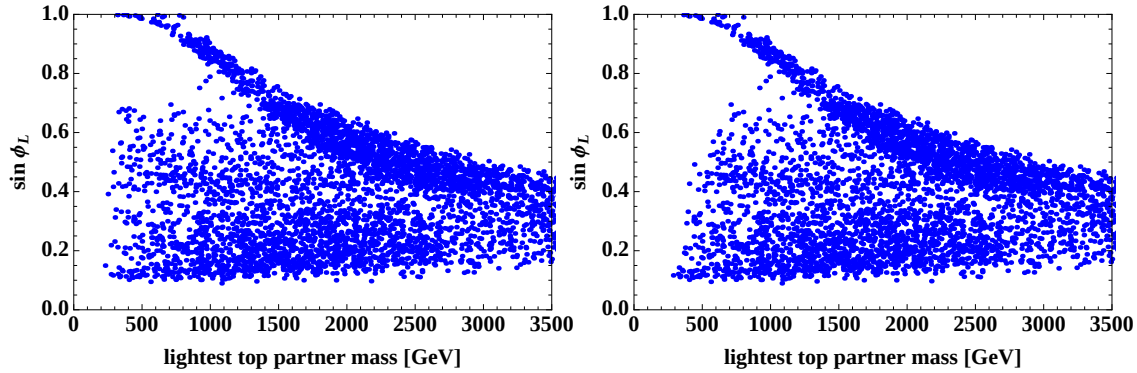

Figure 10. A sample of parameters passing the χ^2 test of the EW precision tests for $|V_{tb}| > 0.77$ (left) and $|V_{tb}| > 0.92$ (right) in the case of $f = 750$ [GeV]. The vertical axis is the compositeness of the left handed sector and the horizontal axis is the lightest top partner mass m_{t3}.

the small compositeness region, the main component of ψ_{t3} is the singlet $\tilde{T}$ and the other states are rather heavy. On the other hand, in the large compositeness region the exotic charge state ψ_X becomes light below 1 [TeV].
The direct top partner search at the LHC is also experimental constraints. This constraint is roughly 700 [GeV] [47]. However, we check that this constraint gives no significant influence to the Higgs couplings we discuss in the next section; hence we ignore this constraint in our analysis.

We comment on the parameters we use for the numerical simulations. The ranges of the parameters we use are as follows:

$$m_\rho = [2\pi f, 4\pi f], \tag{4.93}$$
$$M = [0, m_\rho], \tag{4.94}$$
$$Y = [-4\pi, 4\pi], \tag{4.95}$$
$$\sin\phi_L = [0, 1], \tag{4.96}$$
$$\sin\phi_R = [0, 1]. \tag{4.97}$$

The first parameter m_ρ is the cut-off scale of the theory; we find that for this range the result does not change significantly. In regard to the other parameters, we vary them as large as possible although perhaps they may be somewhat unphysical.

As a conclusion of this section we plot the contributions to the ϵ_1 and ϵ_b parameters from the fermionic resonances for the parameter region passing the χ^2 tests in the case of $f = 750$ [GeV], see the Fig. 11. We find the contribution to the ϵ_b parameter corresponding to the $Zb_L\bar{b}_L$ coupling tends to be large and gives a severe constraint; this result is consistent with the Ref. [46]. We can see it is possible to get in agreement with the EW precision tests by having a small positive contribution to both $(\epsilon_1^{\rm fermion} - \epsilon_1^{\rm SM,fermion})/\epsilon_1^{\rm SM,fermion}$ and $(\epsilon_b^{\rm fermion} - \epsilon_b^{\rm SM,fermion})/\epsilon_b^{\rm SM,fermion}$.

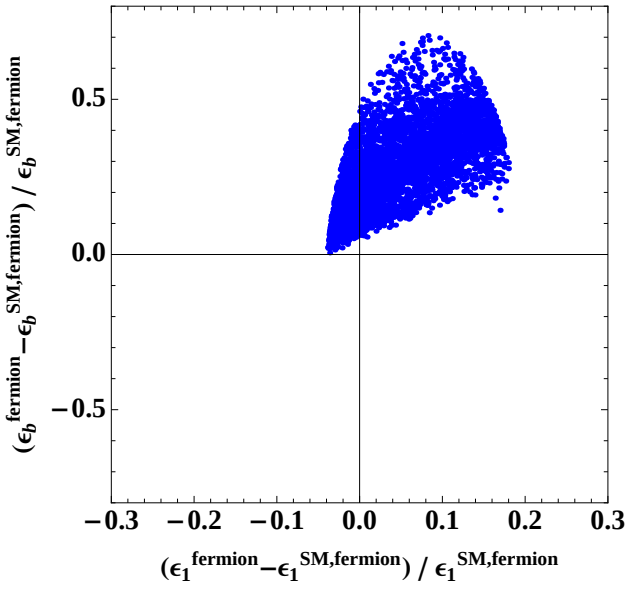

Figure 11. Scatter plot of the contributions to the ϵ_1 and ϵ_b parameters from the ferimionic resonances. In this plot we ignore the small contribution $\delta\epsilon_1^{IR}$.

4.1.3 Decay widths and couplings: numerical result

We now study the decay widths of the Higgs boson in the MHCM5. In this subsection we present the decay widths in terms of the parameters of the Lagrangian in the mass eigenbasis, and then perform the monte carlo simulation in the case of $f = 750$ [GeV] as a reference value. We include the contributions from all of the fermionic resonances taking into account the top and bottom quarks, and apply the experimental constraints considered in the previous subsection.

Using the results in the Sec. 2.2, the ratios of the decay widths to those of the SM can be expressed in the following forms.

$h \to VV^*$ mode:

$$\frac{\Gamma(h \to VV^*)}{\Gamma(h \to VV^*)_{SM}} = 1 - \frac{v^2}{f^2}. \tag{4.98}$$

This mode is completely determined by the decay constant. This result is derived by the resummation of the Higgs kinetic term (4.7); therefore this is valid in all order of $\frac{v^2}{f^2}$. For the value of $f = 750$ [GeV], the ratio is $\Gamma/\Gamma_{SM} = 0.892$.

$h \to bb$ mode:

$$\frac{\Gamma(h \to bb)}{\Gamma(h \to bb)_{SM}} = \frac{\mathcal{Y}^b_{L22}}{\frac{m_b}{v}} = \frac{\mathcal{Y}^b_{R22}}{\frac{m_b}{v}}. \tag{4.99}$$

The hermiticity of the Lagrangian leads the relation $\mathcal{Y}^b_{L22} = \mathcal{Y}^b_{R22}$. Since we construct the bottom quark mass by the explicit breaking of the partial compositeness, this mode is the

almost same as the SM case, see the Fig. 12. The difference is lower than $\mathcal{O}(10^{-5})$ %.

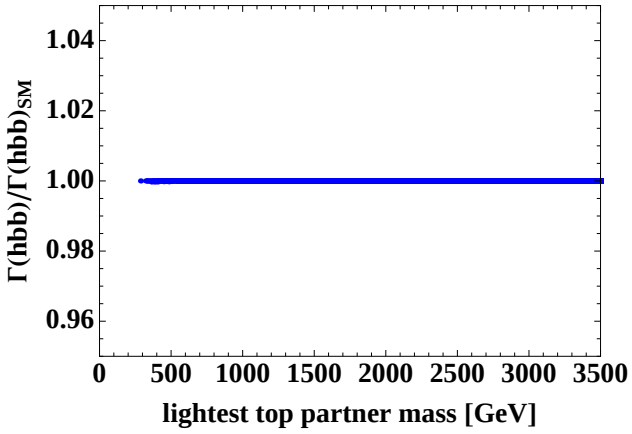

Figure 12. The ratio of the $h \to bb$ mode decay widths for $f = 750$ [GeV]. The vertical axis is the ratio of $\Gamma(h \to bb)$ and the SM one, and the horizontal axis is the lightest top partner mass. The ratio is almost one; the difference is less than $\mathcal{O}(10^{-5})$ %. This result is unchanged before and after imposing the experimental constraints.

$h \to gg$ mode:

$$\frac{\Gamma(h \to gg)}{\Gamma(h \to gg)_{SM}} = \left|\frac{2}{v}A_{1/2}(\tau_t) + \frac{2}{v}A_{1/2}(\tau_b)\right|^{-2} \times \left|\sum_{i=1}^{4}\frac{2\mathcal{Y}^t_{Lii}}{m_{ti}}A_{1/2}(\tau_{ti}) + \sum_{\alpha=1}^{2}\frac{2\mathcal{Y}^b_{L\alpha\alpha}}{m_{b\alpha}}A_{1/2}(\tau_{b\alpha})\right|^2, \tag{4.100}$$

where we define $\tau_\phi = \left(\frac{2m_\phi}{m_h}\right)^2$, and the loop function $A_{1/2}$ is expressed in the App. A. This mode is important for the production of the Higgs boson because the gluon fusion process is the dominant process at the LHC. In particular, if we ignore the other Higgs production modes we get the relation

$$\frac{\Gamma(h \to gg)}{\Gamma(h \to gg)_{SM}} = \frac{\sigma(pp \to h)}{\sigma(pp \to h)_{SM}}. \tag{4.101}$$

In the MCHM5 this mode is significantly suppressed because of the structure of the top yukawa coupling; in the Higgs low energy theorem limit the top yukawa coupling is suppressed by $\frac{1-2\xi}{\sqrt{1-\xi}}$. Due to this suppression the small value of f is undesirable from the view point of the LHC experiment. For example, in the case of $f = 500$ [GeV] we find

$$\frac{\sigma(gg \to h)}{\sigma(gg \to h)_{SM}} \times \frac{\mathrm{BR}(h \to \gamma\gamma)}{\mathrm{BR}(h \to \gamma\gamma)_{SM}} \sim 0.33 \quad (\text{for } f = 500[\text{GeV}]). \tag{4.102}$$

This value is too small to explain the experimental data. In this thesis we therefore consider the decay constant is larger than 750 [GeV] (although the production is still a bit small for

the decay constant below 1000 [GeV]). We show the result in the Fig. 13 with/without the constraints of the EW precision measurements and the CKM matrix element $|V_{tb}|$. The suppression of the width is larger than 30%. Without the constraints, the ratio can vary by about 10 %. In the small ratio region the top quark yukawa coupling is small and the coupling of one of the partner becomes large. However, in such a case the contributions to the ϵ_1 and ϵ_b parameters from the fermion loop turn out to be rather small compared with those of the SM. After imposing the constraints, we find that the possible value of the ratio is within a few % of the result of the Higgs low energy theorem limit.

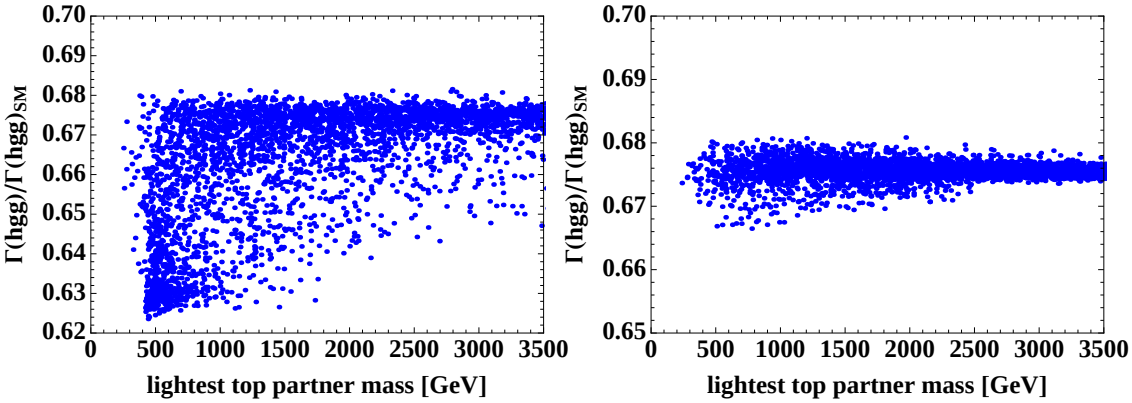

Figure 13. The ratio of the $h \to gg$ mode decay widths for $f = 750$ [GeV] without the constraints (left) and with the constraints (right). The vertical axis is the ratio of $\Gamma(h \to gg)$ and the SM one, and the horizontal axis is the lightest top partner mass. Since the top yukawa coupling receives the large suppression, this mode shows the large deviation from the SM prediction.

$h \to \gamma\gamma$ mode:

$$\frac{\Gamma(h \to \gamma\gamma)}{\Gamma(h \to \gamma\gamma)_{SM}} = \left| \frac{2}{v} 1^2 A_1(\tau_W) + \frac{6}{v}\left(\frac{2}{3}\right)^2 A_{1/2}(\tau_t) + \frac{6}{v}\left(\frac{-1}{3}\right)^2 A_{1/2}(\tau_b) \right|^{-2} \times \left| \frac{2}{v} 1^2 \sqrt{1 - \frac{v^2}{f^2}} A_1(\tau_W) + \sum_{i=1}^{4} \frac{6\mathcal{Y}^t_{Lii}}{m_{ti}}\left(\frac{2}{3}\right)^2 A_{1/2}(\tau_{ti}) + \sum_{\alpha=1}^{2} \frac{6\mathcal{Y}^b_{L\alpha\alpha}}{m_{b\alpha}}\left(\frac{-1}{3}\right)^2 A_{1/2}(\tau_{b\alpha}) \right|^2, \quad (4.103)$$

where the loop function A_1 is defined in the App. A. The W boson also contributes to this mode and its contribution is large and opposite compared with the fermionic contribution. Therefore, the suppression is relatively smaller than that of the $h \to gg$ mode. From the Fig. 14 we can see that the difference whether the constraints are imposed or not is not significant. The width is suppressed by about 5 %.

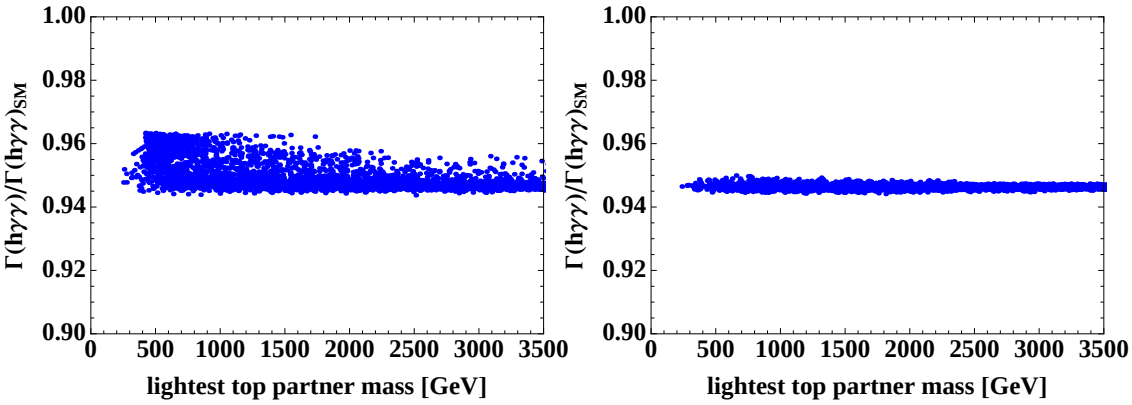

Figure 14. The ratio of the $h \to \gamma\gamma$ mode decay widths for $f = 750$ [GeV] without the constraints (left) and with the constraints (right). The vertical axis is the ratio of $\Gamma(h \to \gamma\gamma)$ and the SM one, and the horizontal axis is the lightest top partner mass. The plots are almost flat with respect to the lightest top partner mass because the dominant contribution coming from the W boson is determined only by the decay constant.

$h \to Z\gamma$ mode:

$$\begin{aligned}\frac{\Gamma(h \to Z\gamma)}{\Gamma(h \to Z\gamma)_{SM}} = \Bigg| & \frac{g m_W}{s_W c_W} A_V(m_W) \\ & + \frac{6}{g s_W}\left[\frac{2}{3}\frac{g}{c_W}\left(\frac{1}{2} - 2s_W^2\frac{2}{3}\right)\frac{2m_t}{v} m_t A_F(m_t, m_t)\right. \\ & \left. + \frac{-1}{3}\frac{g}{c_W}\left(-\frac{1}{2} - 2s_W^2\frac{-1}{3}\right)\frac{2m_b}{v} m_b A_F(m_b, m_b)\right]\Bigg|^{-2} \times \\ & \Bigg| \frac{g m_W}{s_W c_W}\sqrt{1 - \frac{v^2}{f^2}} A_V(m_W) \\ & + \sum_{i,j=1}^{4} \frac{4}{g s_W}(\mathcal{Y}^t_{Lij} + \mathcal{Y}^t_{Rij})(\mathcal{N}^t_{Lij} + \mathcal{N}^t_{Rij}) m_{ti} A_F(m_{ti}, m_{tj}) \\ & + \sum_{\alpha,\beta=2}^{4} \frac{-2}{g s_W}(\mathcal{Y}^b_{L\alpha\beta} + \mathcal{Y}^b_{R\alpha\beta})(\mathcal{N}^b_{L\alpha\beta} + \mathcal{N}^b_{R\alpha\beta}) m_{b\alpha} A_F(m_{b\alpha}, m_{b\beta})\Bigg|^2 ,\end{aligned} \tag{4.104}$$

where the loop functions A_V and A_F are defined in the App. A. The striking feature of this mode is that different mass eigenstates can be appeared in the loop because there exists the off-diagonal interactions in both Higgs-fermions and Z boson-fermions interactions. Therefore, although the W contribution is similarly dominant in this mode, the width exhibits a different behavior from the $h \to \gamma\gamma$ mode. This mode is already studied in the Ref. [48], including only composite sector. In this thesis we include the fundamental sector and compute the width including the exact dependence on the all fermion masses and the off-diagonal interactions. Before imposing the constraints the possible range is quite wide; especially the ratio can be larger than unity. This is because that the sign of the fermionic

contribution can be changed, and off-diagonal contributions can be entered. After applying the constraints, we find the large ratio region is excluded but still have the fairly wider possible range than that of the $h \to \gamma\gamma$ mode; this process is also interesting for the collider search.

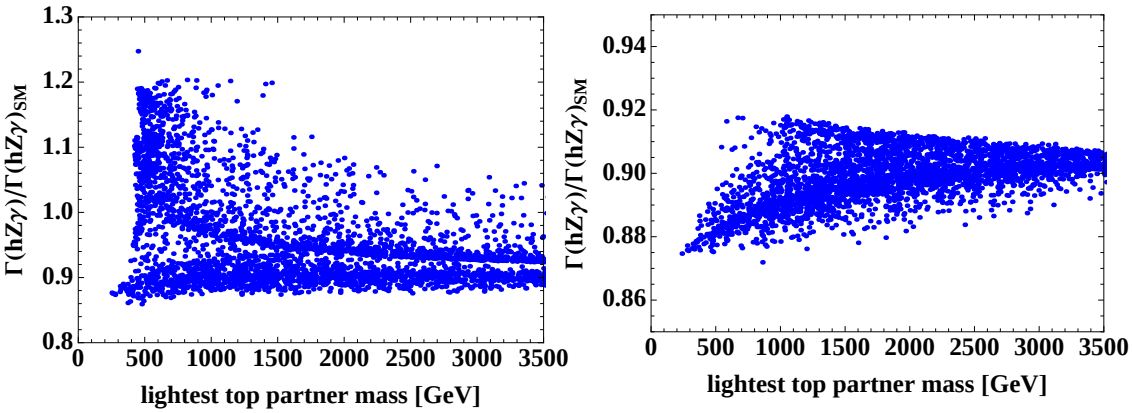

Figure 15. The ratio of the $h \to Z\gamma$ mode decay width for $f = 750$ [GeV] without the constraints (left) and with the constraints (right). The vertical axis is the ratio of $\Gamma(h \to Z\gamma)$ and the SM one, and the horizontal axis is the lightest top partner mass. In the light mass region the contribution of the heavy fermions gives relatively large deviation compared with the heavy mass limit.

We summarize the result of the ratios of the decay widths in the Fig. 16. In the MCHM5 the $h \to gg$ mode shows the largest deviation from the SM about larger than 30 %. On the other hand, the $h \to bb$ mode is almost the same as the SM case. The other three modes receives the suppressions about $5 \sim 10$ %.

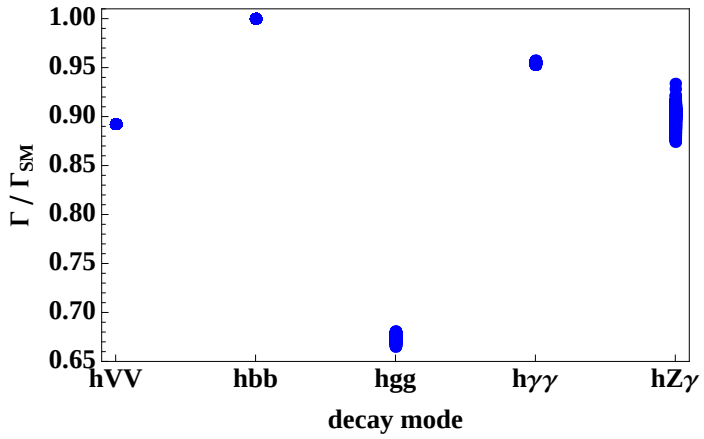

Figure 16. The summary of the ratios of the decay widths of $h \to XX$ for $f = 750$ [GeV]. The vertical axis is the ratio of $\Gamma(h \to XX)$ and the SM one for various decay modes. We perform the numerical calculation and show the result for the parameters which are allowed by the EW precision tests and the $|V_{tb}|$ constraint.

Next we define the deviation of the Higgs couplings from the SM prediction in accordance with the Ref. [15] in order to compare with the experimental sensitivity. In the perspective of the effective coupling, we can define the deviation of the coupling from that of the SM using the decay widths computed above:

$$d(hXX) = \sqrt{\frac{\Gamma(h \to XX)}{\Gamma(h \to XX)_{SM}}} - 1, \tag{4.105}$$

According to the Ref. [15], the future experiments can reveal this deviation with high precision for various modes. In this thesis we use the following modes: hWW, hZZ and hbb for the tree level couplings; hgg, $h\gamma\gamma$ and $hZ\gamma$ for the one-loop effective couplings. Although the experimental sensitivity of the $hZ\gamma$ coupling has not studied yet, we also present the result of this coupling to show the impact on new physics search of this mode. As a reference analysis, we study the possible deviations of the Higgs coupling in the case of $f = 750$ [GeV]. We show the result in the Fig. 17. The thin line (LHC14) shows the 1σ confidence intervals for the LHC sensitivity at 14 [TeV] with 300 $[\text{fb}^{-1}]$. The bold line (ILC250) shows the 1σ confidence intervals for the ILC sensitivity at 250 [GeV] with 250 $[\text{fb}^{-1}]$. If the plots are below these lines, we can observe the deviations of the couplings. In the present case the hgg coupling can be distinguished from the SM at both the LHC and ILC, and the hVV coupling is detectable only at the ILC. For the $h\gamma\gamma$ mode, it is difficult to observe the deviation due to the small difference. The interesting point is that if we can measure the $hZ\gamma$ coupling with the sensitivity close to the $h\gamma\gamma$ mode the deviation of this coupling is likely to be observed.

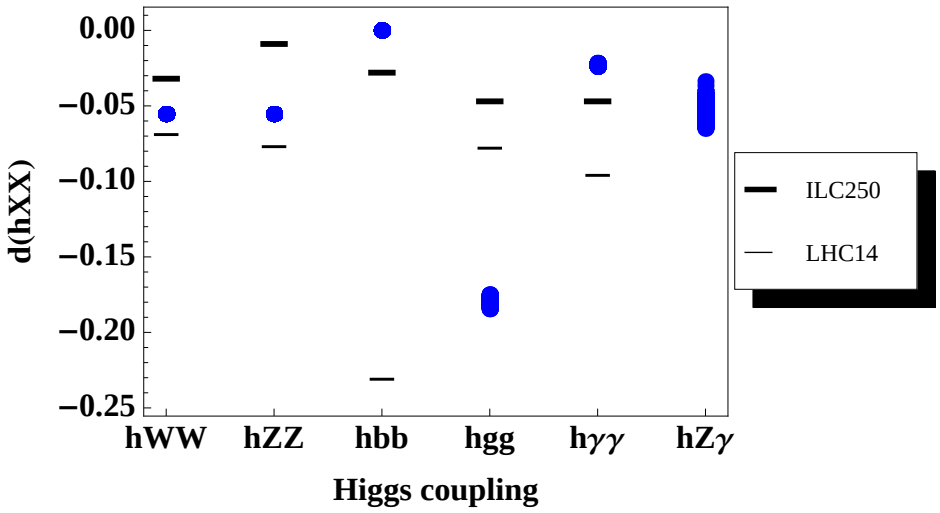

Figure 17. The deviations of the Higgs couplings for $f = 750$ [GeV] and the experimental sensitivities. The vertical axis is the deviation of the coupling from those of the SM. The thin (bold) line is the 1σ confidence sensitivity at 14 [TeV] LHC with 300 $[\text{fb}^{-1}]$ (250 [GeV] ILC with 250 $[\text{fb}^{-1}]$).

Finally we perform the numerical calculation with varying the decay constant f from 750 [GeV] to 2000 [GeV]. Using the fine tuning measure defined in the Ref. [36], we find $f = 2000$ [GeV] corresponds to about 1 % fine tuning. It probably seems to be unnatural; however, we here allow up to 1 % fine tuning in the light of recent experimental results that we have found no new particles at the LHC. In our numerical calculation we first determine the decay constant f from 750 [GeV] to 2000 [GeV] and then randomly choose the input parameters in accordance to the Eqs. (4.93)-(4.97). The ratio of decay widths are denoted in the Fig. 18. As we saw the displacements of each ratio is not large for the fixed f. Hence the wide possible ranges in the figure are due to the change of f; the possible range moves from the bottom to the top as f becomes large. If we take $f \to \infty$ limit, the theory can reproduce the SM and all of the ratios converge to unity.

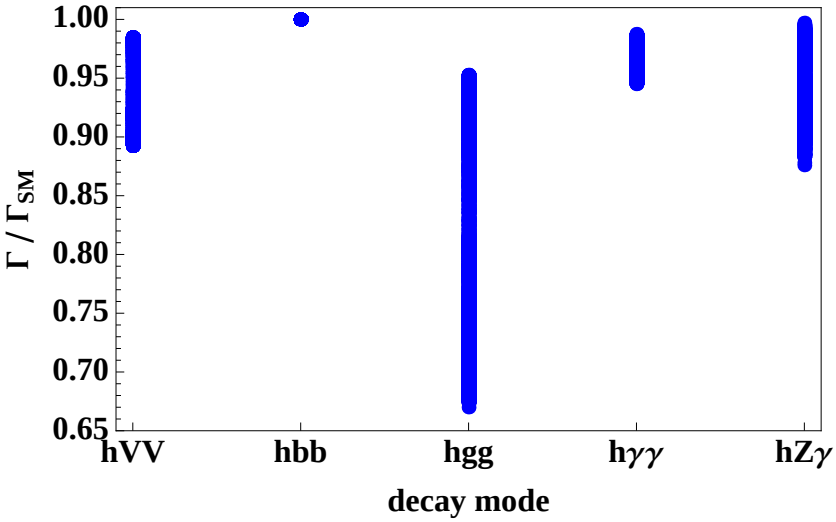

Figure 18. The summary of the ratios of the decay width of $h \to XX$ for $f = [750, 2000]$ [GeV]. The vertical axis is the ratio of $\Gamma(h \to XX)$ and the SM one for various decay modes. We perform the numerical calculation and show the result for the parameters which are allowed by the EW precision tests and the $|V_{tb}|$ constraint.

The summarized results of the deviations of the couplings and the experimental sensitivities are shown in the Fig. 19. For the wide range of f we can detect the non-SM hgg coupling at both the LHC and the ILC. For the ILC case we can probe f up to about 1500 [GeV]. In addition, the hZZ coupling is a useful probe to search the large value of f because of the high accuracy at the ILC; we find $f \leq 1850$ [GeV] can be investigated. The $hZ\gamma$ coupling could be an interesting target up to around $f \sim 1000$ [GeV].

4.2 Other models

In this section we study other models compared with the MCHM5. As comparison models we study the RS model and the extra singlet Higgs model. With respect to the SUSY

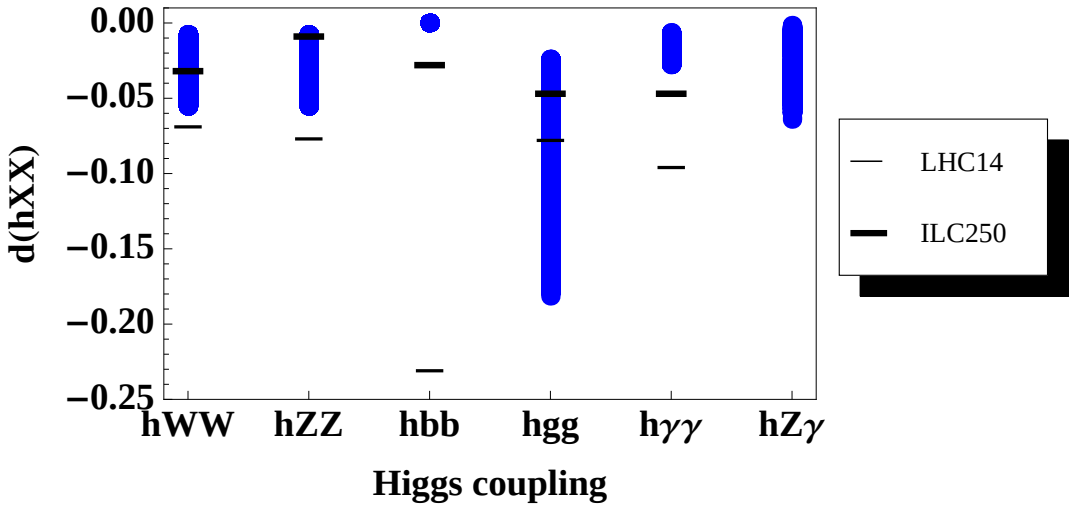

Figure 19. The deviations of the Higgs couplings for $f = [750, 2000]$ [GeV] and the experimental sensitivities. The vertical axis is the deviation of the coupling from those of the SM. The thin (bold) line is the 1σ confidence sensitivity at the 14 [TeV] LHC with 300 [fb^{-1}] (250 [GeV] ILC with 250 [fb^{-1}]).

model, we will give a comment later. Here we just explain the structure of the Higgs coupling, and the actual numerical simulation will be done in the next section.

4.2.1 Randall-Sundrum model

The RS model is one of solution of the gauge hierarchy problem with one AdS extra space dimension. In addition to the background metric, we introduce a massive five dimensional scalar field which interacts at the brane in order to stabilize the distance between branes, which is known as the Goldberger-Wise mechanism [49]. This scalar field generates the potential for the radion field. Considering the scalar perturbation which is corresponding to the radion, we find the metric is given by

$$ds^2 = e^{-2(kr_c\phi + F(x,\phi))}\eta_{\mu\nu}dx^\mu dx^\nu - (1 + 2F(x,\phi))^2 r_c^2 d\phi^2. \tag{4.106}$$

The fifth dimension has the topology S_1/Z_2 and is parametrized by ϕ $(0 < \phi < \pi)$. Here $kr_c\pi$ is the product of the fifth dimensional curvature k and the size of the fifth dimension $r_c\pi$, and F is a scalar perturbation $F(x,\phi) = r(x)R(\phi)$ [50] where $r(x)$ is the radion field and $R(\phi)$ is determined by the Einstein equation. If the back reaction is negligibly small, the scalar perturbation is

$$F(x,\phi) = \frac{r(x)}{\Lambda_\phi} e^{2kr_c(\phi-\pi)}, \tag{4.107}$$

where Λ_ϕ is the VEV of the radion $\Lambda_\phi = \sqrt{6} m_{pl} e^{-kr_c\pi} \sim$ TeV. In this thesis we consider the case in which all fields except for the Higgs boson propagate along the fifth dimension;

the effect of the higher dimensional operators are suppressed, and there arises Kaluza-Klein (KK) particles in the four dimensional effective theory.

Let us first show the KK reduction of the bulk gauge fields in the case of an $U(1)$ gauge theory [51]. The extension to the non-abelian gauge theory is straightforward. The five dimensional action of the bulk gauge field is

$$S_V = -\frac{1}{4}\int d^4x \int d\phi \sqrt{-G} G^{AB} G^{CD} F_{AC} F_{BD}, \tag{4.108}$$

where $G^{AB}(A, B = 0 \sim 4)$ is the five dimensional metric and G is its determinant such that $\sqrt{-G} = e^{-4kr_c\phi} r_c$. We introduce the Z_2 parity and assign the Z_2 even and odd to V_μ and V_4, respectively. Z_2 even states can have the zeroth modes which are identified to be the SM fields. We can rewrite the five dimensional action as

$$S_V \supset -\frac{1}{4}\int d^4x \int d\phi\, r_c \left(\eta^{\mu\nu}\eta^{\lambda\tau} F_{\mu\lambda} F_{\nu\tau} - 2\eta^{\mu\nu} V_\nu \partial_4 (e^{-2kr_c\phi}\partial_4 V_\nu)\right). \tag{4.109}$$

The KK reduction of the gauge fields is realized using the fifth dimensional wave function of the n-th KK mode $\xi^{(n)}$:

$$V_\mu(x,\phi) = \sum_{n=0}^{\infty} V_\mu^{(n)}(x) \frac{\xi^{(n)}(\phi)}{\sqrt{r_c}}. \tag{4.110}$$

The wave function has to satisfy the following two conditions: the first one is the orthonormality condition;

$$\int_{-\pi}^{\pi} d\phi\, \xi^m \xi^n = \delta^{mn}, \tag{4.111}$$

the second one is the bulk differential equation;

$$-\frac{1}{r_c^2}\frac{d}{d\phi}\left(e^{-2kr_c\phi}\frac{d}{d\phi}\xi^{(n)}\right) = m_n^2 \xi^{(n)}, \tag{4.112}$$

where m_n is a mass of the n-th KK mode. From these conditions we can analytically express the n-th wave function:

$$\xi^{(n)} = \frac{e^{kr_c\phi}}{N_n}[J_1(z_n) + \alpha_n Y_1(z_n)], \tag{4.113}$$

where $J_n(Y_n)$ is the Bessel function of the first (second) kind, see the App. A, and $z_n = \frac{m_n}{k} e^{kr_c\pi}$. We here introduce the normalization factor N_n which is determined by the Eq. (4.111), and

$$\alpha_n = -\frac{\pi}{2(\log(m_n/2k) - kr_c\pi + \gamma + 1/2)}, \tag{4.114}$$

where γ is the Euler-Mascheroni constant. In particular, the zeroth mode of the wave function is $\xi^{(0)} = \frac{1}{\sqrt{2\pi}}$. Moreover, the boundary conditions at the visible brane lead the following equation which determines the masses of each KK mode:

$$J_1(z_n) + \frac{m_n}{k} J_1'(z_n) + \alpha_n \left(Y_1(z_n) + \frac{m_n}{k} Y_1'(z_n)\right) = 0. \tag{4.115}$$

In this thesis we neglect the small correction to the wave function and to the KK mass of the massive gauge bosons from the EW symmetry breaking.

Next we present the KK reduction of the bulk massive fermions [52].

$$\begin{aligned} S_f = \int d^4x \int d\phi \sqrt{-G} \Bigg[& e_a^A \left\{ \frac{i}{2} \bar{Q} \gamma^a \partial_A Q - \partial_A \bar{Q} \gamma^a Q + \omega_{bcA} \bar{Q} \frac{1}{2} \{\gamma^a, \sigma^{bc}\} Q \right\} \\ & - m_Q \, \mathrm{sgn}(\phi) \bar{Q} Q + \sum_{q=u,d} \left(\frac{i}{2} \bar{q} \gamma^a \partial_A q - \partial_A \bar{q} \gamma^a q + \omega_{bcA} \bar{q} \frac{1}{2} \{\gamma^a, \sigma^{bc}\} q \right) \\ & - \sum_{q=u,d} m_q \, \mathrm{sgn}(\phi) \bar{q} q - \frac{v}{\sqrt{2} r_c} (\bar{u}_L Y_{5D} u_R + \bar{d}_L Y_{5D} d_R) \delta(|\phi| - \pi) \Bigg], \end{aligned} \tag{4.116}$$

where $e_a^A = \mathrm{Diag}(e^{kr_c\phi}, e^{kr_c\phi}, e^{kr_c\phi}, e^{kr_c\phi}, 1/r_c)$ is an inverse vielbein, ω_{bcA} is a spin connection, $u_{L(R)}, d_{L(R)}$ are five dimensional up and down quarks, and $q(Q)$ is an $SU(2)_L$ singlet (doublet). Note that our assumption of the localized Higgs field only allows the localized yukawa interaction on the visible brane. In order to construct the chiral effective theory we impose the appropriate Z_2 parity to the quark fields. Integrating this action by parts, we get the following action after some simplifications:

$$\begin{aligned} S_f = \int d^4x \int d\phi \, r_c \Bigg[& e^{-3kr_c\phi} \left(\bar{Q} i \not{\partial} Q + \sum_{q=u,d} \bar{q} i \not{\partial} q \right) \\ & - e^{-4kr_c\phi} \, \mathrm{sgn}(\phi) \left(c_Q k \bar{Q} Q + \sum_{q=u,d} c_q k \bar{q} q \right) \\ & - \frac{1}{2r_c} \left\{ \bar{Q}_L (e^{-4kr_c\phi} \partial_\phi + \partial_\phi e^{-4kr_c\phi}) Q_R + \sum_{q=u,d} \bar{q}_L (e^{-4kr_c\phi} \partial_\phi + \partial_\phi e^{-4kr_c\phi}) q_R + (\text{h.c.}) \right\} \\ & - e^{-3kr_c\phi} \frac{v}{\sqrt{2} r_c} (\bar{u}_L Y_{5D} u_R + \bar{d}_L Y_{5D} d_R) \delta(|\phi| - \pi) \Bigg], \end{aligned} \tag{4.117}$$

where we rewrite $m_Q(q) = c_{Q(q)} k$; naively we expect the coefficient $c_{Q(q)}$ is $\mathcal{O}(1)$. The KK reduction of the five dimensional fermion Ψ is performed by

$$\Psi(x, \phi) = \sum_{n=0}^{\infty} \psi_n^{L,R}(x) \frac{e^{2kr_c\phi}}{\sqrt{2}} f_n^{L,R}(\phi), \tag{4.118}$$

where $f_n^{L(R)}(\phi)$ is the left (right) handed fifth dimensional wave function of the n-th KK mode and ψ_n is the n-th order four dimensional fermion. As with the gauge field we have the two conditions. The orthonormality condition is

$$\int_{-\pi}^{\pi} e^{kr_c\phi} f_m^{A*}(\phi) f_n^B(\phi) = \delta_{mn} \delta^{AB}, \tag{4.119}$$

where $A, B = L, R$. The differential equation of the wave function is

$$\left(\pm \frac{1}{r_c} \partial_\phi - m_n \right) f_n^{L,R}(\phi) = -m_n e^{kr_c\phi} f_n^{R,L}(\phi) + e^{kr_c\phi} \frac{v}{\sqrt{2} r_c} Y_{5D} f_n^{R,L} \delta(\phi - \pi). \tag{4.120}$$

Then we get the following wave function:

$$f_n^{L,R}(\phi) = \frac{e^{kr_c\phi/2}}{N_n^{L,R}} \left(J_{c_{L,R}\mp 1/2}\left(\frac{m_n}{k}e^{kr_c\phi}\right) + \beta_n^{L,R} Y_{c_{L,R}\mp 1/2}\left(\frac{m_n}{k}e^{kr_c\phi}\right)\right). \tag{4.121}$$

We define the function $\beta_n^{L,R}$ for each Z_2 parity:

$$(\beta_n^{L,R})_{\text{even}} = \frac{\left(\frac{1}{2}+c_{L,R}\right) J_{c_{L,R}\mp 1/2}\left(\frac{m_n}{k}\right) + \frac{m_n}{k} J'_{c_{L,R}\mp 1/2}\left(\frac{m_n}{k}\right)}{\left(\frac{1}{2}+c_{L,R}\right) Y_{c_{L,R}\mp 1/2}\left(\frac{m_n}{k}\right) + \frac{m_n}{k} Y'_{c_{L,R}\mp 1/2}\left(\frac{m_n}{k}\right)}, \tag{4.122}$$

$$(\beta_n^{L,R})_{\text{odd}} = -\frac{J_{c_{L,R}\mp 1/2}\left(\frac{m_n}{k}\right)}{Y_{c_{L,R}\mp 1/2}\left(\frac{m_n}{k}\right)}. \tag{4.123}$$

In particular the zeroth mode is given by

$$f_0^{L,R}(\phi) = \frac{e^{\pm c_{L,R}\phi}}{N_0^{L,R}}, \quad \text{with} \quad N_0^{L,R} = \sqrt{\frac{2(e^{kr_c\pi(1+2c_{L,R})}-1)}{kr_c(1+2c_{L,R})}}. \tag{4.124}$$

The profile of the wave function is controlled by the bulk mass, i.e. the parameter $c_{L,R}$ in this case. If the fermion is localized near the visible brane, its coupling with the Higgs boson becomes large because the Higgs field is localized on the visible brane. Such a situation is realized by the small $c_{L,R}$. We can relax the hierarchy problem of the yukawa couplings by choosing appropriate $\mathcal{O}(1)$ parameters.

At this point we can illustrate the interactions of the Higgs field and the radion field with the SM fields and the KK modes [53]. The radion interactions are similar to those of the Higgs; the interaction is realized through the mass of the interacting particles. The interaction with the massive gauge boson is

$$\begin{aligned}\mathcal{L}_{rVV} =& -\frac{r}{\Lambda_\phi}\left(2m_W^2 W_\mu^{(0)+}W^{(0)+\mu} + 2m_Z^2\frac{Z_\mu^{(0)}Z^{(0)\mu}}{2}\right.\\ &\left. + 4\pi m_W^2\sum_{n=1}^{\infty}\xi_W^{(n)}(\pi)\xi_W^{(n)}(\pi)W_\mu^{(n)+}W^{(n)+\mu} + \cdots\right),\end{aligned} \tag{4.125}$$

$$\begin{aligned}\mathcal{L}_{hVV} =& -\frac{h}{v}\left(2m_W^2 W_\mu^{(0)+}W^{(0)+\mu} + 2m_Z^2\frac{Z_\mu^{(0)}Z^{(0)\mu}}{2}\right.\\ &\left. + 4\pi m_W^2\sum_{n=1}^{\infty}\xi_W^{(n)}(\pi)\xi_W^{(n)}(\pi)W_\mu^{(n)+}W^{(n)+\mu} + \cdots\right),\end{aligned} \tag{4.126}$$

where $V_\mu^{(0)}$ is the SM vector boson and $V_\mu^{(n)}$ is the n-th KK mode. $\xi_W^{(n)}(\pi)$ is the wave function of the n-th KK mode on the visible brane. The interaction with the fermion is

$$\mathcal{L}_{rff} = \frac{f}{\Lambda_\phi}\left(m_f\bar{\psi}^{(0)}\psi^{(0)} + e^{kr_c\pi}\frac{v}{\sqrt{2}r_c}Y_{5D}\sum_{n=1}^{\infty}f^{(n)*}(\pi)f^{(n)}(\pi)\bar{\psi}^{(n)}\psi^{(n)}\right), \tag{4.127}$$

$$\mathcal{L}_{hff} = \frac{h}{v}\left(m_f\bar{\psi}^{(0)}\psi^{(0)} + e^{kr_c\pi}\frac{v}{\sqrt{2}r_c}Y_{5D}\sum_{n=1}^{\infty}f^{(n)*}(\pi)f^{(n)}(\pi)\bar{\psi}^{(n)}\psi^{(n)}\right), \tag{4.128}$$

where $\psi^{(0)}$ is the SM fermion field and $\psi^{(n)}$ is the n-th KK mode. $f^{(n)}(\pi)$ is the wave function of the n-th KK mode on the visible brane. The loop induced effective couplings to gg and $\gamma\gamma$ are also well known. Note that in the radion case there exists the tree level coupling [54]:

$$\mathcal{L}_{rgg,r\gamma\gamma} = -\frac{r}{4\Lambda_\phi}\left(\left(\frac{1}{kr_c\pi}+\frac{\alpha_s}{2\pi}b^r_{QCD}\right)G^a_{\mu\nu}G^{a\mu\nu}+\left(\frac{1}{kr_c\pi}+\frac{\alpha_s}{2\pi}b^r_{EM}\right)F_{\mu\nu}F^{\mu\nu}\right), \quad (4.129)$$

where

$$b^r_{QCD} = 7+(A_{1/2}(\tau_f)+A^{fKK}_{1/2}), \quad (4.130)$$

$$b^r_{EM} = -\frac{11}{3}+\frac{8}{3}(A_{1/2}(\tau_f)+A^{fKK}_{1/2})+(A_1(\tau_W)+A^{WKK}_1), \quad (4.131)$$

and the KK mode contributions $A^{fKK}_{1/2}$ and A^{WKK}_1 are computed as follows:

$$A^{fKK}_{1/2} = e^{kr_c\pi}\frac{v}{\sqrt{2}r_c}Y_{5D}\sum_{n=1}^{\infty}\frac{f^{(n)*}(\pi)f^{(n)}(\pi)}{m^{(n)}_{f_{KK}}}A^f_{1/2}, \quad (4.132)$$

$$A^{SKK}_1 = 2\pi\left(\frac{m_W}{m^{(n)}_{W_{KK}}}\right)^2\sum_{n=1}^{\infty}\xi^{(n)}_W(\pi)\xi^{(n)}_W(\pi)A^W_1, \quad (4.133)$$

where $m^{(n)}_{f_{KK}}$ and $m^{(n)}_{W_{KK}}$ are the mass of the n-th KK mode. Note that the sum of all KK modes is finite [55]. For the Higgs boson case the interaction is obtained as

$$\mathcal{L}_{hgg,h\gamma\gamma} = -\frac{r}{4v}\left(\frac{\alpha_s}{2\pi}b^h_{QCD}G^a_{\mu\nu}G^{a\mu\nu}+\frac{\alpha_s}{2\pi}b^h_{EM}F_{\mu\nu}F^{\mu\nu}\right), \quad (4.134)$$

Next we consider the radion-Higgs mixing [56]. The mixing is induced by a curvature-Higgs mixing term in the four dimensional effective Lagrangian:

$$\mathcal{L}_\xi = \sqrt{g_{\rm ind}}\xi R(g_{\rm ind})H^\dagger H, \quad (4.135)$$

where ξ is a parameter and $g_{\rm ind}$ is an induced metric which is given by $e^{-2(kr_c\pi+r/\Lambda_\phi)}\eta_{\mu\nu}$. $R(g_{\rm ind})$ is the Ricci scalar calculated from the induced metric. After simplification we get the Higgs boson and the radion quadratic terms as

$$\mathcal{L} = -\frac{1}{2}h\partial^2 h-\frac{1}{2}m_h^2h^2-\frac{1}{2}(1+6\xi\gamma^2)f\partial^2 r-\frac{1}{2}m_r^2r^2+6\xi\gamma h\partial^2 r, \quad (4.136)$$

where we introduce the notation $\zeta = \frac{v}{\Lambda_\phi}$. In order to obtain the canonical kinetic terms, we first rescale the fields as follows:

$$h = h'+\frac{6\xi\zeta r'}{Z}, \quad (4.137)$$

$$r = \frac{r'}{Z}, \quad (4.138)$$

where $Z^2 = 1+6\xi\zeta^2(1-6\xi)$. The positivity of Z^2 requires the following relation:

$$\frac{1}{12}\left(1-\sqrt{1+\frac{4}{\zeta^2}}\right) < \xi < \frac{1}{12}\left(1+\sqrt{1+\frac{4}{\zeta^2}}\right). \quad (4.139)$$

Then we perform the orthogonal transformation as

$$\begin{pmatrix} h' \\ r' \end{pmatrix} = \begin{pmatrix} \cos\theta & \sin\theta \\ -\sin\theta & \cos\theta \end{pmatrix} \begin{pmatrix} h_m \\ r_m \end{pmatrix}, \tag{4.140}$$

where the subscript m denotes the mass eigenstate, and the mixing angle is

$$\tan 2\theta = 12\xi\zeta Z \frac{m_h^2}{m_r^2 - m_h^2(Z^2 - 36\xi^2\zeta^2)}. \tag{4.141}$$

Finally we get the following relation between the gauge eigenstate and the mass eigenstate:

$$h = \left(\cos\theta - \frac{6\xi\zeta}{Z}\sin\theta\right) h_m + \left(\sin\theta + \frac{6\xi\zeta}{Z}\cos\theta\right) r_m, \tag{4.142}$$

$$r = -\sin\theta\frac{h_m}{Z} + \cos\theta\frac{r_m}{Z}. \tag{4.143}$$

From now on we study the couplings of h_m, and the subscript m is omitted for simplicity.

In our numerical calculation, we use the following parameters. We set the cut-off scale $\Lambda_\phi = 10$ [TeV] in order to evade the experimental constraints [57]. The bulk mass parameters c_L and c_R are changed from -1 to 1 with the constraints that the SM fermion masses are reproduced. We vary the mixing parameter ξ also from -1 to 1. The range of the radion mass eigenvalue is set as $m_r = [200, 1000]$ [GeV]. The lower bound is determined from the view point that the radion cannot be produced at the ILC 250 [GeV], and the upper bound is just put on 1 [TeV].

4.2.2 Extra singlet Higgs model

We consider a theory where an extra gauge singlet Higgs boson mixes with the SM Higgs boson [58]. This singlet may spontaneously break symmetries in some hidden sector group. The Lagrangian of the Higgs sector is changed from the SM as follows:

$$\begin{aligned} \mathcal{L} \supset\ & (D_\mu H)^\dagger D^\mu H + \mu^2|H|^2 - \lambda|H|^4 \\ & + \partial_\mu\Phi^\dagger\partial^\mu\Phi + \mu'^2|\Phi|^2 - \lambda'|\Phi|^4 - \lambda''|\Phi|^2|H|^2. \end{aligned} \tag{4.144}$$

We have two CP-even mass eigenstates which are linear combinations of H and Φ with the mixing angle θ_H:

$$\begin{pmatrix} h \\ H \end{pmatrix} = \begin{pmatrix} \cos\theta_H & -\sin\theta_H \\ \sin\theta_H & \cos\theta_H \end{pmatrix} \begin{pmatrix} H_{\text{CP even, neutral}} \\ \Phi_{\text{CP even, neutral}} \end{pmatrix}, \tag{4.145}$$

where we denote the Higgs fields in the right handed side as CP-even neutral components. The lighter mass eigenstate is identified to the observed Higgs boson, i.e. $m_h = 126$ [GeV], which requires $\sin^2\theta_H < 0.5$. With respect to the Higgs couplings, all we need is the mixing angle to describe the couplings. We can express the couplings of the CP-even mass eigenstate in unit of those of the SM Higgs:

$$g_h^2 = \cos^2\theta_H g_{SM}^2 \tag{4.146}$$

$$g_H^2 = \sin^2\theta_H g_{SM}^2. \tag{4.147}$$

The deviation of the Higgs couplings from the SM is

$$d(hXX) = -\frac{\sin^2\theta_H}{2}. \tag{4.148}$$

The striking feature of this model is that all of the Higgs couplings are changed in the same way.

The experimental constraints come from the direct detection of H and the EW precision tests. In this thesis we focus on the region where the direct detection cannot be achieved and the EW precision tests are satisfied. In according to the Ref. [58], this requirement restricts the mixing parameter as $\sin^2\theta_H < 0.11$; hence the amount of the deviation of the Higgs coupling is within 6%.

4.3 Model discrimination using the correlation of Higgs couplings

In this section we compare the deviations of the Higgs couplings among the models we studied in the previous sections. As we emphasized, the correlations of the deviations are important for the model discrimination because they could extract the peculiar information of the model we consider. We focus on the correlation between the hZZ and hbb coupling deviations for the tree level process. The hZZ mode is a well-measurable mode at the LHC and ILC; the hWW mode is not considered because the sensitivity of this mode is similar to that of the hZZ mode. The hbb mode can be measured with high sensitivity at the ILC, and bb final state is a main decay mode of the Higgs boson. For the loop induced process, we focus on the correlation between hgg, $h\gamma\gamma$ and $hZ\gamma$ coupling deviations. The hgg mode is important for the production of the Higgs boson at the LHC and sensitive to the new colored particles which interact with the Higgs boson. The $h\gamma\gamma$ mode gives us the information of the Higgs mass and the new charged particles which interact with the Higgs boson. The $hZ\gamma$ mode is not yet studied experimentally, but we can also use this mode for new physics search. Although the branching ratios of these modes are relatively small, the loop process is useful to discriminate the models which are degenerate at tree level. We investigate on the experimental accessibility of the model discrimination by using the date of the Ref. [15].

First we consider the correlation between the deviations of the hbb and hZZ couplings at the LHC. In this section we denote the numerical results of the MCHM5 and the RS model as blue and red points respectively while the extra singlet Higgs model which ca be analytically studied is expressed by the green line. Experimental sensitivities are shown by the black line, and we can survey the region outside the line from the origin $(0, 0)$ which is corresponding to the SM case. Due to the small deviations, we cannot observe the tree level couplings at the LHC. In the MCHM5 the bottom yukawa coupling is almost the same as that of the SM as we saw. For the RS and extra singlet Higgs models, the tree level coupling deviations are determined only by the mixing angle; hence the correlation shows the same behavior and the red points are on the green line in the figure.

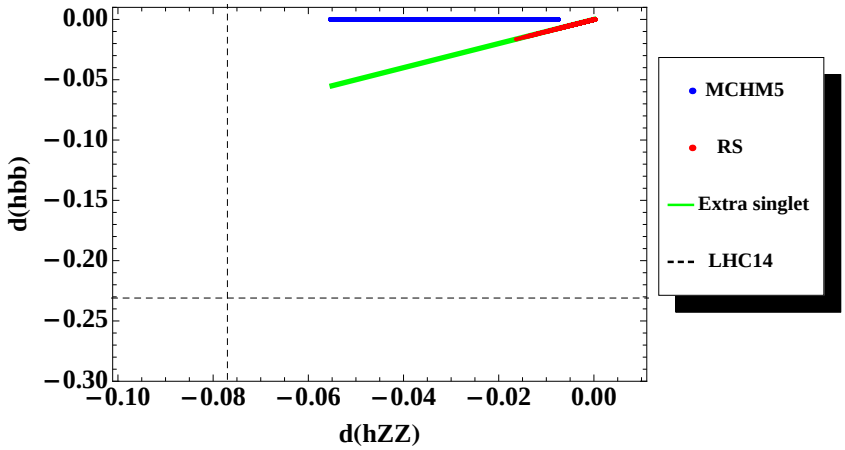

Figure 20. The correlation between the coupling deviations of the hbb and hZZ couplings. The blue point, red point and green line denote the MCHM5, the RS model and the extra singlet Higgs model, respectively. The red points are on the green line because only the mixing angle determines the deviations for both models. The black dashed line gives the 1σ interval sensitivity of the LHC 14 [TeV] with 300 [fb^{-1}]. This line means that we can probe the region outside the line from the origin $(0, 0)$. We find we cannot observe the deviations at the LHC.

Next we investigate the correlation between the deviations of the $h\gamma\gamma$ and hgg couplings at the LHC. We find that the hgg coupling is promising for the search of the MCHM5 and RS models. For the MCHM5 we can investigate f up to about 1100 [GeV]. The interesting point is the different behavior of the $h\gamma\gamma$ coupling deviation. As we saw it cannot be large to detect in the MCHM5; however the RS model shows it can possibly be large to be observed in the positive direction. This is because the contribution of the KK mode can be opposite to that of the SM by changing the wave function profile; the bulk mass parameters c_L and c_R are independent and can especially have the opposite signs. Therefore the deviations of the $h\gamma\gamma$ and hgg couplings show the negative correlation. Using the correlation, we perhaps distinguish the RS model from the MHCM5 if the negative $d(hgg)$ and positive $d(h\gamma\gamma)$ are observed within the prediction of the model. No deviation can be found in the extra singlet Higgs model.

Then we study the correlation between the deviations of the hbb and hZZ couplings at the ILC. In this thesis we use the ILC sensitivity of the coupling measurements for the 250 [GeV] with 300 [fb^{-1}] and 1000 [GeV] with 1000 [fb^{-1}] cases. Because of the high sensitivity of the ILC experiment, we can probe the very wide parameter region using this correlation. For the MHCM5 with f below 2000 [GeV], we definitely observe the modified hZZ coupling at the ILC1000 while the hbb coupling deviation can be never seen because the coupling is almost the same as the SM case. On the other hand, both of the deviations can be detected in the RS and extra singlet Higgs models if the mixing angle is not too tiny; for the extra singlet Higgs model we can investigate the mixing angle as $\sin^2\theta_h \geq 0.012$.

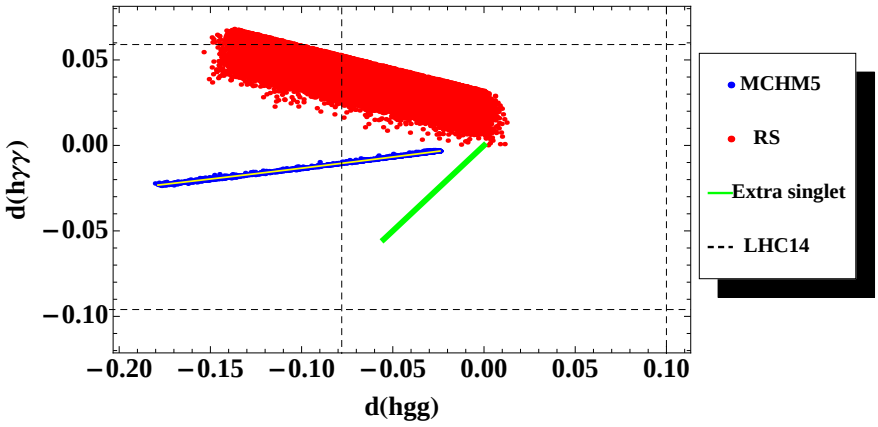

Figure 21. The correlation between the coupling deviations of the $h\gamma\gamma$ and hgg couplings. The blue point, red point and green line denote the MCHM5, the RS model and the extra singlet Higgs model, respectively. The result of the Higgs low energy theorem limit for the MCHM5 is expressed as the yellow line. The black dashed line gives the 1σ interval sensitivity of the LHC 14 [TeV] with 300 [fb^{-1}]. This line means that we can probe the region outside the line from the origin $(0, 0)$. The deviations of the extra singlet Higgs model are too small to observe. On the other hand, the hgg coupling is promising for the MCHM5 and the RS model.

We find that in any case the RS and extra singlet Higgs models can be distinguished from the MCHM5 because the case where the hZZ coupling deviation is observed alone is only possible in the MCHM5. This is due to the great sensitivity of the hbb coupling at the ILC experiment.

The correlation between the deviations of the $h\gamma\gamma$ and hgg couplings at the ILC is also useful for the model discrimination. The hgg mode is quite powerful for the MCHM5; at the ILC250 the decay constant can be searched up to about 1500 [GeV], and at the ILC1000 we can absolutely detect the deviation. The difference of the correlations of the RS and extra singlet Higgs models is available to discriminate them. For the RS model, the $h\gamma\gamma$ coupling deviation could be large because of the KK contribution even in the small mixing region. On the other hand, for the extra singlet Higgs model negative $d(h\gamma\gamma)$ could be observed. Therefore this correlation resolves the degeneracy of the RS and extra singlet Higgs models at the tree level.

Finally we also show the result of the correlation of the $h\gamma\gamma$ and $hZ\gamma$ couplings. For this study we use the result of the TLEP with $\sqrt{s} = 350$ [GeV] and 2600 [fb^{-1}] [59], which is the best sensitivity proposed at the present. Since the $hZ\gamma$ mode is not well studied experimentally, we naively expect that the sensitivity of this mode is different by only the statistics compared with the $h\gamma\gamma$ mode. The branching ratio of the $h \to Z\gamma$ mode is about two-thirds of the $h \to \gamma\gamma$ mode, and we cannot use the invisible decay of the Z boson whose

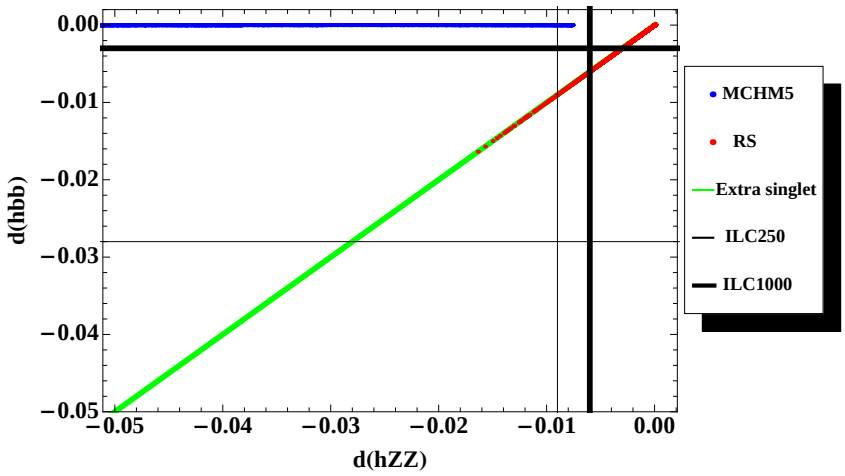

Figure 22. The correlation between the coupling deviations of the hbb and hZZ couplings. The blue point, red point and green line denote the MCHM5, the RS model and the extra singlet Higgs model, respectively. The red point is on the green line because only the mixing angle determines the deviations for both models. The black thin (thick) line gives the 1σ interval sensitivity of the ILC 250 [GeV] with 300 [fb^{-1}] (1000 [GeV] with 1000 [fb^{-1}]). This line means that we can probe the region outside the line from the origin $(0, 0)$. Due to the high sensitivity at the ILC, we can measure the deviations in the wide parameter regions of each model.

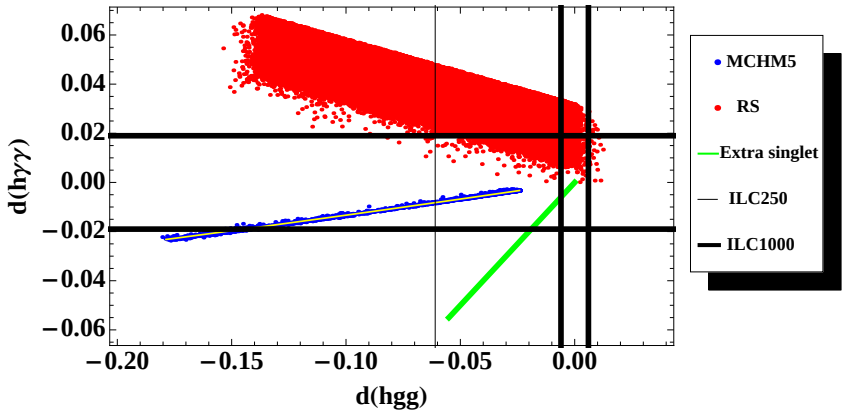

Figure 23. The correlation between the coupling deviations of the $h\gamma\gamma$ and hgg couplings. The blue point, red point and green line denote the MCHM5, the RS model and the extra singlet Higgs model, respectively. The result of the Higgs low energy theorem limit for the MCHM5 is expressed as the yellow line. The black thin (thick) line gives the 1σ interval sensitivity of the ILC 250 [GeV] with 300 [fb^{-1}] (1000 [GeV] with 1000 [fb^{-1}]). This line means that we can probe the region outside the line from the origin $(0, 0)$. The hgg mode is quite powerful, and the positive deviation of the $h\gamma\gamma$ coupling is useful to distinguish the RS model and the extra singlet Higgs model.

branching ratio is about 20 %; the error of the coupling measurement is expected to be $\sqrt{\frac{15}{8}}$ times of the $h\gamma\gamma$ one[13]. If we have such a good sensitivity, this mode is also interesting for new physics search. For the MCHM5, the $hZ\gamma$ mode can be searched up to about $f = 1200$ [GeV]. We find the $hZ\gamma$ deviation shows different behavior compared with the $h\gamma\gamma$ case for the RS model. The reason why is that the possible wave function profile is asymmetric for the positive and negative values, and the relative sign of the fermionic contribution to $h\gamma\gamma$ and $hZ\gamma$ is opposite. Therefore the plots shows the negative correlation.

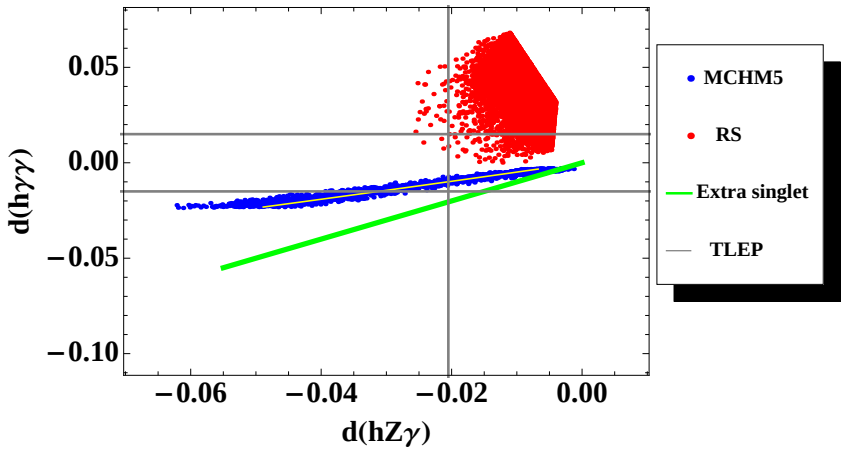

Figure 24. The correlation between the coupling deviations of the $h\gamma\gamma$ and $hZ\gamma$ couplings. The blue point, red point and green line denote the MCHM5, the RS model and the extra singlet Higgs model, respectively. The result of the Higgs low energy theorem limit for the MCHM5 is expressed as the yellow line. The gray line gives the 1σ interval sensitivity of the TLEP 350 [GeV] with 2600 [fb^{-1}]. This line means that we can that we can probe the region outside the line from the origin $(0, 0)$. The future experiment gives us interesting possibilities for the measurement of the $h\gamma\gamma$ and $hZ\gamma$ modes.

4.4 Conclusions

After the discovery of the Higgs boson, the precise study of the Higgs property is becoming important and interesting. Some of the Higgs couplings are observed at the LHC; then the parameter fitting of the theories we are interested in becomes possible [60]. It is important to examine the modified Higgs couplings of models beyond the SM and to clarify the correlation of the couplings in order to discriminate the models.

We have studied the modified Higgs couplings for the three explicit model: the MCHM5, the RS model, the extra singlet Higgs model. We especially focused on the MCHM5 and computed the tree level and the one-loop level (effective) couplings including exact mass dependences of all fermionic resonances. The constrains of the EW precision tests and

[13] In addition the hadronic decay of the Z boson is not easy for experimental analysis.

the CKM matrix element $|V_{tb}|$ are imposed, and the possible range of the decay widths with/without the constraints are shown. We have found that the finite mass effect of the heavy fermions is small except for the $hZ\gamma$ mode, and the Higgs low energy theorem limit well describes the modified couplings. In the MCHM5, the hZZ and hgg modes are promising to be observed at the collider experiments, and the $hZ\gamma$ mode is also an interesting target at the future collider experiments.

We have shown the correlation of the deviations of both the tree level couplings and the loop induced effective couplings. At the LHC, the deviations of the $h\gamma\gamma$ and hgg couplings are useful to investigate the MCHM5 and RS models. In some region we can observe both $d(h\gamma\gamma)$ and $d(hgg)$ for the RS model, which can be a discriminator of these models. At the ILC we can discriminate the three models in the wide parameter regions; especially we can investigate the decay constant up to about 2000 [GeV] for the MCHM5 and the mixing angle up to 0.012 for the other models. Using the correlation of the tree level couplings, we can distinguish the MCHM5 from the other models. In addition, the correlation of h$\gamma\gamma$-hgg modes allows us to discriminate the RS model and the extra singlet Higgs model because in the RS model the KK mode contribution could enhance the $h\gamma\gamma$ coupling in the positive direction while the extra singlet Higgs model always show the negative deviation.

Let us comment on the SUSY model. Since the number of model parameters is large, it is difficult to determine the general features of coupling correlations using a small DOFs. However, tree level couplings can be investigated generally by treating the quantum corrections to the Higgs mass matrix as parameters. According to the Ref. [58], the deviation of the hbb coupling tends to be positive, which is a strong discriminator for the comparison with the three models we studied.

We have clarified the importance and usefulness of the correlation of the Higgs couplings. It is important to study the modified Higgs couplings for more models and to investigate discrimination possibilities of the models at the future collider experiments.

5 Concluding remarks

The LHC has discovered the Higgs boson, and the next important step would be to measure accurately its properties. Many models beyond the SM predict the modified Higgs interactions which may produce indirect signals of new physics. It is important to study the features of the signals for each model and to clarify how we can discriminate models at the future collider experiments.

In this thesis we focused on the two aspects of the Higgs interactions. The first one is the perturbative unitarity of the scattering amplitudes of the scalar particles. This is directly connected with the mechanism of the EW symmetry breaking. If the coupling between the Higgs boson and the longitudinal gauge boson deviates from that of the SM, the unitarity breaks down at some high energy, which indicates the energy scale of new physics. The second one is the deviations of the Higgs couplings. In the SM all couplings to other particles are determined by the mass parameters which are already known. Therefore,

the deviation of Higgs couplings is a clear evidence of physics beyond the SM, and the future experiment can measure it about typically $\mathcal{O}(1)$ % precision.

In the chapter 3 we studied the perturbative unitarity violation caused by the dimension-six Higgs derivative interactions. The theory which modifies the Higgs sector would produce these interactions in the low energy effective theory, and the scattering amplitudes of the scalar particles grow with the energy. A more fundamental theory has to replace the effective theory before reaching at least the energy scale of the unitarity violation. We focused on one and two Higgs doublets case and gave the formula of the unitarity bound in terms of the parameters of the Lagrangian. The strongest bound is obtained from the largest eigenvalue of the scattering amplitude matrices which consist of the charge-conserving two-body to two-body scattering processes. We actually estimated the violation scales in various models and found them to be rather low, especially in the two doublets case, compared with the naive dimensional analysis.

In the chapter 4 we examined the deviations of Higgs couplings in the three models: the MCHM5, the RS mode, the extra singlet Higgs model. We focused on the MCHM5 and computed the tree level and the one-loop level (effective) couplings of the Higgs boson including the exact mass dependences of all heavy fermionic resonances. We found that the effect of the heavy resonances is small, and the Higgs low energy theorem limit is good approximation, except for the $hZ\gamma$ mode. We clarified the correlation of the Higgs couplings for each model, which is found to be quite powerful to discriminate the models. In particular, the high sensitivity of coupling measurements at the ILC permits us to distinguish the models in most parameter regions we consider.

Era of the precision measurement of Higgs physics has begun. The precise measurement of the Higgs properties provides a rich variety of new physics search; this kind of indirect search is complementary to the direct search. By clarifying the properties, we could get hints for Higgs physics beyond the SM: the origin of the EW symmetry breaking, the structure of the yukawa couplings and the meaning of the fine tuning, etc. These information could be a foothold for a more fundamental theory of the nature. Therefore, Higgs physics is one of the most interesting targets of the future collider experiments. It is important to study how we determine the new physics scenario using the high sensitivity of the experiments. In future we will obtain more and more data; we expect we can find the physics beyond the SM by using them.

Acknowledgments

I am strongly indebted to my supervisor, Yasuhiro Okada, for his support throughout my five-years Ph. D. program. Through many discussions, he has expanded my knowledge and has given me useful advices. His nice joke makes me work in a comfortable office environment.

I would like to thank Mihoko M. Nojiri, Kazunori Kohri, Yasuhiro Yamamoto and Hirohisa Kubota for our collaboration works. I appreciate them for fruitful discussions,

and always having time for my questions. I would also thank Keisuke Fujii and Akiya Miyamoto for their useful comments on the ILC experiment.

A special thanks goes to Ian Low, who accepted me during his sabbatical at the KITP. It was a great experience to discuss with him about Higgs physics.

I thank to the Cafe Prime at the KEK. This thesis would be never possible without the curry with fried pork cutlets I ate every night.

Further, I am very grateful to all members of KEK theory center and to my friends. I want to thank in particular Susumu Okazawa, Junya Nakamura, Kohsaku Tobioka, Hiraku Fukushima, Natsumi Nagata, Hikaru Matsuo and Manami Hashi.

A Loop functions and special functions

In this appendix we collect the definitions of various functions.

Loop functions used in the calculation of the decay widths are defined as follows:

$$A_1(\tau) = -\tau^2[2\tau^{-2} + 3\tau^{-1} + 3(2\tau^{-1} - 1)f(\tau)], \tag{A.1}$$

$$A_{1/2}(\tau) = 2\tau^2[\tau^{-1} + (\tau^{-1} - 1)f(\tau)], \tag{A.2}$$

$$A_0(\tau) = -\tau^2[\tau^{-1} - f(\tau)], \tag{A.3}$$

$$A_V(m_V) = 2\left(\frac{m_h^2}{m_V^2}(1 - 2c_W^2) + 2(1 - 6c_W^2)\right) C_2(m_V) + 4(1 - 4c_W^2)C_0(m_V), \tag{A.4}$$

$$\begin{aligned} A_F(m_1, m_2) =& C_0(m_1, m_2, m_2) + C_1(m_1, m_2, m_2) - C_1(m_2, m_1, m_1) \\ &+ 2C_2(m_1, m_2, m_2) + 2C_2(m_2, m_1, m_1), \end{aligned} \tag{A.5}$$

where

$$C_2(m_a) = \frac{\lambda_a\tau_a}{8m_a^2(\lambda_a - \tau_a)} + \frac{\lambda_a\tau_a^2}{8m_a^2(\lambda_a - \tau_a)^2}\left(\lambda_a(f(\lambda_a) - f(\tau_a)) + 2(F(\lambda_a) - F(\tau_a))\right), \tag{A.6}$$

$$C_0(m_a) = -\frac{\lambda_a\tau_a}{2m_a^2(\lambda_a - \tau_a)}(f(\lambda_a) - f(\tau_a)), \tag{A.7}$$

$$\begin{aligned} C_1(m_1, m_2, m_2) \equiv& C_{11}(m_Z^2, 0, m_h^2; m_1, m_2, m_2) \\ =& \frac{B_0(m_h^2; m_1, m_2) - B_0(m_Z^2; m_1, m_2)}{m_Z^2 - m_h^2} - C_0(m_Z^2, 0, m_h^2; m_1, m_2, m_2), \end{aligned} \tag{A.8}$$

$$\begin{aligned} C_2(m_1, m_2, m_2) =& C_{12}(m_Z^2, 0, m_h^2; m_1, m_2, m_2) + C_{23}(m_Z^2, 0, m_h^2; m_1, m_2, m_2) \\ =& \frac{m_1^2 - m_2^2 - m_Z^2}{2(m_Z^2 - m_h^2)^2}\left[B_0(m_h^2; m_1, m_2) - B_0(m_Z^2; m_1, m_2)\right] \\ &+ \frac{1}{2(m_Z^2 - m_h^2)m_h^2}\left[m_h^2 + 2m_2^2m_h^2C_0(m_Z^2, 0, m_h^2; m_1, m_2, m_2)\right. \\ &\left. + (m_2^2 - m_1^2)B_0(m_h^2; m_1, m_2) + A_0(m_1) - A_0(m_2)\right]. \end{aligned} \tag{A.9}$$

Here we define $\lambda_a = (2m_a/m_Z)^2$, $\tau_a = (2m_a/m_h)^2$ and

$$f(\tau) = \begin{cases} \arcsin^2 \sqrt{\frac{1}{\tau}}, & \tau \geq 1, \\ -\frac{1}{4}\left(\mathrm{Log}\,\frac{1+\sqrt{1-\tau}}{1-\sqrt{1-\tau}} - i\pi\right)^2, & \tau < 1, \end{cases} \tag{A.10}$$

$$F(\tau) = \begin{cases} \sqrt{\tau-1}\arcsin\sqrt{\frac{1}{\tau}}, & \tau \geq 1, \\ \frac{\sqrt{1-\tau}}{2}\left(\log\frac{1+\sqrt{1+\tau}}{1-\sqrt{1-\tau}} - i\pi\right), & \tau < 1. \end{cases} \tag{A.11}$$

The expressions of the scalar one-, two-, three- point functions A_0, B_0 and C_0 are

$$A_0(m) = m^2\left[1 - \log\frac{m^2}{\mu^2}\right], \tag{A.12}$$

$$\begin{aligned} B_0(p^2, m_1, m_2) = {} & 2 - \log\frac{m_1 m_2}{\mu} + \frac{m_1^2 - m_2^2}{p^2}\log\frac{m_2}{m_1} \\ & + \frac{\lambda^{1/2}(p^2, m_1^2, m_2^2)}{p^2}\log\frac{m_1^2 + m_2^2 - p^2 + \lambda^{1/2}(p^2, m_1^2, m_2^2)}{2m_1 m_2}, \end{aligned} \tag{A.13}$$

$$C_0(M_2^2, 0, M_1^2; m_1, m_2, m_2) = \frac{1}{M_1^2 - M_2^2}\sum_{i=1}^{2}\sum_{\sigma=\pm 1}(-1)^i \mathrm{Li}_2\left[\frac{2M_i^2}{m_2^2 - m_1^2 + M_i^2 + \sigma\lambda^{1/2}(M_i^2, m_1^2, m_2^2)}\right], \tag{A.14}$$

where μ is renormalization scale, and the ultraviolet poles in A_0 and B_0 are subtracted since the amplitudes are finite; λ is the usual two-body phase space function: $\lambda(x, y, z) = x^2 + y^2 + z^2 - 2(xy + yz + xz)$.

We also define loop functions appeared in the calculation of the ϵ parameters:

$$\theta_+(x_1,x_2) = x_1+x_2-\frac{2x_1x_2}{x_1-x_2}\log\frac{x_1}{x_2}-2(x_1\log x_1+x_2\log x_2)+\frac{x_1+x_2}{2}\Delta, \tag{A.15}$$

$$\theta_-(x_1,x_2) = 2\sqrt{x_1x_2}\left(\frac{x_1+x_2}{x_1-x_2}\log\frac{x_1}{x_2}-2+\log(x_1x_2)-\frac{\Delta}{2}\right), \tag{A.16}$$

$$F_{SM}(m) = \frac{\frac{m^2}{m_W^2}}{8\sin^2\theta_W\left(\frac{m^2}{m_W^2}-1\right)^2}\left(\frac{m^4}{m_W^4}-7\frac{m^2}{m_W^2}+6+\left(3\frac{m^2}{m_W^2}+2\right)\log\frac{m^2}{m_W^2}\right), \tag{A.17}$$

$$\begin{aligned}F_1(g_L,g_R,m) = \frac{1}{8\sin^2\theta_W}\Bigg\{&\frac{m^2}{m_W^2}g_L\left(2-\frac{4}{\frac{m^2}{m_W^2}-1}\log\frac{m^2}{m_W^2}\right)\\ &-\frac{m^2}{m_W^2}g_R\left(\Delta+\frac{2\frac{m^2}{m_W^2}-5}{\frac{m^2}{m_W^2}-1}+\frac{\frac{m^4}{m_W^4}-2\frac{m^2}{m_W^2}+4}{\left(\frac{m^2}{m_W^2}-1\right)^2}\log\frac{m^2}{m_W^2}\right)\Bigg\},\end{aligned} \tag{A.18}$$

$$\begin{aligned}F_2(g_L,g_R,m_1,m_2) = \frac{1}{8\sin^2\theta_W\left(\frac{m_2^2}{m_W^2}-\frac{m_1^2}{m_W^2}\right)}\Bigg\{&\\ 2g_L\left(\frac{\frac{m_1^2}{m_W^2}-1}{\frac{m_2^2}{m_W^2}-1}\frac{m_2^4}{m_W^4}\log\frac{m_2^2}{m_W^2}-\frac{\frac{m_2^2}{m_W^2}-1}{\frac{m_1^2}{m_W^2}-1}\frac{m_1^4}{m_W^4}\log\frac{m_1^2}{m_W^2}\right)&-2g_R\sqrt{\frac{m_1^2}{m_W^2}\frac{m_2^2}{m_W^2}}\Bigg(\\ (\Delta+1)\left(\frac{m_2^2}{m_W^2}-\frac{m_1^2}{m_W^2}\right)+\frac{\frac{m_2^2}{m_W^2}-4}{\frac{m_2^2}{m_W^2}-1}\frac{m_2^2}{m_W^2}\log\frac{m_2^2}{m_W^2}-\frac{\frac{m_1^2}{m_W^2}-4}{\frac{m_1^2}{m_W^2}-1}\frac{m_1^2}{m_W^2}\log\frac{m_1^2}{m_W^2}\Bigg)\Bigg\},&\end{aligned} \tag{A.19}$$

where Δ is the divergent part which we don't specify its explicit form because the divergence cancels out.

The Bessel functions of the first and second kind are the following:

$$J_\nu(z) = \left(\frac{z}{2}\right)^\nu\sum_{k=0}^{\infty}(-1)^k\frac{\left(\frac{z^2}{4}\right)^k}{k!\Gamma(\nu+k+1)}, \tag{A.20}$$

$$Y_\nu(z) = \frac{J_\nu(z)\cos(\nu\pi)-J_{-\nu}(z)}{\sin(\nu\pi)}. \tag{A.21}$$

Their derivatives with respect to order are defined as

$$\frac{\partial J_\nu(z)}{\partial\nu} = J_\nu(z)\log\frac{z}{2}-\left(\frac{z}{2}\right)^\nu\sum_{k=0}^{\infty}(-)^k\frac{\psi(\nu+k+1)}{\Gamma(\nu+k+1)}\frac{\left(\frac{4}{z^2}\right)^k}{k!}, \tag{A.22}$$

$$\frac{\partial Y_\nu(z)}{\partial\nu} = \cot(\nu\pi)\left(\frac{\partial J_\nu(z)}{\partial\nu}-\pi Y_\nu(z)\right)-\csc(\nu\pi)\frac{\partial J_{-\nu}(z)}{\partial\nu}-\pi J_\nu(z), \tag{A.23}$$

where $\psi(z) = \Gamma'(z)/\Gamma(z)$.

B Unitarity matrices and other bounds

Here we derive the matrices given by the zeroth modes of partial wave amplitudes for various VBS processes in 2HDMs. Using the largest eigenvalue of each, the perturbative unitarity bound is obtained with Eq. (3.30).

B.1 Neutral two-body states

The matrix for partial wave amplitudes of neutral two-body states is shown here. Initial and final states are given by eight states, namely, $C_1^+C_1^-$, $C_1^+C_2^-$, $C_2^+C_1^-$, $C_2^+C_2^-$, $N_1N_1^\dagger$, $N_1N_2^\dagger$, $N_2N_1^\dagger$ and $N_2N_2^\dagger$. If all of the coefficients, except for c_{1111}^H, are turned off, the matrix

becomes the one in the case of 1HDM given in Eq. (3.11).

$$
\begin{pmatrix}
\frac{3c^T_{1111}+c^H_{1111}}{2} & \frac{3c^T_{1112}+c^H_{1112}}{2} & \frac{3c^T_{1112}+c^H_{1112}}{2} & \frac{3c^T_{1221}-c^H_{1221}+2c^H_{1122}}{2} \\
\frac{3c^T_{1112}+c^H_{1112}}{2} & \frac{3c^T_{1122}+2c^H_{1221}-c^H_{1122}}{2} & \frac{3c^T_{1212}+c^H_{1212}}{2} & \frac{3c^T_{2221}+c^H_{2221}}{2} \\
\frac{3c^T_{1112}+c^H_{1112}}{2} & \frac{3c^T_{1212}+c^H_{1212}}{2} & \frac{3c^T_{1122}+2c^H_{1221}-c^H_{1122}}{2} & \frac{3c^T_{2221}+c^H_{2221}}{2} \\
\frac{3c^T_{1221}-c^H_{1221}+2c^H_{1122}}{2} & \frac{3c^T_{2221}+c^H_{2221}}{2} & \frac{3c^T_{2221}+c^H_{2221}}{2} & \frac{3c^T_{2222}+c^H_{2222}}{2} \\
c^H_{1111} & c^H_{1112} & c^H_{1112} & c^H_{1122} \\
c^H_{1112} & c^H_{1221} & c^H_{1212} & c^H_{2221} \\
c^H_{1112} & c^H_{1212} & c^H_{1221} & c^H_{2221} \\
c^H_{1122} & c^H_{2221} & c^H_{2221} & c^H_{2222}
\end{pmatrix}
\begin{pmatrix}
c^H_{1111} & c^H_{1112} & c^H_{1112} & c^H_{1122} \\
c^H_{1112} & c^H_{1221} & c^H_{1212} & c^H_{2221} \\
c^H_{1112} & c^H_{1212} & c^H_{1221} & c^H_{2221} \\
c^H_{1122} & c^H_{2221} & c^H_{2221} & c^H_{2222} \\
\frac{3c^T_{1111}+c^H_{1111}}{2} & \frac{3c^T_{1112}+c^H_{1112}}{2} & \frac{3c^T_{1112}+c^H_{1112}}{2} & \frac{3c^T_{1221}-c^H_{1221}+2c^H_{1122}}{2} \\
\frac{3c^T_{1112}+c^H_{1112}}{2} & \frac{3c^T_{1122}+2c^H_{1221}-c^H_{1122}}{2} & \frac{3c^T_{1212}+c^H_{1212}}{2} & c^T_{2221} \\
\frac{3c^T_{1112}+c^H_{1112}}{2} & \frac{3c^T_{1212}+c^H_{1212}}{2} & \frac{3c^T_{1122}+2c^H_{1221}-c^H_{1122}}{2} & c^T_{2221} \\
\frac{3c^T_{1221}-c^H_{1221}+2c^H_{1122}}{2} & c^T_{2221} & c^T_{2221} & \frac{3c^T_{2222}+c^H_{2222}}{2}
\end{pmatrix}
. \tag{B.1}
$$

If we impose $SO(4)$ symmetry on the above matrix and eliminate c^T_{1122} and c^T_{1212} with

Eqs. (C.12) and (C.13), the matrix is simplified as follows:

$$
\begin{pmatrix}
\frac{c^H_{1111}}{2} & \frac{c^H_{1112}}{2} & \frac{c^H_{1112}}{2} & \frac{3c^T_{1221}-c^H_{1221}+2c^H_{1122}}{2} \\
\frac{c^H_{1112}}{2} & \frac{c^H_{1221}+c^H_{1212}-c^H_{1122}}{2} & -\frac{3c^T_{1221}-c^H_{1221}}{2} & \frac{c^H_{2221}}{2} \\
\frac{c^H_{1112}}{2} & -\frac{3c^T_{1221}-c^H_{1221}}{2} & \frac{c^H_{1221}+c^H_{1212}-c^H_{1122}}{2} & \frac{c^H_{2221}}{2} \\
\frac{3c^T_{1221}-c^H_{1221}+2c^H_{1122}}{2} & \frac{c^H_{2221}}{2} & \frac{c^H_{2221}}{2} & \frac{c^H_{2222}}{2} \\
c^H_{1111} & c^H_{1112} & c^H_{1112} & c^H_{1122} \\
c^H_{1112} & c^H_{1221} & c^H_{1212} & c^H_{2221} \\
c^H_{1112} & c^H_{1212} & c^H_{1221} & c^H_{2221} \\
c^H_{1122} & c^H_{2221} & c^H_{2221} & c^H_{2222}
\end{pmatrix}
\begin{pmatrix}
c^H_{1111} & c^H_{1112} & c^H_{1112} & c^H_{1122} \\
c^H_{1112} & c^H_{1221} & c^H_{1212} & c^H_{2221} \\
c^H_{1112} & c^H_{1212} & c^H_{1221} & c^H_{2221} \\
c^H_{1122} & c^H_{2221} & c^H_{2221} & c^H_{2222} \\
\frac{c^H_{1111}}{2} & \frac{c^H_{1112}}{2} & \frac{c^H_{1112}}{2} & \frac{3c^T_{1221}-c^H_{1221}+2c^H_{1122}}{2} \\
\frac{c^H_{1112}}{2} & \frac{c^H_{1221}+c^H_{1212}-c^H_{1122}}{2} & -\frac{3c^T_{1221}-c^H_{1221}}{2} & 0 \\
\frac{c^H_{1112}}{2} & -\frac{3c^T_{1221}-c^H_{1221}}{2} & \frac{c^H_{1221}+c^H_{1212}-c^H_{1122}}{2} & 0 \\
\frac{3c^T_{1221}-c^H_{1221}+2c^H_{1122}}{2} & 0 & 0 & \frac{c^H_{2222}}{2}
\end{pmatrix}
. \tag{B.2}
$$

B.2 Singly charged two-body states

The matrix for the zeroth mode partial wave amplitudes of singly charged two-body states is shown below. Initial and final states consist of the following four states: $C_1^+ N_1^\dagger$, $C_1^+ N_2^\dagger$,

$C_2^+ N_1^\dagger$, and $C_2^+ N_2^\dagger$:

$$\begin{pmatrix} -\frac{3c^T_{1111}+c^H_{1111}}{2} & -\frac{3c^T_{1112}+c^H_{1112}}{2} & -\frac{3c^T_{1112}+c^H_{1112}}{2} & -\frac{3c^T_{1221}+c^H_{1221}}{2} \\ -\frac{3c^T_{1112}+c^H_{1112}}{2} & -\frac{3c^T_{1122}+c^H_{1122}}{2} & -\frac{3c^T_{1212}+c^H_{1212}}{2} & -\frac{3c^T_{2221}+c^H_{2221}}{2} \\ -\frac{3c^T_{1112}+c^H_{1112}}{2} & -\frac{3c^T_{1212}+c^H_{1212}}{2} & -\frac{3c^T_{1122}+c^H_{1122}}{2} & -\frac{3c^T_{2221}+c^H_{2221}}{2} \\ -\frac{3c^T_{1221}+c^H_{1221}}{2} & -\frac{3c^T_{2221}+c^H_{2221}}{2} & -\frac{3c^T_{2221}+c^H_{2221}}{2} & -\frac{3c^T_{2222}+c^H_{2222}}{2} \end{pmatrix}. \tag{B.3}$$

We explicitly impose $SO(4)$ symmetry as in the case of the neutral states:

$$\begin{pmatrix} -\frac{c^H_{1111}}{2} & -\frac{c^H_{1112}}{2} & -\frac{c^H_{1112}}{2} & -\frac{3c^T_{1221}+c^H_{1221}}{2} \\ -\frac{c^H_{1112}}{2} & \frac{c^H_{1221}-c^H_{1212}-c^H_{1122}}{2} & \frac{3c^T_{1221}-c^H_{1221}}{2} & -\frac{c^H_{2221}}{2} \\ -\frac{c^H_{1112}}{2} & \frac{3c^T_{1221}-c^H_{1221}}{2} & \frac{c^H_{1221}-c^H_{1212}-c^H_{1122}}{2} & -\frac{c^H_{2221}}{2} \\ -\frac{3c^T_{1221}+c^H_{1221}}{2} & -\frac{c^H_{2221}}{2} & -\frac{c^H_{2221}}{2} & -\frac{c^H_{2222}}{2} \end{pmatrix}. \tag{B.4}$$

B.3 Doubly charged two-body states

The entries of the following matrices are the coefficients of VBS processes for the doubly charged states: $C_1^+ C_1^+$, $C_1^+ C_2^+$, and $C_2^+ C_2^+$. If processes have the same particles in their final states, the unitarity bound becomes weak, as mentioned in the Subsec 2.3.1. The effect has been included in the following matrix:

$$\begin{pmatrix} -\frac{c^T_{1111}-c^H_{1111}}{2} & c^H_{1112}-c^T_{1112} & -\frac{c^T_{1212}-c^H_{1212}}{2} \\ -\frac{c^T_{1112}-c^H_{1112}}{2} & -\frac{3c^T_{1221}+3c^T_{1122}+c^H_{1221}+c^H_{1122}}{2} & -\frac{c^T_{2221}-c^H_{2221}}{2} \\ -\frac{c^T_{1212}-c^H_{1212}}{2} & c^H_{2221}-c^T_{2221} & -\frac{c^T_{2222}-c^H_{2222}}{2} \end{pmatrix}. \tag{B.5}$$

We also impose $SO(4)$ symmetry on the above:

$$\begin{pmatrix} \frac{c^H_{1111}}{2} & c^H_{1112} & \frac{3c^T_{1221}-c^H_{1221}+4c^H_{1212}}{6} \\ \frac{c^H_{1112}}{2} & -\frac{3c^T_{1221}+c^H_{1212}+c^H_{1122}}{2} & \frac{c^H_{2221}}{2} \\ \frac{3c^T_{1221}-c^H_{1221}+4c^H_{1212}}{6} & c^H_{2221} & \frac{c^H_{2222}}{2} \end{pmatrix}. \tag{B.6}$$

C Custodial symmetry of derivative interactions

Dimension-six derivative interactions of Higgs doublets naively violate custodial symmetry. We study the conditions of the derivative interactions that ensure symmetry in the case of 2HDMs. In the following discussion, we refer to results and notations in the Ref. [6, 61].

Derivative interactions are classified into three kinds of operators: operators including unique indices are called type I, e.g. $\partial(H_1^\dagger H_1)\partial(H_1^\dagger H_1)$; in type II, only one of four doublets has a different index, e.g. $\partial(H_1^\dagger H_1)\partial(H_1^\dagger H_2)$; the others belong to type III, e.g. $\partial(H_1^\dagger H_2)\partial(H_2^\dagger H_1)$. For type I and II, current-current interactions, namely O^T operators, violate custodial symmetry because they produce additional contributions to the mass of the Z boson. This is interpreted from a different viewpoint with the nonlinear representation. For type I, as studied in the Ref. [62], operators belonging to O^T are built from the generator of the hypercharge, i.e. the third generator of $SU(2)_R$:

$$(hT^{R3}\partial h)(hT^{R3}\partial h) = \frac{1}{2}O^T_{1111}, \tag{C.1}$$

where h is a real scalar multiplet that corresponds to the Higgs doublet. Since the generator violates $SO(4)$ symmetry, custodial symmetry cannot be preserved after the EW symmetry breaking. In other words, operators that consist of $SO(4)$ symmetric combinations of generators produce the custodial symmetric derivative interactions. This is also the case for operators of type II.[14]

For type III derivative interactions, the situation is different, that is, certain combinations of $SU(2)_R$ violating operators recover $SU(2)_R$ symmetry. In this type, the following operators produce real DOF of derivative interactions:

$$T^{L\alpha}_{11}T^{L\alpha}_{22} = \frac{1}{4}(3O^H_{1221} - O^T_{1122} + O^T_{1221}), \tag{C.2}$$

$$T^{L\alpha}_{12}T^{L\alpha}_{12} = \frac{1}{2}(3O^H_{1122} + 3O^H_{1212} + 3O^H_{2121} + O^T_{1122} - O^T_{1221}), \tag{C.3}$$

$$T^{R\beta}_{11}T^{R\beta}_{22} = \frac{1}{4}(3O^H_{1212} + 3O^H_{2121} + O^T_{1122} - O^T_{1212} - O^T_{2121}), \tag{C.4}$$

$$T^{R\beta}_{12}T^{R\beta}_{12} = \frac{1}{2}(3O^H_{1122} + 3O^H_{1221} - O^T_{1122} + O^T_{1212} + O^T_{2121}), \tag{C.5}$$

$$S^{\alpha 3}_{12}S^{\alpha 3}_{12} = \frac{1}{2}(3O^H_{1122} - 3O^H_{1212} - 3O^H_{2121} + O^T_{1122} - O^T_{1221}), \tag{C.6}$$

$$S^{\alpha\beta}_{12}S^{\alpha\beta}_{12} = \frac{3}{2}(2O^H_{1122} - O^H_{1221} - O^H_{1212} - O^H_{2121}), \tag{C.7}$$

$$T^{R3}_{11}T^{R3}_{22} = \frac{1}{2}O^T_{1122}, \tag{C.8}$$

$$T^{R3}_{12}T^{R3}_{12} = \frac{1}{2}(O^T_{1221} + O^T_{1212} + O^T_{2121}), \tag{C.9}$$

$$U_{12}U_{12} = \frac{1}{2}(O^T_{1221} - O^T_{1212} - O^T_{2121}), \tag{C.10}$$

[14] It is also true for imaginary DOF of derivative interactions. Any imaginary DOF of coefficients violate, in addition to CP symmetry, custodial symmetry. There are no relations to ensure custodial symmetry for imaginary DOF, so we discuss only real DOF here.

where $X^A_{ij} := (hX^A_{(i,j)}\partial h)$ and h includes eight real scalar fields interpreted as two Higgs doublets. Generators $T^{L\alpha}_{(i,j)}$, $T^{R\beta}_{(i,j)}$, $S^{\alpha\beta}_{(i,j)}$ and $U_{(i,j)}$ are, respectively, $(\mathbf{3},\mathbf{1})$, $(\mathbf{1},\mathbf{3})$, $(\mathbf{3},\mathbf{3})$, and $(\mathbf{1},\mathbf{1})$ representations of $SU(2)_L \times SU(2)_R$. Explicit forms of these matrices are given in the Ref. [6]. If we naively follow the discussion for type I and II, the coefficients of operators (C.6), (C.8), and (C.9) should vanish for $SO(4)$ symmetry. However, we have found that some operators preserving $SU(2)_R$ can be given by a certain combination of operators violating $SU(2)_R$. Since these operators are not linearly independent of each other, several relations are derived. In these relations, the above operators violating $SU(2)_R$ symmetry appear with a certain proportional relation:

$$a^S_{1212} : a^Y_{1122} : a^Y_{1212} = 1 : -2 : 1, \tag{C.11}$$

where they are respectively coefficients of operators (C.6), (C.8) and (C.9). This condition is expressed as

$$c^T_{1122} + c^T_{1221} + c^T_{1212} = 0, \tag{C.12}$$
$$3c^T_{1122} + c^H_{1212} - c^H_{1221} = 0, \tag{C.13}$$

where $c^{H,T}_{ijkl}$ are defined as the coefficients of $O^{H,T}_{ijkl}$. The result is consistent with the custodial symmetric conditions shown in the Refs. [6].

The above analysis is easily extended to models including N Higgs doublets. In this case, two other classes of derivative interactions should be defined: operators including three deferent indices are called type IV, e.g. $\partial(H_i^\dagger H_j)\partial(H_i^\dagger H_k)$; the other operators whose indices are totally different from each other are classified as type V, e.g. $\partial(H_i^\dagger H_j)\partial(H_k^\dagger H_l)$. With similar discussions to those given above, the following proportional relations are obtained:

$$a^S_{ijik} : a^Y_{iijk} : a^Y_{ijik} = 1 : -2 : 1, \tag{C.14}$$
$$a^S_{ijkl} : a^S_{ijkl} : a^Y_{ijkl} : a^Y_{ikjl} : a^Y_{iljk} = 1 : -1 : 1 : -2 : 1, \tag{C.15}$$
$$a^S_{ikjl} : a^S_{iljk} : a^Y_{ijkl} : a^Y_{ikjl} : a^Y_{iljk} = 1 : 1 : -1 : 1 : 1, \tag{C.16}$$

where a^Y_{ijkl} and a^S_{ijkl} are, respectively, coefficients of $T^{R3}_{ij}T^{R3}_{kl}$ and $S^{\alpha 3}_{ij}S^{\alpha 3}_{kl}$, the first relation is for type IV and the others are for type V. The following relations are induced for the coefficients of the derivative interactions: for type IV,

$$c^T_{iijk} + c^T_{ijik} + c^T_{ijki} = 0, \tag{C.17}$$
$$3c^T_{iijk} + c^H_{ijki} - c^H_{ijik} = 0; \tag{C.18}$$

for type V,

$$c^H_{ijkl} - c^H_{ijlk} - c^H_{ikjl} + c^H_{iklj} + c^H_{iljk} - c^H_{ilkj} = 0, \tag{C.19}$$
$$3(c^T_{ijkl} + c^T_{ijlk}) - c^H_{ikjl} + c^H_{iklj} - c^H_{iljk} + c^H_{ilkj} = 0, \tag{C.20}$$
$$3(c^T_{ikjl} + c^T_{iklj}) - c^H_{ijkl} + c^H_{ijlk} + c^H_{iljk} - c^H_{ilkj} = 0, \tag{C.21}$$
$$3(c^T_{iljk} + c^T_{ilkj}) + c^H_{ijkl} - c^H_{ijlk} + c^H_{ikjl} - c^H_{iklj} = 0. \tag{C.22}$$

	with	without
I	N	$2N$
II	$N(N-1)$	$2N(N-1)$
III	$2N(N-1)$	$3N(N-1)$
IV	$2N(N-1)(N-2)$	$3N(N-1)(N-2)$
V	$N(N-1)(N-2)(N-3)/3$	$N(N-1)(N-2)(N-3)/2$
Sum	$N^2(N^2+2)/3$	$N^2(N^2+3)/2$

Table 3. Real DOF of dimension-six derivative interactions on models including N Higgs doublets with/without $SO(4)$ symmetry for each type.

After imposing these conditions to ensure $SO(4)$ symmetry on the derivative interactions, we get their remaining DOF. The result is shown in the Tab. 3.

References

[1] G. Aad *et al.* [ATLAS Collaboration], "Observation of a new particle in the search for the Standard Model Higgs boson with the ATLAS detector at the LHC," Phys. Lett. B **716**, 1 (2012) [arXiv:1207.7214 [hep-ex]]; S. Chatrchyan *et al.* [CMS Collaboration], "Observation of a new boson at a mass of 125 GeV with the CMS experiment at the LHC," Phys. Lett. B **716**, 30 (2012) [arXiv:1207.7235 [hep-ex]].

[2] F. Englert and R. Brout, "Broken Symmetry and the Mass of Gauge Vector Mesons," Phys. Rev. Lett. **13**, 321 (1964). P. W. Higgs, Phys. Lett. **12**, 132 (1964).

[3] M. Gell-Mann, M. L. Goldberger, N. M. Kroll and F. E. Low, "Amelioration of divergence difficulties in the theory of weak interactions," Phys. Rev. **179**, 1518 (1969). S. Weinberg, "Physical Processes in a Convergent Theory of the Weak and Electromagnetic Interactions," Phys. Rev. Lett. **27**, 1688 (1971). S. D. Joglekar, "S matrix derivation of the Weinberg model," Annals Phys. **83**, 427 (1974). C. H. Llewellyn Smith, "High-Energy Behavior and Gauge Symmetry," Phys. Lett. B **46**, 233 (1973). J. M. Cornwall, D. N. Levin and G. Tiktopoulos, "Derivation of Gauge Invariance from High-Energy Unitarity Bounds on the s Matrix," Phys. Rev. D **10**, 1145 (1974) [Erratum-ibid. D **11**, 972 (1975)].

[4] B. W. Lee, C. Quigg and H. B. Thacker, "Weak Interactions at Very High-Energies: The Role of the Higgs Boson Mass," Phys. Rev. D **16** (1977) 1519. B. W. Lee, C. Quigg and H. B. Thacker, "The Strength of Weak Interactions at Very High-Energies and the Higgs Boson Mass," Phys. Rev. Lett. **38**, 883 (1977).

[5] G. F. Giudice, C. Grojean, A. Pomarol and R. Rattazzi, "The Strongly-Interacting Light Higgs," JHEP **0706**, 045 (2007) [hep-ph/0703164].

[6] Y. Kikuta, Y. Okada and Y. Yamamoto, "Structure of dimension-six derivative interactions in pseudo Nambu-Goldstone N Higgs doublet models," Phys. Rev. D **85**, 075021 (2012) [arXiv:1111.2120 [hep-ph]].

[7] G. Aad *et al.* [ATLAS Collaboration], "Measurements of Higgs boson production and couplings in diboson final states with the ATLAS detector at the LHC," Phys. Lett. B **726**, 88 (2013) [arXiv:1307.1427 [hep-ex]]. S. Chatrchyan *et al.* [CMS Collaboration], "Observation

of a new boson with mass near 125 GeV in pp collisions at $\sqrt{s} = 7$ and 8 TeV," JHEP **1306**, 081 (2013) [arXiv:1303.4571 [hep-ex]].

[8] K. Agashe, R. Contino and A. Pomarol, "The Minimal composite Higgs model," Nucl. Phys. B **719**, 165 (2005) [hep-ph/0412089].

[9] L. Randall and R. Sundrum, "A Large mass hierarchy from a small extra dimension," Phys. Rev. Lett. **83**, 3370 (1999) [hep-ph/9905221]. L. Randall and R. Sundrum, "An Alternative to compactification," Phys. Rev. Lett. **83**, 4690 (1999) [hep-th/9906064].

[10] S. Weinberg, "A Model of Leptons," Phys. Rev. Lett. **19**, 1264 (1967).

[11] R. Belusevic and T. Higo, "A CLIC-Prototype Higgs Factory," arXiv:1208.4956 [physics.acc-ph].

[12] D. M. Asner, T. Barklow, C. Calancha, K. Fujii, N. Graf, H. E. Haber, A. Ishikawa and S. Kanemura *et al.*, "ILC Higgs White Paper," arXiv:1310.0763 [hep-ph].

[13] M. Spira, A. Djouadi, D. Graudenz and P. M. Zerwas, "Higgs boson production at the LHC," Nucl. Phys. B **453**, 17 (1995) [hep-ph/9504378].

[14] SHeinemeyer *et al.* [LHC Higgs Cross Section Working Group Collaboration], "Handbook of LHC Higgs Cross Sections: 3. Higgs Properties," arXiv:1307.1347 [hep-ph].

[15] M. E. Peskin, "Comparison of LHC and ILC Capabilities for Higgs Boson Coupling Measurements," arXiv:1207.2516 [hep-ph].

[16] M. Klute, R. Lafaye, T. Plehn, M. Rauch and D. Zerwas, "Measuring Higgs Couplings at a Linear Collider," Europhys. Lett. **101**, 51001 (2013) [arXiv:1301.1322 [hep-ph]].

[17] J. Hisano and K. Tsumura, "Higgs boson mixes with an SU(2) septet representation," Phys. Rev. D **87**, no. 5, 053004 (2013) [arXiv:1301.6455 [hep-ph]].

[18] M. S. Chanowitz and M. K. Gaillard, "The TeV Physics of Strongly Interacting W's and Z's," Nucl. Phys. B **261**, 379 (1985).

[19] J. R. Ellis, M. K. Gaillard and D. V. Nanopoulos, "A Phenomenological Profile of the Higgs Boson," Nucl. Phys. B **106**, 292 (1976). M. A. Shifman, A. I. Vainshtein, M. B. Voloshin and V. I. Zakharov, "Low-Energy Theorems for Higgs Boson Couplings to Photons," Sov. J. Nucl. Phys. **30**, 711 (1979) [Yad. Fiz. **30**, 1368 (1979)].

[20] B. A. Kniehl and M. Spira, "Low-energy theorems in Higgs physics," Z. Phys. C **69**, 77 (1995) [hep-ph/9505225].

[21] R. Barbieri and A. Strumia, "The 'LEP paradox'," hep-ph/0007265.

[22] M. Farina, D. Pappadopulo and A. Strumia, "A modified naturalness principle and its experimental tests," JHEP **1308**, 022 (2013) [arXiv:1303.7244 [hep-ph]].

[23] Y. Kikuta and Y. Yamamoto, "Perturbative unitarity of Higgs derivative interactions," arXiv:1210.5674 [hep-ph].

[24] N. Arkani-Hamed, A. G. Cohen, E. Katz and A. E. Nelson, "The Littlest Higgs," JHEP **0207**, 034 (2002) [hep-ph/0206021]; H. -C. Cheng and I. Low, "TeV symmetry and the little hierarchy problem," JHEP **0309**, 051 (2003) [hep-ph/0308199]; H. -C. Cheng and I. Low, "Little hierarchy, little Higgses, and a little symmetry," JHEP **0408**, 061 (2004) [hep-ph/0405243]; I. Low, "T parity and the littlest Higgs," JHEP **0410**, 067 (2004) [hep-ph/0409025].

[25] N. Mahajan, "Littlest Higgs model and unitarity constraints," hep-ph/0310098,

[26] S. Chang and H. -J. He, "Unitarity of little Higgs models signals new physics of UV completion," Phys. Lett. B **586**, 95 (2004) [hep-ph/0311177].

[27] H. Georgi, "Generalized dimensional analysis," Phys. Lett. B **298**, 187 (1993) [hep-ph/9207278].

[28] R. Contino, D. Marzocca, D. Pappadopulo and R. Rattazzi, "On the effect of resonances in composite Higgs phenomenology," JHEP **1110**, 081 (2011) [arXiv:1109.1570 [hep-ph]].

[29] R. Contino, C. Grojean, M. Moretti, F. Piccinini and R. Rattazzi, "Strong Double Higgs Production at the LHC," JHEP **1005**, 089 (2010) [arXiv:1002.1011 [hep-ph]].

[30] N. Arkani-Hamed, A. G. Cohen and H. Georgi, "(De)constructing dimensions," Phys. Rev. Lett. **86**, 4757 (2001) [hep-th/0104005]; N. Arkani-Hamed, A. G. Cohen and H. Georgi, "Electroweak symmetry breaking from dimensional deconstruction," Phys. Lett. B **513**, 232 (2001) [hep-ph/0105239]; N. Arkani-Hamed, A. G. Cohen, T. Gregoire and J. G. Wacker, "Phenomenology of electroweak symmetry breaking from theory space," JHEP **0208**, 020 (2002) [hep-ph/0202089].

[31] M. Schmaltz, D. Stolarski and J. Thaler, "The Bestest Little Higgs," JHEP **1009**, 018 (2010) [arXiv:1006.1356 [hep-ph]].

[32] T. Brown, C. Frugiuele and T. Gregoire, "UV friendly T-parity in the SU(6)/Sp(6) little Higgs model," JHEP **1106**, 108 (2011) [arXiv:1012.2060 [hep-ph]].

[33] G. Aad *et al.* [ATLAS Collaboration], "Search for a heavy top-quark partner in final states with two leptons with the ATLAS detector at the LHC," arXiv:1209.4186 [hep-ex].

[34] R. Contino, C. Grojean, D. Pappadopulo, R. Rattazzi and A. Thamm, "Strong Higgs Interactions at a Linear Collider," arXiv:1309.7038 [hep-ph].

[35] M. Farina, C. Grojean and E. Salvioni, "(Dys)Zphilia or a custodial breaking Higgs at the LHC," JHEP **1207**, 012 (2012) [arXiv:1205.0011 [hep-ph]].

[36] R. Barbieri, B. Bellazzini, V. S. Rychkov and A. Varagnolo, "The Higgs boson from an extended symmetry," Phys. Rev. D **76**, 115008 (2007) [arXiv:0706.0432 [hep-ph]], R. Contino, "A Holographic composite Higgs model," hep-ph/0609148.

[37] R. Contino, L. Da Rold and A. Pomarol, "Light custodians in natural composite Higgs models," Phys. Rev. D **75**, 055014 (2007) [hep-ph/0612048], M. S. Carena, E. Ponton, J. Santiago and C. E. M. Wagner, "Light Kaluza Klein States in Randall-Sundrum Models with Custodial SU(2)," Nucl. Phys. B **759**, 202 (2006) [hep-ph/0607106], A. D. Medina, N. R. Shah and C. E. M. Wagner, "Gauge-Higgs Unification and Radiative Electroweak Symmetry Breaking in Warped Extra Dimensions," Phys. Rev. D **76**, 095010 (2007) [arXiv:0706.1281 [hep-ph]], G. Panico, E. Ponton, J. Santiago and M. Serone, "Dark Matter and Electroweak Symmetry Breaking in Models with Warped Extra Dimensions," Phys. Rev. D **77**, 115012 (2008) [arXiv:0801.1645 [hep-ph]].

[38] A. Azatov and J. Galloway, "Light Custodians and Higgs Physics in Composite Models," Phys. Rev. D **85**, 055013 (2012) [arXiv:1110.5646 [hep-ph]].

[39] M. Montull, F. Riva, E. Salvioni and R. Torre, "Higgs Couplings in Composite Models," Phys. Rev. D **88**, 095006 (2013) [arXiv:1308.0559 [hep-ph]].

[40] G. Altarelli and R. Barbieri, "Vacuum polarization effects of new physics on electroweak

processes," Phys. Lett. B **253**, 161 (1991), G. Altarelli, R. Barbieri and S. Jadach, "Toward a model independent analysis of electroweak data," Nucl. Phys. B **369**, 3 (1992) [Erratum-ibid. B **376**, 444 (1992)], G. Altarelli, R. Barbieri and F. Caravaglios, "Nonstandard analysis of electroweak precision data," Nucl. Phys. B **405**, 3 (1993).

[41] S. Schael *et al.* [ALEPH and DELPHI and L3 and OPAL and SLD and LEP Electroweak Working Group and SLD Electroweak Group and SLD Heavy Flavour Group Collaborations], "Precision electroweak measurements on the Z resonance," Phys. Rept. **427**, 257 (2006) [hep-ex/0509008].

[42] T. E. W. Group [CDF and D0 Collaborations], "2012 Update of the Combination of CDF and D0 Results for the Mass of the W Boson," arXiv:1204.0042 [hep-ex].

[43] M. Gillioz, R. Grober, C. Grojean, M. Muhlleitner and E. Salvioni, "Higgs Low-Energy Theorem (and its corrections) in Composite Models," JHEP **1210**, 004 (2012) [arXiv:1206.7120 [hep-ph]].

[44] V. M. Abazov *et al.* [D0 Collaboration], "Evidence for s-channel single top quark production in $p\bar{p}$ collisions at $\sqrt{s} = 1.96$ TeV," arXiv:1307.0731 [hep-ex].

[45] T. E. W. Group [CDF and D0 Collaborations], "Combination of CDF and D0 Measurements of the Single Top Production Cross Section," arXiv:0908.2171 [hep-ex].

[46] C. Anastasiou, E. Furlan and J. Santiago, "Realistic Composite Higgs Models," Phys. Rev. D **79**, 075003 (2009) [arXiv:0901.2117 [hep-ph]].

[47] M. Carena, I. Low and C. E. M. Wagner, "Implications of a Modified Higgs to Diphoton Decay Width," JHEP **1208**, 060 (2012) [arXiv:1206.1082 [hep-ph]].

[48] A. Azatov, R. Contino, A. Di Iura and J. Galloway, "New Prospects for Higgs Compositeness in h $\to$ Z gamma," arXiv:1308.2676 [hep-ph].

[49] W. D. Goldberger and M. B. Wise, "Modulus stabilization with bulk fields," Phys. Rev. Lett. **83**, 4922 (1999) [hep-ph/9907447].

[50] C. Csaki, M. L. Graesser and G. D. Kribs, "Radion dynamics and electroweak physics," Phys. Rev. D **63**, 065002 (2001) [hep-th/0008151].

[51] H. Davoudiasl, J. L. Hewett and T. G. Rizzo, "Bulk gauge fields in the Randall-Sundrum model," Phys. Lett. B **473**, 43 (2000) [hep-ph/9911262]. A. Pomarol, "Gauge bosons in a five-dimensional theory with localized gravity," Phys. Lett. B **486**, 153 (2000) [hep-ph/9911294]. T. Gherghetta and A. Pomarol, "Bulk fields and supersymmetry in a slice of AdS," Nucl. Phys. B **586**, 141 (2000) [hep-ph/0003129]. S. Chang, J. Hisano, H. Nakano, N. Okada and M. Yamaguchi, "Bulk standard model in the Randall-Sundrum background," Phys. Rev. D **62**, 084025 (2000) [hep-ph/9912498].

[52] S. Casagrande, F. Goertz, U. Haisch, M. Neubert and T. Pfoh, "Flavor Physics in the Randall-Sundrum Model: I. Theoretical Setup and Electroweak Precision Tests," JHEP **0810**, 094 (2008) [arXiv:0807.4937 [hep-ph]]. M. Bauer, S. Casagrande, U. Haisch and M. Neubert, "Flavor Physics in the Randall-Sundrum Model: II. Tree-Level Weak-Interaction Processes," JHEP **1009**, 017 (2010) [arXiv:0912.1625 [hep-ph]].

[53] H. Kubota and M. Nojiri, "Radion-higgs mixing state at the LHCwith the KK contributions to the production and decay," Phys. Rev. D **87**, 076011 (2013) [arXiv:1207.0621 [hep-ph]].

[54] C. Csaki, J. Hubisz and S. J. Lee, "Radion phenomenology in realistic warped space models," Phys. Rev. D **76**, 125015 (2007) [arXiv:0705.3844 [hep-ph]].

[55] M. Carena, S. Casagrande, F. Goertz, U. Haisch and M. Neubert, "Higgs Production in a Warped Extra Dimension," JHEP **1208**, 156 (2012) [arXiv:1204.0008 [hep-ph]].

[56] D. Dominici, B. Grzadkowski, J. F. Gunion and M. Toharia, "The Scalar sector of the Randall-Sundrum model," Nucl. Phys. B **671**, 243 (2003) [hep-ph/0206192]. V. Barger and M. Ishida, "Randall-Sundrum Reality at the LHC," Phys. Lett. B **709**, 185 (2012) [arXiv:1110.6452 [hep-ph]]. B. Grzadkowski, J. F. Gunion and M. Toharia, "Higgs-Radion interpretation of the LHC data?," Phys. Lett. B **712**, 70 (2012) [arXiv:1202.5017 [hep-ph]]. H. de Sandes and R. Rosenfeld, "Radion-Higgs mixing effects on bounds from LHC Higgs Searches," Phys. Rev. D **85**, 053003 (2012) [arXiv:1111.2006 [hep-ph]].

[57] K. Agashe, R. Contino, L. Da Rold and A. Pomarol, "A Custodial symmetry for Zb anti-b," Phys. Lett. B **641**, 62 (2006) [hep-ph/0605341]. C. Csaki, A. Falkowski and A. Weiler, "The Flavor of the Composite Pseudo-Goldstone Higgs," JHEP **0809**, 008 (2008) [arXiv:0804.1954 [hep-ph]]. O. Gedalia, G. Isidori and G. Perez, "Combining Direct & Indirect Kaon CP Violation to Constrain the Warped KK Scale," Phys. Lett. B **682**, 200 (2009) [arXiv:0905.3264 [hep-ph]].

[58] R. S. Gupta, H. Rzehak and J. D. Wells, "How well do we need to measure Higgs boson couplings?," Phys. Rev. D **86**, 095001 (2012) [arXiv:1206.3560 [hep-ph]].

[59] M. Bicer, H. Duran Yildiz, I. Yildiz, G. Coignet, M. Delmastro, T. Alexopoulos, C. Grojean and S. Antusch *et al.*, "First Look at the Physics Case of TLEP," arXiv:1308.6176 [hep-ex].

[60] K. Cheung, J. S. Lee and P. -Y. Tseng, "Higgs Precision (Higgcision) Era begins," JHEP **1305**, 134 (2013) [arXiv:1302.3794 [hep-ph]].

[61] J. Mrazek, A. Pomarol, R. Rattazzi, M. Redi, J. Serra and A. Wulzer, "The Other Natural Two Higgs Doublet Model," Nucl. Phys. B **853**, 1 (2011) [arXiv:1105.5403 [hep-ph]].

[62] I. Low, R. Rattazzi and A. Vichi, "Theoretical Constraints on the Higgs Effective Couplings," JHEP **1004**, 126 (2010) [arXiv:0907.5413 [hep-ph]].